FLEXOR TENDON MOTION AND SHEAR: IMPLICATIONS FOR WORK

FLEXOR TENDON MOTION AND SHEAR IN THE CARPAL TUNNEL: IMPLICATIONS FOR WORK

By AARON M. KOCIOLEK, M.Sc.

A Thesis Submitted to the School of Graduate Studies in Partial Fulfilment of the Requirements for the Degree Doctor of Philosophy

DOCTOR OF PHILOSOPHY (2015) McMaster University

(Kinesiology) Hamilton, Ontario

TITLE: Flexor tendon motion and shear in the carpal tunnel: implications for work

AUTHOR: Aaron M. Kociolek, M.Sc. (McMaster University), B.Sc. Honours (Laurentian University)

SUPERVISOR: Dr. Peter J. Keir

NUMBER OF PAGES: xxiv, 185

ABSTRACT

Carpal tunnel syndrome is characterized by non-inflammatory fibrosis of the subsynovial connective tissue next to the tendons in the carpal tunnel, suggesting a shear injury owing to repetitive wrist and finger motion at work. I tested the effects of several well-established biomechanical predictors of injury on tendon and subsynovial connective tissue motion and shear in the carpal tunnel. These included non-neutral finger and wrist posture, speed of work, and forceful exertion. A cadaveric paradigm was used to directly measure tendon gliding characteristics, which showed that concurrent exposure to multiple biomechanical risk factors disproportionately increased tendon frictional work (Chapter 2). Given that tendon shear cannot be directly measured *in vivo*, colour flow ultrasound was used to assess relative motion between tendon and subsynovial connective tissue as a metric of shear potential (Chapter 3 − 5). Healthy participants completed middle finger movements while colour flow ultrasound imaged carpal tunnel structures and optical motion capture recorded finger joint kinematics. From the data, I developed regression equations to predict both tendon and subsynovial connective tissue displacements as a function of finger joint angles, which can be used as an ergonomic method to calculate the relative displacement (Chapter 3). Furthermore, relative motion between tendon and subsynovial connective tissue increased with wrist flexion angle, suggesting a greater susceptibility to shear injury during repetitive work when the wrist is flexed (Chapter 4). Using colour flow imaging, electrogoniometry, and fine-wire EMG, relative displacement was found to increase with tendon velocity and force (Chapter 5). Relative displacements in Chapters 3 to 5 were combined into a prediction model, and

further compared to a tendon friction model derived from Chapter 2. The relative displacement model showed an additive relationship with combined physical exposures, including finger and wrist position, tendon velocity, and force (Chapter 6). The relative displacement model was more responsive to lower physical exposures whereas the friction model produced greater overall changes (with higher exposures). While both models infer a greater risk of shear injury due to repetitive and forceful wrist/finger movement, future studies will aim to set protective guidelines based on tendon motion and shear during hand-intensive work. Overall, this thesis showed that tendon friction and relative motion between tendon and subsynovial connective tissue both increased in response to well-established biomechanical risk factors. We propose the current models for use in ergonomics, representing a move towards mechanistic-based injury risk assessment of the wrist and hand.

Keywords: Carpal tunnel syndrome, friction, tendon travel, subsynovial connective tissue

ACKNOWLEDGEMENTS

This thesis is a labour of love that was only made possible by the magnanimous support of my colleagues, mentors, and family. First, I would like to thank Dr. Peter Keir. You are someone that I aspire to be. While many know Peter as an accomplished researcher, he is also a deeply generous and caring person. Thank you for always being in my corner. I am forever grateful for your guidance and supervision. I would also like to thank Dr. Jim Potvin and Dr. Richard Wells, for your continued and unwavering support, particularly as I tested and developed new methods while going well over-time before eyeing completion.

I would like to thank my collaborator, Jimmy Tat. It was a pleasure to get to know you. I am very proud of the body of research that we contributed during our time at McMaster. Thank you to Dr. Joshua Cashaback, who kindly shared his distribution-moment model of skeletal muscle for use in my thesis. I would also like to thank Dr. Joanne Hodder for training me in the use of fine-wire EMG. Thank you, Alison McDonald, Samantha Ebata, Katherine Wilson, David Cocchiarella, Calvin Tse, and Mike Rizzuto, for you help with data collection and analysis. Thank you to all members (past and present) of the Occupational Biomechanics Laboratory for your loyal friendship. Hamilton will always stand out as a truly magical time in my life. Special thanks to Justin Weresch, Jeff Graham, Nicholas LaDelfa, Jim Burkitt, Michel Sonne, Joanne Hodder, Michael Holmes, and Joshua Cashaback.

Lastly, I would like to thank my family, especially my sister, Amy, and Mom and Dad, Micheline and John Kociolek. You taught me the true meaning of unconditional

love, which keeps me grounded. Thank you to my brother-in-law, James Batchelor. Even though Jim is the youngest in his family, he is wise beyond his years, and certainly did more for me than could ever be expected of a little brother. Thank you Jody and Brian Batchelor, for your love and support in my academic pursuit, even though that has meant moving your daughter and grandson far away to further my career. Finally, thank you to my wife, Allyson, and son, Adam. Allyson, you have sacrificed much to make this thesis possible. Adam and Allyson, whenever I find myself lacking for energy, I need only look to you, and I realize how blessed I am to have you. I love you both.

THESIS FORMAT AND ORGANIZATION

This thesis contains PhD work conducted by Aaron M. Kociolek, prepared in the "sandwich" format as outlined in the McMaster University School of Graduate Studies' Guide for the Preparation of Thesis.

This thesis begins with a general introduction into work-related wrist and hand musculoskeletal disorders, including tendon shear in the development of carpal tunnel syndrome (Chapter 1). Next, three studies that explore the relationship between biomechanical predictors of injury and flexor tendon motion and shear are presented in four manuscripts, which comprise Chapters 2 to 5.

Chapter 2 used a cadaveric protocol to measure flexor tendon gliding resistance and frictional work through the carpal tunnel in response to biomechanical work factors, and was recently published in the Journal of Biomechanics.

Chapters 3 and 4 used ultrasound and motion capture to assess relative displacement between tendon and subsynovial connective tissue as healthy participants performed different finger movements. Chapter 3 describes a model to predict relative displacement based on finger joint angles, and was recently published in Ergonomics. Chapter 4 characterized the relation between wrist angle and relative displacement, and will be submitted to the Journal of Orthopaedic Research.

Chapter 5 used colour ultrasound, electrogoniometry, and fine-wire EMG to determine the effects of movement frequency and finger force, and by extension tendon velocity and

force, on the relative displacement between tendon and subsynovial connective tissue. This manuscript will be submitted to the Journal of Biomechanics.

This thesis ends with a final summary (Chapter 6), which compares two models that predict (i) relative displacement and (ii) tendon friction, for future use in ergonomics. The material in this chapter may ultimately form the start of a review paper detailing injury mechanisms of the wrist and hand, and implications for work.

CONTRIBUTIONS TO PAPERS WITH MULTIPLE AUTHORS

Chapter 2

Kociolek, A.M., Tat, J., Keir, P.J., 2015. Biomechanical risk factors and flexor tendon frictional work in the cadaveric carpal tunnel. Journal of Biomechanics 48 (3), 449−455.

Contributions

This study was conceived by Aaron M. Kociolek and Dr. Peter J. Keir. Method development and data collection were conducted equally by Jimmy Tat and Aaron Kociolek with input from Dr. Keir. Data analysis, interpretation, and manuscript preparation were performed by Aaron Kociolek. Jimmy Tat also assisted with data analysis. Dr. Keir was a major contributor to both data interpretation and manuscript preparation with input from Jimmy Tat. All co-authors contributed to the paper, which was recently published in Journal of Biomechanics.

Chapter 3

Kociolek, A.M., Keir, P.J., 2015. Development of a kinematic model to predict finger flexor tendon and subsynovial connective tissue displacement in the carpal tunnel. Ergonomics, Accepted, January 20, 2015.

Chapter 4

Kociolek, A.M., Keir, P.J. Relative motion between the flexor digitorum superficialis tendon and subsynovial connective tissue increases with wrist flexion angle. Prepared for Journal of Orthopaedic Research.

Contributions

Aaron Kociolek and Dr. Keir both contributed substantially to Chapters 3 and 4. The study paradigm, methods, data collection, analysis, interpretation, and manuscript preparation were conducted by Aaron Kociolek with major contributions from Dr. Keir throughout the study.

Chapter 5

Kociolek, A.M., Tat, J., Keir, P.J. Relative displacement between flexor tendon and subsynovial connective tissue increases with movement frequency and finger force. Prepared for Journal of Biomechanics.

Contributions

This study was conceived by Aaron Kociolek and Dr. Keir. The methods were developed by Aaron Kociolek with input from Dr. Keir. Aaron Kociolek and Jimmy Tat both collected the data over the entire study. Data analysis was primarily performed by Aaron Kociolek with assistance from Jimmy Tat and input from Dr. Keir. Data interpretation and manuscript development was conducted by Aaron Kociolek with major contributions from Dr. Keir. All co-authors contributed to the paper.

TABLE OF CONTENTS

LIST OF TABLES

CHAPTER 1

CHAPTER 2

CHAPTER 3

CHAPTER 4

CHAPTER 5

LIST OF FIGURES

CHAPTER 1

CHAPTER 2

CHAPTER 3

CHAPTER 4

CHAPTER 5

CHAPTER 6

LIST OF ABBREVIATIONS

aEMG ..... Average electromyography

ANOVA ..... Analysis of variance

A2 ..... 2nd annular pulley

CDI ..... Colour Doppler imaging

CMC ..... Carpometacarpal joint

CTP ..... Carpal tunnel pressure

CTS ..... Carpal tunnel syndrome

DIP ..... Distal interphalangeal joint

DMA ..... Distribution moment approximation

ED ..... Extensor digitorum

EMG ..... Electromyograhy

FDP ..... Flexor digitorum profundus

FDS ..... Flexor digitorum superficialis

FF ..... Full finger flexion

FPL ..... Flexor pollicis longus

F/E ..... Flexion/extension

IC ..... Intercarpal joint

IOM ..... Institute of Medicine

MCP ..... Metacarpophalangeal joint

MVE ..... Maximum voluntary effort

MVR ..... Maximum velocity ratio

NIOSH ..... National Institute for Occupational Safety and Health

NRC ..... National Research Council

NSERC ..... National Sciences and Engineering Research Council

OR ..... Odds ratio

PIP ..... Proximal interphalangeal joint

PIP + DIP ..... Combined proximal and distal interphalangeal joints

RDI ..... Relative displacement index

RMSE ..... Root mean squared error

RULA ..... Rapid Upper Limb Assessment

R^2 ..... Coefficient of determination

SSCT ..... Subsynovial connective tissue

TCL ..... Transverse carpal ligament

TLV for HAL ..... Threshold Limit Value for Hand Activity Level

LIST OF APPENDICES

CHAPTER ONE: INTRODUCTION

1.1. Workplace Injury Statistics

The annual incidence of wrist and hand claims in Ontario was 1,429 from 2004 to 2013, which accounted for 10.0 % of all workplace injuries (WSIB, 2013). Zakaria et al. (2004) estimated wrist/hand claim rates of 36.3 and 58.9 per 100,000 male and female Ontario workers, respectively. Claim rates are generally highest in industries with widespread exposure to repetitive motions (Davis et al., 2001; Gerr et al., 2002; Silverstein et al., 1998), though Zakaria (2004) showed that industrial claim rates of carpal tunnel syndrome (CTS) differed between male and female workers. Temporal trends in CTS show increasing diagnosis rates, especially in individuals over the age of 45, which may have profound economic implications due to the aging workforce (Bongers et al., 2007; Gelfman et al., 2009).

Wrist and hand disorders are generally more costly to rehabilitate compared to other anatomical regions. Manktelow et al. (2004) reviewed claims in Ontario from 1996 and found 964 workers diagnosed with CTS. Seventy-five percent of workers required surgery before returning to work 3 ± 3.5 months later. A four-year follow-up of 731 workers demonstrated that 50% still experienced moderate to severe pain or numbness, while only 14% were symptom-free. Successful return to work (i.e. performing the same job) occurred in 64% of cases with or without modification. The average cost per worker exceeded $13,700 each year, for a total annual cost of $13,200,000 (CAD). Similarly, the annual cost of treatment and indemnity for each claim of CTS in Washington was $13,031 (USD), for a total of $77,800,000 each year (Silverstein et al., 1998). This

economic burden underscores the need to better understand the development of wrist and hand disorders, which may lead to reduced injuries in the workplace and improve outcomes of surgery and rehabilitation.

1.2. Occupational Risk Factors

In the late 1990's, the National Institute for Occupational Safety and Health (NIOSH) conducted an extensive review of musculoskeletal disorders (Bernard, 1997). There was strong evidence that a combination of repetitive motion, non-neutral posture, and forceful work increased the risk of wrist/hand tendinitis and CTS. While few studies have assessed these risk factors alone, there was an association between each repetition, posture, and force (separately) and wrist/hand tendinitis. There was also evidence that both repetition and force independently increased the risk of CTS. However, there was insufficient evidence of a positive association between posture and CTS. A follow-up review conducted by the National Research Council (NRC) and Institute of Medicine (IOM) in 2001 found similar associations between physical exposures and wrist/hand musculoskeletal disorders, with stronger evidence for a combination of biomechanical risk factors.

Researchers have attempted to extrapolate dose-response relationships between physical exposures and wrist/hand musculoskeletal disorders with some success (Bonfiglioli et al., 2007; Frost et al., 1998; Gerr et al., 2002; Russo et al., 2002; Scheuerle et al., 2000; Silverstein et al., 1986, 1987; Thomsen et al., 2002). Frost et al. (1998) found that CTS risk increased with cumulative exposure to repetitive and forceful work for up to 10 years, and remained relatively constant thereafter. Bonfiglioli et al. (2007)

studied the prevalence of CTS in cashiers exposed to different weekly durations of 'biomechanical load', and logistical regression found that the prevalence of symptoms was higher in full-time (OR – 2.74) and part-time (OR – 1.26) cashiers compared to office workers (OR – 1.00).

Despite these findings, dose-response relationships between physical exposures and wrist/hand musculoskeletal disorders remain ambiguous, and well-established ergonomic tools do not adequately reflect the multiplicative interaction of combined biomechanical risk factors (Garg et al., 2012). Several ergonomic methods estimate occupational injury risk based on physical exposures, including the Rapid Upper Limb Assessment, or RULA (McAtamney and Corlett, 1993), Occupational Repetitive Action (Occhipinti, 1998), Strain Index (Moore and Garg, 1995), and Threshold Limit Value for Hand Activity Level, or TLV for HAL (ACGIH, 2002), each with a different (and often discrepant) weighting algorithm. For example, RULA places greater emphasis on posture while the Strain Index is greatly influenced by force. Although the TLV for HAL considers both repetition and force relatively equal, epidemiological studies show mixed results for predicting CTS (Garg et al., 2012; Franzblau et al., 2005; Violante et al., 2007). A mechanistic approach, based on injury mechanics, may be better suited to predict wrist/hand musculoskeletal disorders in the workplace, including CTS.

1.3. Carpal Tunnel Anatomy

A transverse section at the level of the hamate illustrates the structures found inside the carpal tunnel (Figure 1.1). The dorsal carpal tunnel consists of 8 carpal bones in 2 rows (proximal row – scaphoid, lunate, pisiform, and triquetrum; distal row – trapezium,

trapezoid, capitate, and hamate) covered by the volar wrist capsule. The transverse carpal ligament (TCL) forms the roof of the carpal tunnel, which attaches radially to the trapezium and scaphoid, and ulnarly to the hamate and pisiform. The median nerve and nine flexor tendons pass through the carpal tunnel and occupy over 90% of its cross-sectional area (Bower et al., 2006). The flexor pollicis longus (FPL) tendon is located near the radial wall of the carpal tunnel. There are four flexor digitorum superficialis (FDS) tendons in the volar region while four flexor digitorum profundus (FDP) tendons are near the dorsal wall of the carpal tunnel. The tendons are cushioned from the carpal bones by the radial and ulnar bursae.

The flexor tendons are surrounded by the multi-layered subsynovial connective tissue (SSCT), a complex microvacuolar system comprised of collagen layers interconnected by smaller vertical fibres (Guimberteau et al., 2010). SSCT fibrils also attach the tendons and nerve to the visceral synovium in the carpal tunnel (Figure 1.2). During tendon displacement, the SSCT is strained, with the deep layers closest to tendon lengthening first (Ettema et al., 2006a). Load is gradually transferred to the superficial layers until the visceral synovium moves. A gel-like interfibrillar matrix containing glycoproteins also permeates the space between the collagen layers of the SSCT, which serves as a nutrient delivery system and provides boundary lubrication to facilitate smooth tendon gliding inside the carpal tunnel (Amadio, 2005). The gliding mechanism in the carpal tunnel is unique since flexor tendon motion results in paratenon gliding resistance as well as bursal friction (Gelberman et al., 1992).

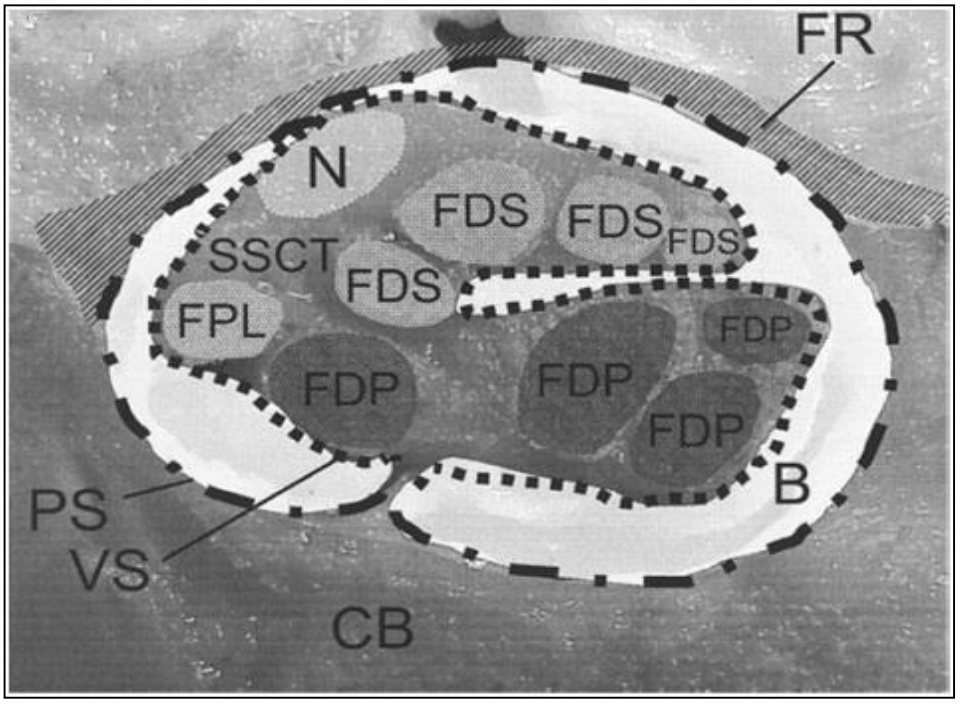

Figure 1.1. Transverse section of the carpal tunnel at the level of the hamate. FR – flexor retinaculum; CB – carpal bones; N – median nerve; FPL – flexor pollicis longus; FDP – flexor digitorum profundus; FDS – flexor digitorum superficialis; B – bursae; SSCT – subsynovial connective tissue; PS – parietal synovium; VS – visceral synovium. From Ettema et al. (2007).

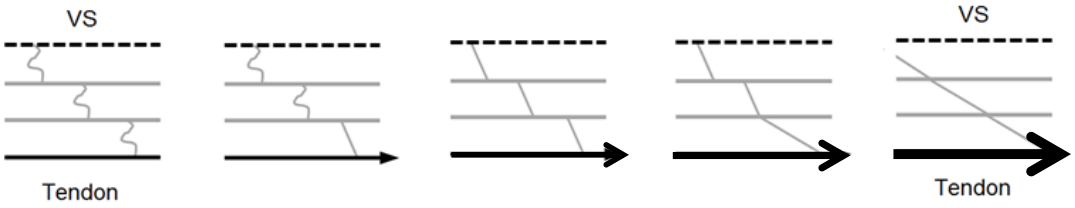

Figure 1.2. Tenosynovial gliding in the carpal tunnel. SSCT layers (horizontal grey lines) tether the tendon (solid black line) to the visceral synovium (dashed black line). During tendon displacement, (solid black arrows), SSCT layers closest to the tendon are lengthened first. With greater tendon displacement (thicker arrows), load is transferred to superficial layers through the perpendicular fibrils (vertical grey lines) until the visceral synovium moves. From Tat (2014).

1.4. Anatomy of the Hand

The hand is comprised of 8 carpals, 5 metacarpals, and 14 phalanges (including proximal and distal thumb phalanges as well as proximal, middle, and distal finger phalanges) that form the intercarpal (IC), carpometacarpal (CMC), metacarpophalangeal (MCP), proximal interphalangeal (PIP), and distal interphalangeal (DIP) joints. The extrinsic finger flexors include the FDP and FDS (Table 1.1). Five ligamentous thickenings of arcing fibres known as annular pulleys constrain the flexor tendons along the finger. Additional thin criss-crossing fibres, the cruciate pulleys, are also located between the annular pulleys. Together, the annular and cruciate pulleys prevent bowstringing and minimize tendon displacement during finger flexion (Goodman and Choueka, 2005). The extrinsic finger extensors include the extensor indicis proprius and extensor digitorum communis that insert into the extensor expansion, a tendinous aponeurosis on the dorsal metacarpals and phalanges.

The intrinsic hand muscles include the lumbricals as well as the palmar and dorsal interossei (Table 1.1). The lumbricals are tiny muscles that originate from the FDP tendons, assisting with MCP joint flexion while maintaining PIP and DIP joint extension. The palmar and dorsal interossei originate from the metacarpal sides and produce MCP adduction and abduction, respectively. The interossei muscles also assist with interphalangeal extension. The lumbricals and interossei insert with the extensor digitorum tendons into the extensor expansion. However, anatomical descriptions of the lumbricals and interossei are typically oversimplified. In reality, multiple insertions of

the lumbricals and interossei exist with a high degree of anatomic variability (Eladoumikdachi et al., 2002a, b).

Table 1.1. Extrinsic and intrinsic finger muscles (MCP – metacarpophalangeal; PIP – proximal interphalangeal; DIP – distal interphalangeal; TCL – transverse carpal ligament). Origins, insertions, and actions from Marieb (2003).

Muscle	**Origin**	**Insertion**	**Action**
	Extrinsic Finger Flexors and Extensors		
Flexor digitorum profundus	Anteromedial surface and coronoid process of ulna; interosseous membrane	By four tendons into distal finger phalanges	Flexes wrist; flexes MCP, PIP and DIP finger joints
Flexor digitorum superficialis	Medial epicondyle of humerus; coronoid process of ulna; radius	By four tendons into middle finger phalanges	Flexes wrist; flexes MCP and PIP joints
Extensor digitorum communis	Lateral epicondyle of humerus	By four tendons into the extensor expansion	Extends wrist; extends MCP, PIP and DIP finger joints
Extensor indicis proprius	Posterior surface of distal ulna; interosseous membrane	Extensor expansion of index finger	Extends wrist; extends index finger
	Intrinsic Midpalmar Muscles		
Lumbricals	Lateral side of flexor digitorum profundus tendons in palm	Lateral edge of extensor expansion at proximal finger phalanges	Flexes MCP joints and extends PIP and DIP finger joints
Palmar interossei	Side of metacarpals facing hand mid-axis	Extensor expansion of proximal finger phalanges	Adducts MCP joints; assists lumbricals
Dorsal interossei	Sides of metacarpals	Extensor expansion of proximal finger phalanges	Abducts MCP joint; assists lumbricals

1.5. Injury Mechanisms of the Wrist and Hand

While it is well-known that CTS is caused by compression of the median nerve, the underlying pathomechanics are complex and likely multi-factorial (Staal et al., 2007). Elevated carpal tunnel pressure (CTP) is evidently involved in the development of CTS (Keir and Rempel, 2005). In the 1980's and 1990's, different animal models were used to artificially increase extraneural pressure while monitoring various pathophysiological processes. Rydevik et al. (1981) studied the effects of extraneural compression on rabbit tibial nerve and found that 20 to 30 mmHg decreased venous blood flow, 30 to 60 mmHg influenced capillary function, and 60 to 80 mmHg resulted in complete ischemia. In rat sciatic nerve, 30 mmHg reduced nutrient transport while 80 mmHg initiated axonal degeneration (Lundborg et al., 1983).

Conduction velocity of the median nerve was found to decrease at experimentally induced CTP of 30 mmHg in 16 human participants, thus establishing a threshold for neurophysiologic impairment (Lundborg et al., 1982). Keir et al. (1998) found that hydrostatic pressure exceeded 30 mmHg in extended as well as radially and ulnarly deviated wrist postures, and effects were greater with the finger straight (versus flexed). Several other studies have shown that awkward (non-neutral) postures increase CTP, including forearm rotation (Rempel et al., 1998; Werner et al., 1997), wrist deviation (Rempel et al., 1997; Weiss et al., 1995), and either full finger flexion (Cobb et al., 1995) or finger extension (Keir et al., 1998). Rempel et al. (1997) also determined that a fingertip force as low as 6 N increased CTP.

While elevated CTP is characteristic of CTS patients compared to healthy controls (Hamanaka et al., 1995; Seradge et al., 1995), histological changes in CTS include fibrosis and thickening of the SSCT (Ettema et al., 2006a; Jinrok et al., 2004, 2006). SSCT fibrosis is also pronounced in the deep layers adjacent to tendon (Figure 1.3), suggesting that repetitive motion results in a shear injury between tendon and SSCT (Ettema et al., 2006a; Schuind et al., 1990). Repetitive shear force is thought to initiate a series of mechanical events, including altered stiffness and permeability of the SSCT (Osamura et al., 2007a, b), increased volume of the carpal tunnel contents (Ettema et al., 2006a), elevated CTP (Hamanaka et al., 1995; Seradge et al., 1995), and ischemia induced compression of the median nerve (Keir and Rempel, 2005).

Finger flexor tendinitis is often considered a precursor to CTS, which may be caused by mechanical abrasion due to relative motion with other carpal tunnel structures, including adjacent tendons and the median nerve (Smutz et al., 1994). Resulting inflammation and edema within the carpal tunnel may also influence motion of the fluid-permeated SSCT (Goetz and Barr, 2014). CTS patients present with increased adherence or dissociation between tendon and SSCT compared to healthy controls (Ettema et al., 2008; van Doesburg et al., 2012) as well as greater relative motion between the median nerve and FDS (Filius et al., 2015). Changes in tenosynovial motion may further influence the permeability and stiffness of the SSCT, resulting in a vicious cycle of shear degradation.

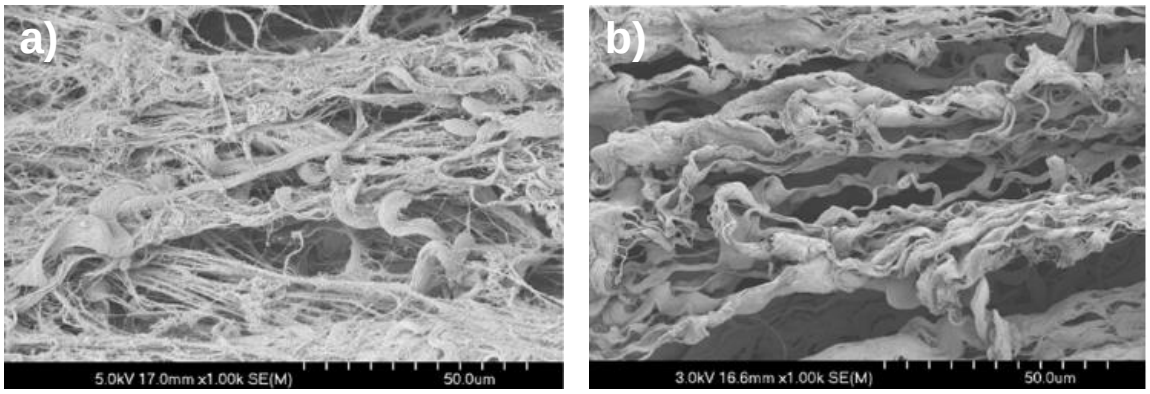

Figure 1.3. Scanning electron microscopy (1000 × magnification) of the SSCT close to tendon in the carpal tunnel. (a) Healthy. (b) CTS. From Ettema et al. (2006a).

1.6. Tendon Friction

Armstrong and Chaffin (1979) characterized the distribution of tendon force on adjacent carpal tunnel structures using a belt-pulley mechanism, which likens a tendon over a curved surface, such as the transverse carpal ligament in wrist flexion, to a belt around a pulley. Contact stress, normal force per unit arc length (f_l), is related to the belt tension (f_t), coefficient of friction (μ), the angle the belt wraps around the pulley (θ), and the radius of curvature (ρ), as described in Equation 1.1.

$$f_l = f_t e^{\theta\mu} / \rho \quad (1.1)$$

The belt-pulley model demonstrates that decreasing the radius of curvature increases the contact stress, thus providing a rational for higher CTS prevalence in female workers compared to male workers (Zakaria, 2004). Keir and Wells (1999) determined the radius of tendon curvature decreased with tendon force and wrist flexion angle,

thereby increasing normal stress on the median nerve in addition to the independent effects of tendon force and wrist angle in the belt-pulley model. The well-established belt-pulley mechanism also provides the conceptual basis to calculate tendon friction inside the carpal tunnel (Moore et al., 1991; Tanaka and McGlothlin, 1993). Moore et al. (1991) quantified tendon displacement and friction using the belt-pulley mechanism, and found that frictional work was a strong predictor of wrist/hand musculoskeletal disorders, including CTS.

An et al. (1993) developed an experimental method to determine friction between the FDP tendon and A2 annular pulley (*in vitro*). FDP force was measured proximal (f_p) and distal (f_d) to the A2 pulley to calculate friction ($f_p - f_d$). Using this paradigm, friction in 9 cadaver index fingers ranged from 0.021 to 0.031 N with a load of 4.9 N (Uchiyama et al., 1995). Using the belt-pulley model, the coefficient of friction was estimated to be 0.022 – 0.063, higher than the coefficient of friction for diarthrodial joints (An, 2007).

Flexor tendon gliding resistance was recently measured in the cadaveric carpal tunnel (Filius et al., 2014; Zhao et al., 2007). Zhao et al. (2007) found that tendon gliding resistance increased exponentially with tendon displacement, presumably due to the strain-dependent characteristics of the viscoelastic SSCT. Gliding resistance also increased with wrist flexion angle and with single-digit versus multi-digit movement. However, the low tendon force (2 N) most likely minimized contact stress with adjacent anatomical structures while the slow velocity (2 mm/sec) diminished viscoelastic gliding resistance of the SSCT. There remains a need to quantify tendon gliding characteristics representative of repetitive and forceful work to better understand the interplay between

contact shear with other anatomical structures and tenosynovial resistance on overall friction in the carpal tunnel.

1.7. Tendon and SSCT Displacement

Pioneering work by Landsmeer (1961) lead to the development of three geometric models that describe joint-tendon interaction (Figure 1.4). Landsmeer's (1961) first model describes a tendon that follows the articular surface of the bone; therefore the radius of curvature is equal to the moment arm (Equation 1.2). The second model constrains the tendon to a single point so that there is an infinite radius of curvature at the joint (Equation 1.3). In the third model, the tendon is able to bowstring from the finger bones, and follows an arc of constant radius between the straight portions of the tendon (Equation 1.4).

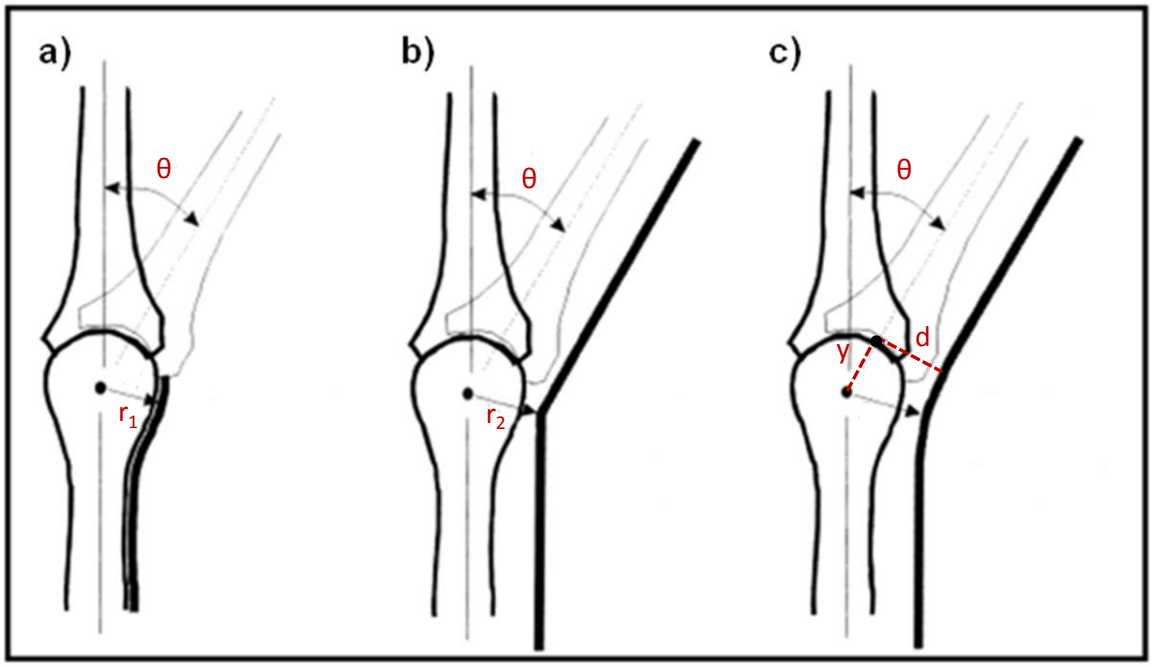

Figure 1.4. Landsmeer's (1961) geometric models of joint-tendon interaction. a) In model I, the tendon is on the curve of the proximal bone articular surface. b) In model II, the tendon is tethered at a single point so there is an infinite radius of curvature. c) In model III, the tendon is curved with an annular pulley enabling bowstringing. From Keir and Wells (1999).

$$x = r_1\theta \quad (1.2)$$

x = tendon displacement (m)
r_1 = distance from joint centre to tendon (m)
θ = joint rotation (rad)

$$x = 2r_2 sin(\theta/2) \quad (1.3)$$

x = tendon displacement (m)
r_2 = distance from joint centre to geometric tendon constraint (m)
θ = joint rotation (rad)

$$x = 2y + \theta d - \theta y/tan(\theta/2) \quad (1.4)$$

x = tendon displacement (m)
y = distance from joint centre to end of curved tendon along bone (m)
d = distance from the bone midline to end of curved tendon (m)
θ = joint rotation (rad)

Several researchers have quantified finger flexor tendon displacements *in vitro* (An et al., 1983; Armstrong and Chaffin, 1978; Brand et al., 1975; Horii et al., 1992; Franko et al., 2011; Yamaguchi et al., 2008). Armstrong and Chaffin (1978) measured FDP and FDS tendon displacements in 4 upper limb cadavers with a displacement micrometer while simultaneously photographing wrist and finger postures. Landsmeer's (1961) first model best fit their data using least squared error regression. Linear regression equations were then developed to calculate tendon displacements based on wrist and finger joint flexion angles as well as the thickness of the finger joints to account for anthropometry (Equations 1.5 and 1.6).

$$te_w = 0.0263x_1 + 0.005x_1x_2 + 0.106x_1x_3 - 0.000960x_1x_2x_4 \quad (1.5)$$

te_w = wrist tendon displacement (mm)
x_1 = wrist angle (°)
x_2 = wrist thickness (mm)
x_3 = 0 for extension; 1 for flexion
x_4 = 0 for FDS; 1 for FDP

$$te_f = 0.103x_5 + 0.00421x_4x_5 - 0.0162x_3x_5 - 0.0304x_1x_5 - 0.0682x_2x_5 + 0.0368x_1x_3x_5 \quad (1.6)$$

te_f = finger tendon excursion (mm)
x_1 = 1 for PIP (0 for other joints)
x_2 = 1 for the DIP (0 for other joints)
x_3 = 0 for FDS; 1 for FDP
x_4 = finger joint thickness (mm)
x_5 = finger joint angle (°)

These well-established regressions have been used to calculate tendon travel associated repetitive wrist and finger motions and to evaluate workplace interventions (Moore et al., 1991; Nelson et al., 2000; Treaster and Marras, 2000; Ugbolue and Nicol,

2012, 2014). For example, Treaster and Marras (2000) used FDP and FDS tendon travel to determine the biomechanical consequences of alternative keyboard features, and found that tendon travel increased with keyboard pitch angle. While tendon travel is most likely related to tendon friction, relative displacement between adjacent carpal tunnel structures (e.g. tendon and median nerve) or alternatively tendon and SSCT may be better suited to predict work-related wrist/hand musculoskeletal disorders, including CTS. The latter approach may prove fruitful since a large portion of tendon gliding resistance is related to the viscoelastic SSCT (Zhao et al., 2007).

Researchers are utilizing ultrasound more frequently in recent years to assess tendon dynamics in the carpal tunnel (Ettema et al., 2006b; Korstanje et al., 2010a; Lopes et al., 2011; Oh et al., 2007; Peolsson et al., 2010; van Doesburg et al., 2012; Yoshii et al., 2009a). Due to advances in image resolution, current methods enable simultaneous assessment of the finger flexor tendons and the adjacent SSCT. Doppler ultrasound transmits a series of pulses (the pulse train), which is returned with a time lag dependent on the tissue velocity. The coinciding Doppler frequency (f_d) is the basis of all Doppler methods (Equation 1.7):

$$f_d = (2 \cdot v \cdot f_t \cdot \cos\theta) / c, \quad (1.7)$$

where v is velocity of scatter (relative to transmitter), f_t is the transmitted frequency, θ is angle of insonation (between scatter and beam), and c the speed of sound in tissue. Colour Doppler imaging (CDI) uses autocorrelation to determine the Doppler

shift (Kukulski et al., 2003), and enables simultaneous assessment of the tendon and adjacent SSCT (Cigali et al., 1996; Oh et al., 2007; Tat et al., 2013, 2015). Tat et al. (2015) recently validated CDI in 8 cadaveric upper limbs, and found relative motion between FDS tendon and SSCT increased with tendon velocities between 50 – 150 mm/sec. Using fluoroscopy, relative displacement in the cadaveric carpal tunnel was found to be influenced by several occupational risk factors, including wrist posture (Yoshii et al., 2008), single-finger movement (Yoshii et al., 2009b), and speed of work (Yoshii et al., 2011).

However, ultrasound technology enables *in vivo* assessment of relative displacement between tendon and SSCT, which may better preserve anatomic fidelity of the tendon gliding system, including the viscoelastic properties of the SSCT. Furthermore, elucidating the relationship between finger angle and relative displacement in cadaveric specimens may be difficult since the tendons are excised from their attachment sites. Lopes et al. (2011) also found that *in vivo* FDS displacements deviated from traditional cadaver-based models of tendon-joint interaction, while FDP displacements were shown to differ between passive versus active finger mobilization (Korstanje et al., 2010b, 2012).

There is a need to assess *in vivo* flexor tendon and SSCT displacement as a function of finger joint angle, thus providing the basis for an ergonomic tool to predict relative displacement during work. There is also a need to account for biomechanical work factors while performing repetitive finger motions, which may lead to improved prediction of wrist/hand disorders, including work-related CTS. Furthermore, there is a

need to understand how ultrasound measures of relative motion between tendon and the SSCT, often equated to "shear-strain", relate to frictional loss inside the carpal tunnel.

1.8. Thesis Objectives

The purpose of this thesis was to determine the relationship between biomechanical risk factors and tendon motion and shear in the carpal tunnel, moving towards mechanistic-based ergonomics for the wrist and hand. I used a cadaveric model to directly measure friction during proximal and distal tendon displacements as well as *in vivo* ultrasound assessment of relative displacement between tendon and subsynovial connective tissue to infer shear potential. The individual studies that comprise this thesis as well as the connections between the studies are shown schematically in Figure 1.5. Specifically, the study objectives were to:

1) Quantify flexor tendon gliding characteristics in the cadaveric carpal tunnel and to determine the relationship between physical exposures, including wrist and finger posture as well as tendon velocity and force, on flexor tendon gliding resistance and frictional work (Chapter 2);
2) Revisit traditional models of tendon-joint interaction and develop a similar model for the adjacent SSCT in healthy participants using ultrasound, and to demonstrate the potential utility of the models as an ergonomic method that predicts relative displacement between tendon and SSCT (Chapter 3);
3) Evaluate the effects of finger motion and wrist posture on ultrasound assessment of relative displacement between FDS tendon and SSCT in healthy participants (Chapter 4);

4) Investigate two well-known occupational risk factors, frequency and force of work, on relative displacement between FDS and SSCT using colour flow imaging (Chapter 5);

5) Compare relative displacement derived from *in vivo* ultrasound assessment in Chapters 3 − 5 with an analytical model of tendon gliding resistance based on cadaveric measurement in Chapter 2, and determine their suitability as an ergonomic tool as well as implications for work-related wrist/hand musculoskeletal disorders, including CTS (Chapters 5 and 6).

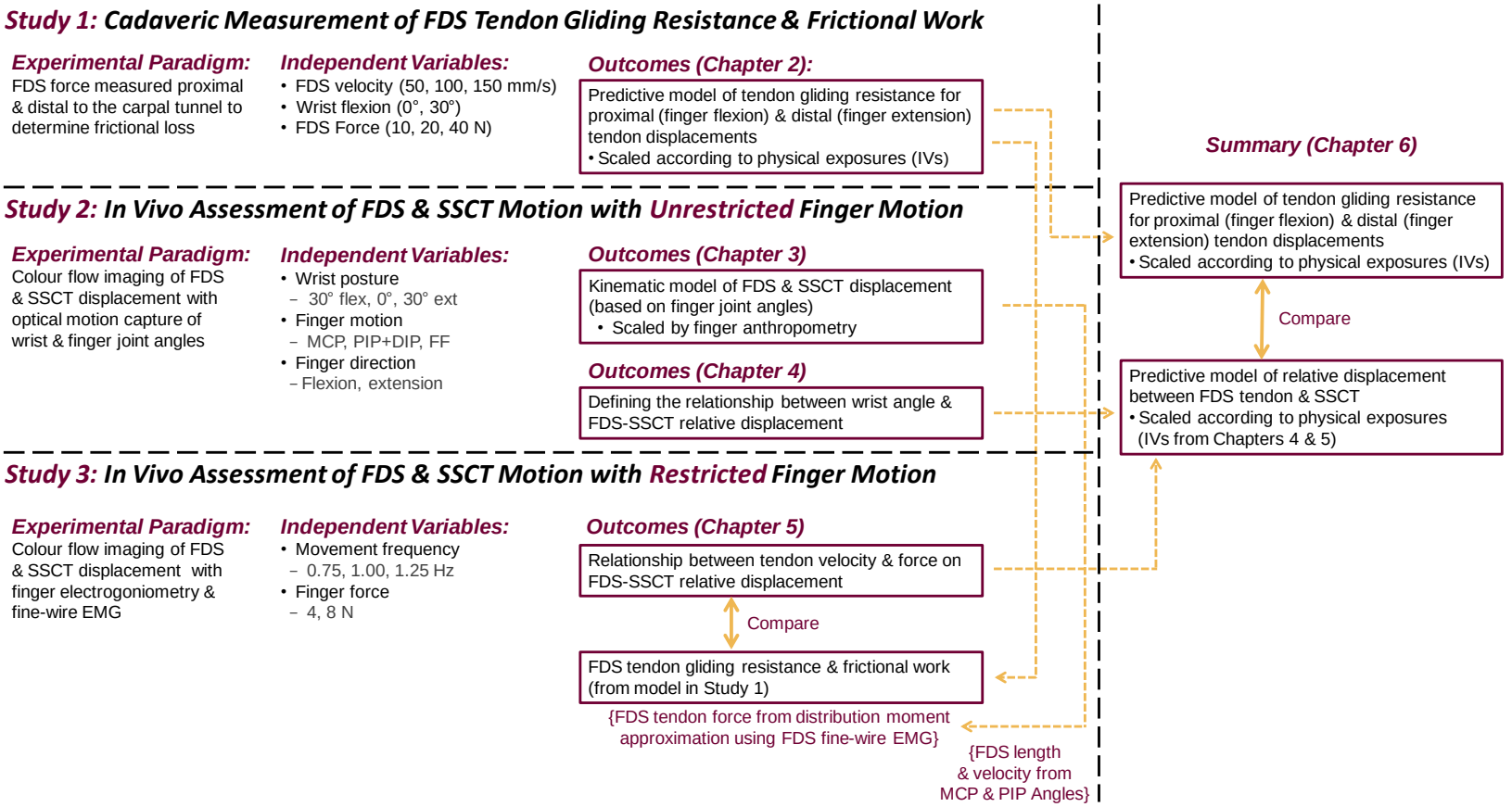

Figure 1.5. Flow diagram of the thesis with arrows indicating connections between the different studies and summary chapter.

CHAPTER TWO

Biomechanical Risk Factors and Flexor Tendon Frictional Work in the Cadaveric Carpal Tunnel

Aaron M. Kociolek, Jimmy Tat, Peter J. Keir

Department of Kinesiology, McMaster University, Hamilton, Ontario, Canada

Kociolek, A.M., Tat, J., Keir, P.J., 2015. Biomechanical risk factors and flexor tendon frictional work in the cadaveric carpal tunnel. Journal of Biomechanics 48 (3), 449−455. http://dx.doi.org/10.1016/j.jbiomech.2014.12.029

2.1 Abstract

Pathological changes in carpal tunnel syndrome patients include fibrosis and thickening of the subsynovial connective tissue (SSCT) adjacent to the flexor tendons in the carpal tunnel. These clinical findings suggest an etiology of excessive shear strain force between the tendon and SSCT, underscoring the need to assess tendon gliding characteristics representative of repetitive and forceful work. A mechanical actuator moved the middle finger flexor digitorum superficialis tendon proximally and distally in eight fresh frozen cadaver arms. Eighteen experimental conditions tested the effects of three well-established biomechanical predictors of injury, including a combination of two wrist postures (0° and 30° flexion), three tendon velocities (50, 100, 150 mm/sec), and three forces (10, 20, 40 N). Tendon gliding resistance was determined with two light-weight load cells, and integrated over tendon displacement to represent tendon frictional work. During proximal tendon displacement, frictional work increased with tendon velocity (58.0% from 50 – 150 mm/sec). There was a significant interaction between wrist posture and tendon force. In wrist flexion, frictional work increased 93.0% between tendon forces of 10 and 40 N. In the neutral wrist posture, frictional work only increased 33.5% (from 10 – 40 N). During distal tendon displacement, there was a similar multiplicative interaction on tendon frictional work. Concurrent exposure to multiple biomechanical work factors markedly increased tendon frictional work, thus providing a plausible link to the pathogenesis of work-related carpal tunnel syndrome. Additionally, our study provides the conceptual basis to evaluate injury risk, including the multiplicative repercussions of combined physical exposures.

Keywords: carpal tunnel; tendon; subsynovial connective tissue; gliding resistance; viscoelastic.

2.2. Introduction

Carpal tunnel syndrome (CTS) is a peripheral entrapment neuropathy due to compression of the median nerve at the wrist. While the etiology of CTS is multi-factorial (Staal et al., 2007), common histopathologic changes include fibrosis and thickening of the subsynovial connective tissue (SSCT) surrounding the flexor tendons in the carpal tunnel (Barr et al., 2004; Ettema et al., 2006; Jinrok et al., 2004). The SSCT loosely attaches the flexor tendons to the visceral synovium, and is comprised of collagen bundles that form adjacent layers interconnected by small perpendicular fibrils. During flexor tendon displacement, the SSCT is strained, with deep layers close to tendon moving before superficial layers near the visceral synovium (Guimberteau et al., 2010). Repetitive tendon motion is thought to promote shear damage at the tendon-SSCT interface, which is supported by the finding that fibrosis is exacerbated in SSCT layers adjacent to flexor tendon (Ettema et al., 2006; Schuind et al., 1990).

Moore et al. (1991) used twelve biomechanical measures to model tissue loads in the wrist/hand and found that flexor tendon frictional work was the best predictor of injury. Tanaka and McGlothlin (1993) also developed a heuristic model of the wrist using frictional energy to predict work-related CTS. Both of these methods utilized the well-established belt-pulley model that likens a tendon gliding over a curved surface, such as the transverse carpal ligament in wrist flexion, to a belt around a pulley (Armstrong and Chaffin, 1979). Keir and Wells (1999) determined the radius of tendon

curvature in the carpal tunnel decreased with both wrist flexion angle and tendon force magnitude thereby increasing normal stress on the median nerve in addition to the effect of tendon tension on contact stress.

More recently, flexor tendon gliding resistance was experimentally measured (*in vitro*) within the carpal tunnel (Filius et al., 2014; Zhao et al., 2007). Zhao et al. (2007) found that tendon gliding resistance increased exponentially with tendon displacement, primarily due to the viscoelastic SSCT. The researchers also quantified the effect of wrist flexion angle on tendon gliding resistance; however, the slow test velocity of 2 mm/sec likely diminished viscoelastic shear strain. There remains a need to quantify tendon gliding characteristics representative of repetitive and forceful work to better understand the interplay between contact shear with other anatomical structures and tenosynovial resistance on overall friction in the carpal tunnel.

The purpose of this study was to quantify flexor tendon gliding resistance and frictional work in two wrist postures (0° and 30° flexion), three tendon velocities (50 mm/sec, 100 mm/sec, 150 mm/sec), and three tendon forces (10 N, 20 N, 40 N). We hypothesized that greater physical exposure, including higher tendon velocity and force, would increase flexor tendon frictional work, especially with wrist flexion.

2.3. Methods

2.3.1. Cadaveric Specimens

Eight unmatched fresh frozen human cadaver upper limbs were amputated at the mid-humerus (age 56.6 ± 15.5 yr, height 178.4 ± 8.8 cm, mass 99.7 ± 26.2 kg). Exclusion

criteria included a known history of wrist tendinopathy, peripheral nerve disease, and CTS. This study was approved by the Hamilton Integrated Research Ethics Board.

Specimens were thawed at 5°C for approximately 12 hours prior to dissection. The flexor digitorum profundus (FDP) and flexor digitorum superficialis (FDS) tendons were exposed on both proximal and distal sides of the transverse carpal ligament. Passive finger flexion/extension movements were used to identify all four tendons of FDP and FDS. The flexor pollicis longus (FPL) tendon and median nerve were also identified. The finger and thumb flexor tendons and median nerve were excised from the proximal and distal attachments. The carpal tunnel was left undisturbed and the mid-humeral amputation ensured that the ulna and radius remained intact to preserve anatomic fidelity of the wrist complex.

2.3.2. Testing Apparatus

Upper limb specimens were secured to the testing apparatus at the proximal forearm with an adjustable clamp as well as the distal forearm (proximal to the wrist crease), hand (3^{rd} metacarpal), and middle finger (3^{rd} distal phalanx) with plastic fasteners (Figure 2.1). The testing apparatus was hinged at the wrist to change the joint angle in the experiment. The middle finger FDS tendon was attached proximally to a cable, connected to a linear actuator (ERC3, IAI America Inc., Torrance, CA) through a series of mechanical pulleys. Distally, the tendon was fixed to a cable that curved around a pulley and attached to a constant force spring (N-series, Vulcan Spring Co, Telford, PA). Both sides of the tendon were attached directly to cable ends with 6 mm aluminum crimping sleeves. Two light-weight load cells (LCM-200, Futek Inc., Irvine, CA) were connected in series with the

tendon proximal and distal to the carpal tunnel. A pulley on the proximal side of the carpal tunnel was also instrumented with a rotary potentiometer (6370 Series, State Electronics Corp., East Hanover, NJ) to calculate displacement of the tendon via the linear actuator.

The proximal ends of the remaining finger flexor tendons (3 FDS and 4 FDP) were connected to an adjustable plate on the testing apparatus. Distally, the tendons were fixed to extension springs to maintain a tension of 250 g. The extension springs connected to another adjustable plate to preserve the tendon lines of action through the carpal tunnel. Since the FPL was only exposed and excised from the origin site, the tendon was fixed to an extension spring on the proximal side of the carpal tunnel while the thumb was secured to the testing apparatus. The distal median nerve branches throughout the hand; thus, tension was provided with an extension spring on the proximal side of the testing apparatus.

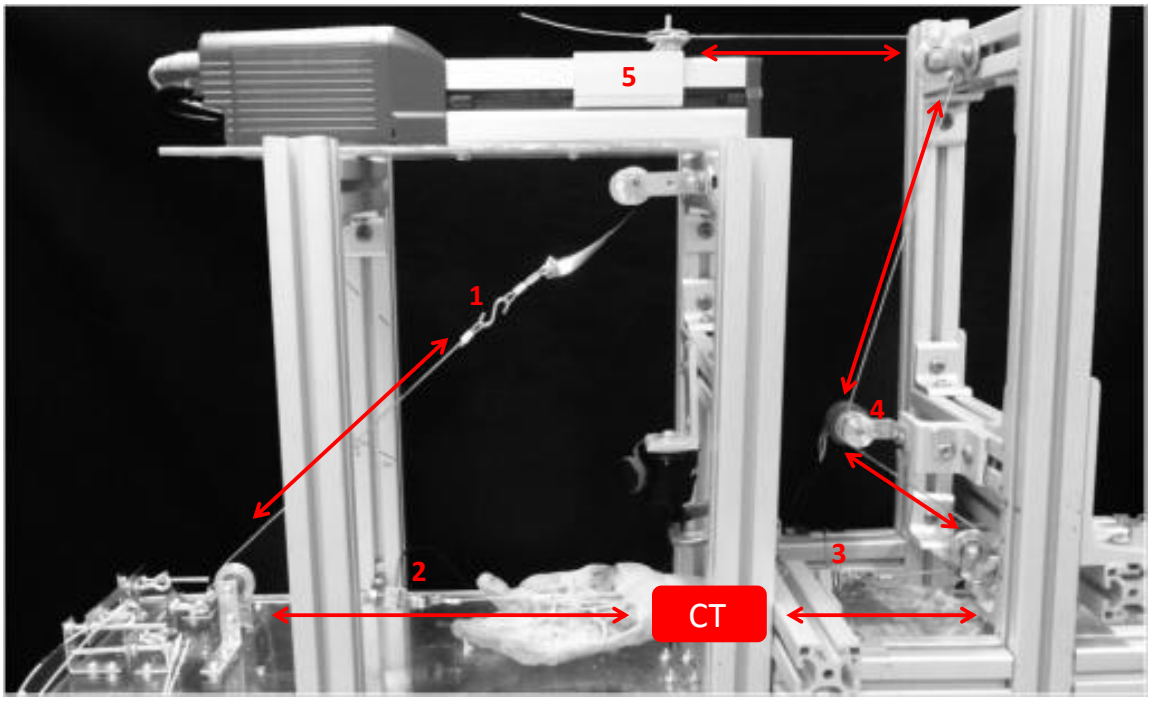

Figure 2.1. A cadaver specimen in the testing apparatus. Gliding characteristics of the middle finger FDS tendon were evaluated as a motor moved the tendon proximally (finger flexion) and distally (finger extension). The apparatus includes the (1) constant force spring, (2) distal load cell, (3) proximal load cell, (4) rotary potentiometer, and (5) linear actuator. Note: the remaining flexor tendons and median nerve are not yet connected so that all the components of the apparatus are clearly visible.

2.3.3. Experimental Protocol

FDS tendon displacements of the middle finger were produced with the linear actuator. The motor was programmed to move 30 mm proximally and distally to represent tendon displacements for full finger flexion and extension, respectively (Kociolek and Keir, 2013). Each specimen was preconditioned with twenty-four continuous tendon displacement cycles (velocity 50 mm/sec; force 10 N). Tendon displacements were tested in eighteen conditions using combinations of two wrist postures (0° and 30° flexion), three tendon velocities (50, 100, 150 mm/sec), and three tendon forces supplied by constant force springs (~ 10, 20, 40 N). While the springs produce constant force with greater deflections, we anticipated different magnitudes for proximal versus distal tendon displacements, due to friction of the mounting axle (William et al., 2013). Spring forces were 25.4% lower for distal deflections compared to proximal deflections (Table 2.1). *Note: from herein we will refer to the tendon forces based on the spring specifications for ease of reading (10, 20, 40 N).*

Four proximal-distal tendon displacement cycles were tested in each experimental condition, for a total of seventy-two cycles (18 conditions × 4 cycles/condition). A balanced design mitigated order effects for wrist posture (i.e. four cadavers started in the neutral posture, four cadavers started in the flexed posture). Tendon force was randomized for each wrist posture, and tendon velocity was block randomized within each force level. The specimens were lightly sprayed with saline solution before starting each wrist posture block. While this represents minimal spraying, the potential for confounded results due to changes in lubrication were minimized (Uchiyama et al., 1997).

Tendon velocities and forces in this study were similar to previous *in vivo* studies. Tendons have been shown to reach velocities up to 150 mm/sec during full finger flexion (Tat et al., 2013). Unrestricted dynamic finger tapping produces tendon force between 8 – 17 N, with higher magnitudes during forceful exertions (Dennerlein, 2005). The impact of wrist posture on tendon friction is well-established (Armstrong and Chaffin, 1979; Tanaka and McGlothin, 1993; Zhao et al., 2007). Representing wrist flexion *in vitro* required meticulous care since the tendons were detached on both sides of the carpal tunnel. During wrist flexion trials, the flexor tendons were displaced 10 mm in the proximal direction to represent the position of the tendon for an intact musculotendon unit (Armstrong and Chaffin, 1978).

Table 2.1. Mean (± standard error of mean) distal tendon force measurements from the constant force springs during proximal and distal tendon displacements.

Manufactured Rating (N)	Prox Disp (N)	Dist Disp (N)
10 N	9.52 ± 0.12	6.39 ± 0.11
20 N	21.93 ± 0.28	16.00 ± 0.20
40 N	39.12 ± 0.62	30.24 ± 0.37

* 10 N, 20 N, and 40 N – Expected force magnitude of the constant force springs from manufacturer specifications.

2.3.4. Data Collection and Analysis

Middle finger FDS tendon forces and displacements were collected at 120 Hz (LabView 8.5, National Instruments Corp., Austin, TX). Load cell and potentiometer data were smoothed with a dual second-order low pass Butterworth filter (f_c = 6 Hz). Tendon gliding resistance was defined as the difference between proximal and distal tendon forces ($F_p - F_d$). Positive gliding resistance represented resistance to proximal tendon displacement while negative gliding resistance represented resistance to distal tendon displacement. Tendon frictional work was calculated by integrating tendon gliding resistance over tendon displacement in both the proximal and distal displacement phase of each cycle.

2.3.5. Statistical Analysis

Due to acceleration and deceleration of the motor, the first 5 mm and last 5 mm of proximal tendon displacement was removed to ensure constant velocity. Thus, we determined tendon gliding resistance for 20 mm of displacement (5 – 25 mm). A smaller displacement interval was used for return distal tendon displacement, since a positive artifact persisted for the first 5 – 10 mm of distal tendon displacement (Figure 2.2). Thus, tendon gliding resistance was determined for a displacement range of 15 mm (10 – 25 mm). This interval ensured only gliding resistance was included for analysis during return distal tendon displacement. FDS tendon gliding resistance was fit with an exponential curve during proximal tendon displacement and a logarithmic curve during distal tendon displacement, based on pilot work of seven specimens and confirmed in a previous study (Zhao et al., 2007). Extensive pilot work also determined that tendon

frictional work increased exponentially with proximal tendon displacement and linearly with distal tendon displacement, and were also characterized with least-squares curve fits.

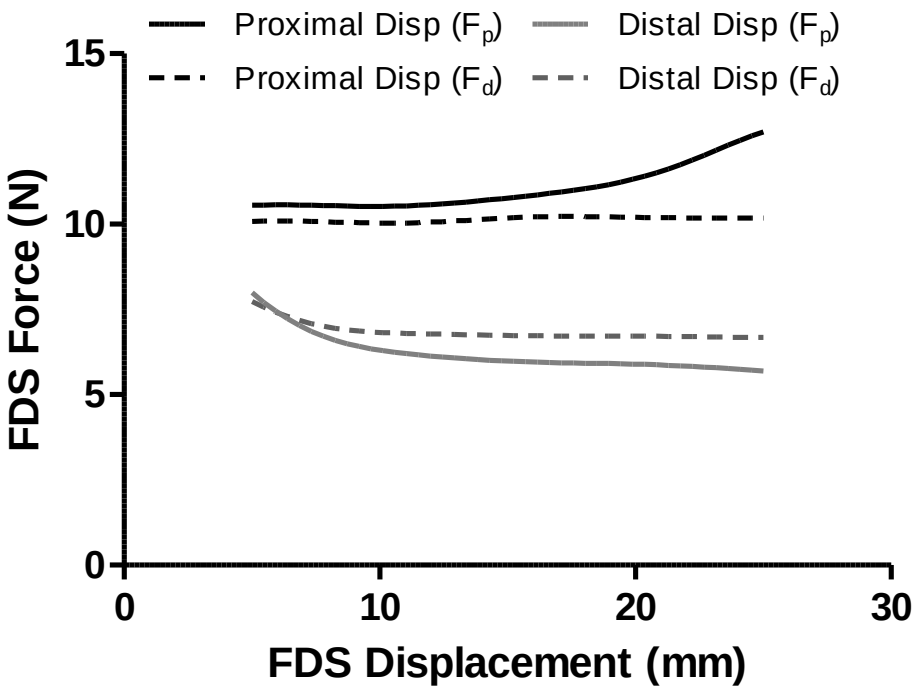

Figure 2.2. FDS tendon forces recorded during proximal tendon displacement (black lines) and distal tendon displacement (grey lines) for one cycle. The difference between the proximal tendon force (F_p) and distal tendon force (F_d) represent tendon gliding resistance. During proximal tendon displacement, the proximal force is greater than the distal force ($F_p > F_d$). During distal tendon displacement, the distal force is greater than the proximal force ($F_d > F_p$). Note that the proximal tendon force is greater than the distal tendon force near the beginning of distal tendon displacement (~ 5 – 10 mm), which was excluded from analysis since this is not representative of tendon gliding resistance.

Three-way repeated measures analysis of variance statistical models were used to test the effects of wrist posture (0°, 30° flexion), tendon velocity (50, 100, 150 mm/sec), and tendon force (10, 20, 40 N) on tendon frictional work over the reduced range of tendon motion. Proximal and distal tendon displacements were tested in separate analyses since different intervals were considered in each movement phase (20 mm for proximal tendon displacement and 15 mm for distal tendon displacement) and different force levels were exhibited by the constant force springs (Table 2.1). Significant main effects and interactions were followed up (post-hoc) with Tukey's HSD ($\alpha = 0.05$).

2.4. Results

Tendon gliding resistance for all eighteen experimental conditions is provided in Table 2.2 (proximal tendon displacement) and Table 2.3 (distal tendon displacement). FDS tendon gliding resistance increased exponentially throughout proximal tendon displacement (Figure 2.3). An exponential model accounted for 97.6 ± 0.8% of the total variance in gliding resistance versus proximal displacement over all eighteen experimental conditions. For distal tendon displacement, a logarithmic relationship explained 90.7 % ± 2.1 % of the total variance in tendon gliding resistance (Figure 2.3).

Table 2.2. Mean (± standard error of mean) flexor tendon gliding resistance (in N) during proximal tendon displacement (simulated finger flexion).

	5 mm	10 mm	15 mm	20 mm	25 mm
Neutral Wrist (0°)					
10 N					
50 mm/sec	0.43 ± 0.13	0.63 ± 0.18	0.81 ± 0.21	1.20 ± 0.27	2.68 ± 0.65
100 mm/sec	0.52 ± 0.13	0.77 ± 0.21	1.07 ± 0.25	1.81 ± 0.32	3.33 ± 0.74
150 mm/sec	0.53 ± 0.13	0.92 ± 0.20	1.49 ± 0.25	2.40 ± 0.41	3.65 ± 0.79
20 N					
50 mm/sec	0.55 ± 0.19	0.75 ± 0.25	0.95 ± 0.28	1.38 ± 0.32	3.24 ± 0.89
100 mm/sec	0.66 ± 0.19	0.89 ± 0.28	1.20 ± 0.32	2.09 ± 0.41	4.04 ± 0.98
150 mm/sec	0.64 ± 0.18	1.04 ± 0.25	1.62 ± 0.27	2.66 ± 0.48	4.23 ± 0.95
40 N					
50 mm/sec	0.60 ± 0.22	0.82 ± 0.32	1.05 ± 0.37	1.59 ± 0.42	3.79 ± 0.95
100 mm/sec	0.73 ± 0.22	1.00 ± 0.33	1.37 ± 0.36	2.43 ± 0.42	4.73 ± 0.96
150 mm/sec	0.74 ± 0.21	1.21 ± 0.30	1.89 ± 0.34	3.10 ± 0.50	4.84 ± 0.95
Flexed Wrist (30°)					
10 N					
50 mm/sec	0.38 ± 0.10	0.63 ± 0.15	0.94 ± 0.22	1.49 ± 0.32	3.16 ± 0.64
100 mm/sec	0.46 ± 0.11	0.84 ± 0.19	1.30 ± 0.28	2.23 ± 0.41	3.83 ± 0.72
150 mm/sec	0.51 ± 0.12	1.06 ± 0.22	1.79 ± 0.34	2.90 ± 0.52	4.27 ± 0.79
20 N					
50 mm/sec	0.69 ± 0.18	1.03 ± 0.26	1.42 ± 0.36	2.10 ± 0.47	4.00 ± 0.75
100 mm/sec	0.82 ± 0.19	1.35 ± 0.34	1.91 ± 0.47	2.97 ± 0.59	4.83 ± 0.86
150 mm/sec	0.82 ± 0.20	1.55 ± 0.34	2.43 ± 0.49	3.68 ± 0.66	5.20 ± 0.91
40 N					
50 mm/sec	1.16 ± 0.33	1.66 ± 0.48	2.30 ± 0.65	3.22 ± 0.79	5.11 ± 1.04
100 mm/sec	1.23 ± 0.31	1.96 ± 0.52	2.71 ± 0.67	4.01 ± 0.82	5.89 ± 1.04
150 mm/sec	1.35 ± 0.36	2.34 ± 0.59	3.42 ± 0.76	4.84 ± 0.91	6.49 ± 1.14

* 10 N, 20 N, and 40 N – Magnitude of tendon force (via constant force springs);

** 50 mm/sec, 100 mm/sec, and 150 mm/sec – Magnitude of tendon velocity (from motor).

Table 2.3. Mean (± standard error of mean) flexor tendon gliding resistance (in N) during distal tendon displacement (finger extension).

	10 mm	**15 mm**	**20 mm**	**25 mm**
Neutral Wrist (0°)				
10 N				
50 mm/sec	-0.59 ± 0.16	-0.74 ± 0.19	-0.91 ± 0.24	-1.09 ± 0.27
100 mm/sec	-0.78 ± 0.18	-1.03 ± 0.19	-1.17 ± 0.23	-1.24 ± 0.27
150 mm/sec	-0.76 ± 0.26	-1.20 ± 0.22	-1.37 ± 0.23	-1.38 ± 0.26
20 N				
50 mm/sec	-0.66 ± 0.21	-0.81 ± 0.25	-0.98 ± 0.31	-1.19 ± 0.35
100 mm/sec	-0.84 ± 0.25	-1.18 ± 0.28	-1.30 ± 0.33	-1.37 ± 0.37
150 mm/sec	-0.71 ± 0.31	-1.28 ± 0.24	-1.50 ± 0.26	-1.53 ± 0.32
40 N				
50 mm/sec	-0.82 ± 0.31	-0.97 ± 0.36	-1.11 ± 0.39	-1.31 ± 0.45
100 mm/sec	-0.93 ± 0.32	-1.28 ± 0.35	-1.38 ± 0.39	-1.46 ± 0.43
150 mm/sec	-0.72 ± 0.36	-1.40 ± 0.33	-1.62 ± 0.36	-1.63 ± 0.40
Flexed Wrist (30°)				
10 N				
50 mm/sec	-0.81 ± 0.12	-1.04 ± 0.13	-1.26 ± 0.17	-1.44 ± 0.22
100 mm/sec	-0.98 ± 0.18	-1.38 ± 0.17	-1.58 ± 0.21	-1.67 ± 0.25
150 mm/sec	-0.91 ± 0.16	-1.51 ± 0.18	-1.78 ± 0.22	-1.82 ± 0.25
20 N				
50 mm/sec	-1.14 ± 0.23	-1.44 ± 0.30	-1.73 ± 0.39	-2.07 ± 0.50
100 mm/sec	-1.42 ± 0.32	-1.94 ± 0.39	-2.25 ± 0.49	-2.45 ± 0.58
150 mm/sec	-1.31 ± 0.34	-2.15 ± 0.40	-2.55 ± 0.49	-2.65 ± 0.56
40 N				
50 mm/sec	-1.19 ± 0.60	-1.69 ± 0.63	-2.17 ± 0.73	-2.75 ± 0.86
100 mm/sec	-1.87 ± 0.46	-2.50 ± 0.56	-2.91 ± 0.69	-3.19 ± 0.81
150 mm/sec	-1.76 ± 0.56	-2.75 ± 0.70	-3.24 ± 0.81	-3.38 ± 0.89

* 10 N, 20 N, and 40 N – Magnitude of tendon force (via constant force springs);
** 50 mm/sec, 100 mm/sec, and 150 mm/sec – Tendon velocity (from motor).

Tendon frictional work also increased exponentially versus proximal tendon displacement. An exponential relationship explained 98.6 ± 0.2% of the total variance in proximally directed tendon frictional work over all experimental conditions (Figure 2.4). For proximal tendon displacement, there was a wrist posture × tendon force interaction on frictional work ($F_{2,14}$ = 11.0, p = 0.01). In wrist flexion, tendon frictional work increased 93.0% from a tendon force of 10 N (31.4 ± 6.0 mJ) to 40 N (60.6 ± 13.0 mJ). In the neutral wrist posture, tendon frictional work only increased 33.5% between 10 – 40 N, from 26.6 ± 4.9 mJ to 35.5 ± 7.0 mJ (Figure 2.5). During proximal tendon displacement, tendon frictional work increased with tendon velocity ($F_{2,14}$ = 92.8, p < 0.001). A frictional work increase of 58.0% was found between 50 and 150 mm/sec (Figure 2.5).

A linear relationship accounted for 95.5 ± 0.6% of the total variance in frictional work against distal tendon displacement (Figure 2.4). For distal tendon displacement, there was a three-way wrist posture × tendon velocity × tendon force interaction on frictional work ($F_{4,28}$ = 3.1, p = 0.032). In a neutral wrist posture, tendon force had very little effect on frictional work (Figure 2.6), but frictional work increased with tendon velocity by 29.0% between 50 mm/sec and 100 mm/sec, and 14.5% from 100 mm/s to 150 mm/s (averaged over all three forces). In wrist flexion, tendon frictional work increased with tendon force between 10 – 40 N (Figure 2.6). Frictional work also increased with velocity, more so at higher forces. At 10 N, frictional work increased 26.1% from 50 mm/sec to 100 mm/sec and another 11.6% from 100 mm/sec to 150 mm/sec (total increase of 37.7%). At 40 N, frictional work increased 37.1% from 50

mm/sec to 100 mm/sec and 11.8% from 100 mm/sec to 150 mm/sec (total increase of 48.9%).

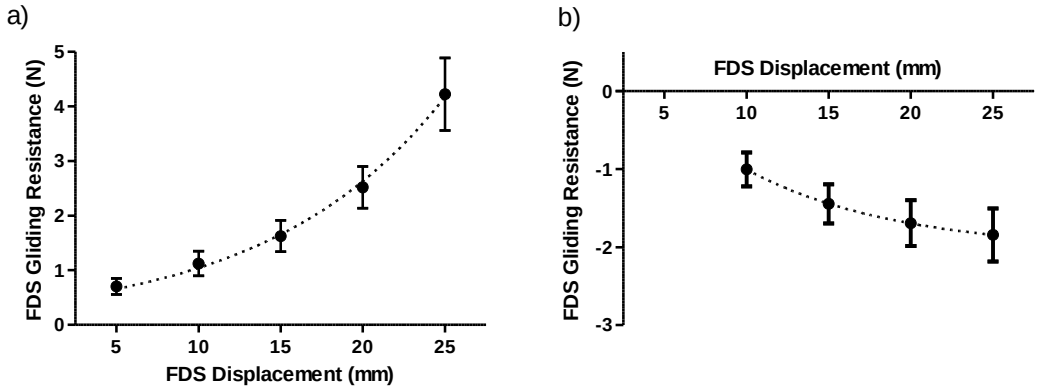

Figure 2.3. FDS gliding resistance versus (a) proximal (simulated finger flexion) and (b) distal (simulated finger extension) tendon displacement.

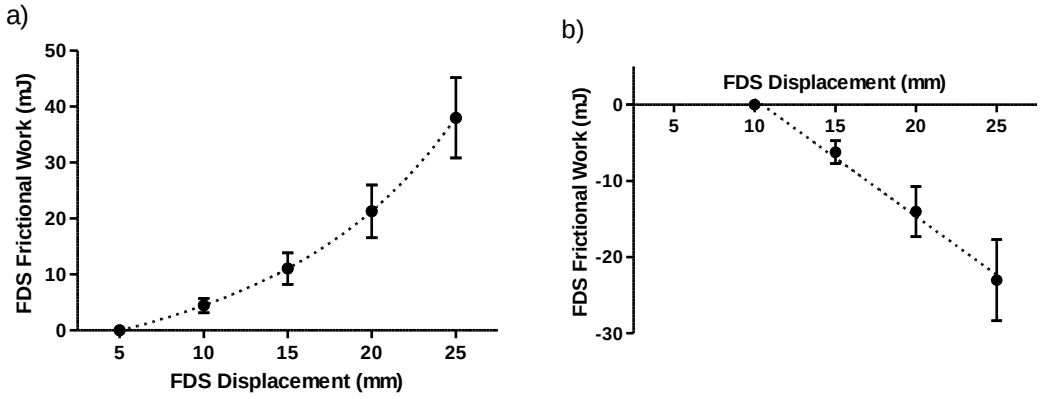

Figure 2.4. FDS frictional work during (a) proximal (simulated finger flexion) and (b) distal (simulated finger extension) tendon displacement.

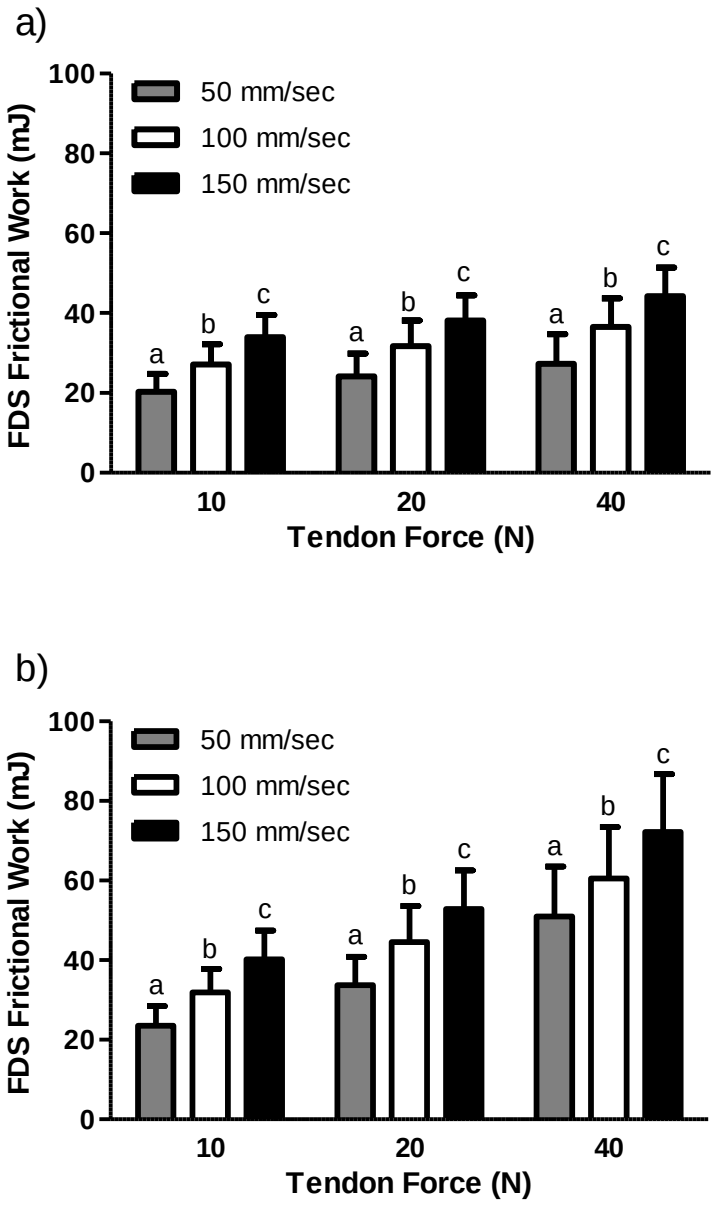

Figure 2.5. Mean (± standard error of the mean) tendon frictional work for proximal tendon displacement in (a) 0° and (b) 30° wrist flexion. Letters indicate significant differences between the three tendon velocities (50, 100, 150 mm/sec) at each force (10, 20, 40 N).

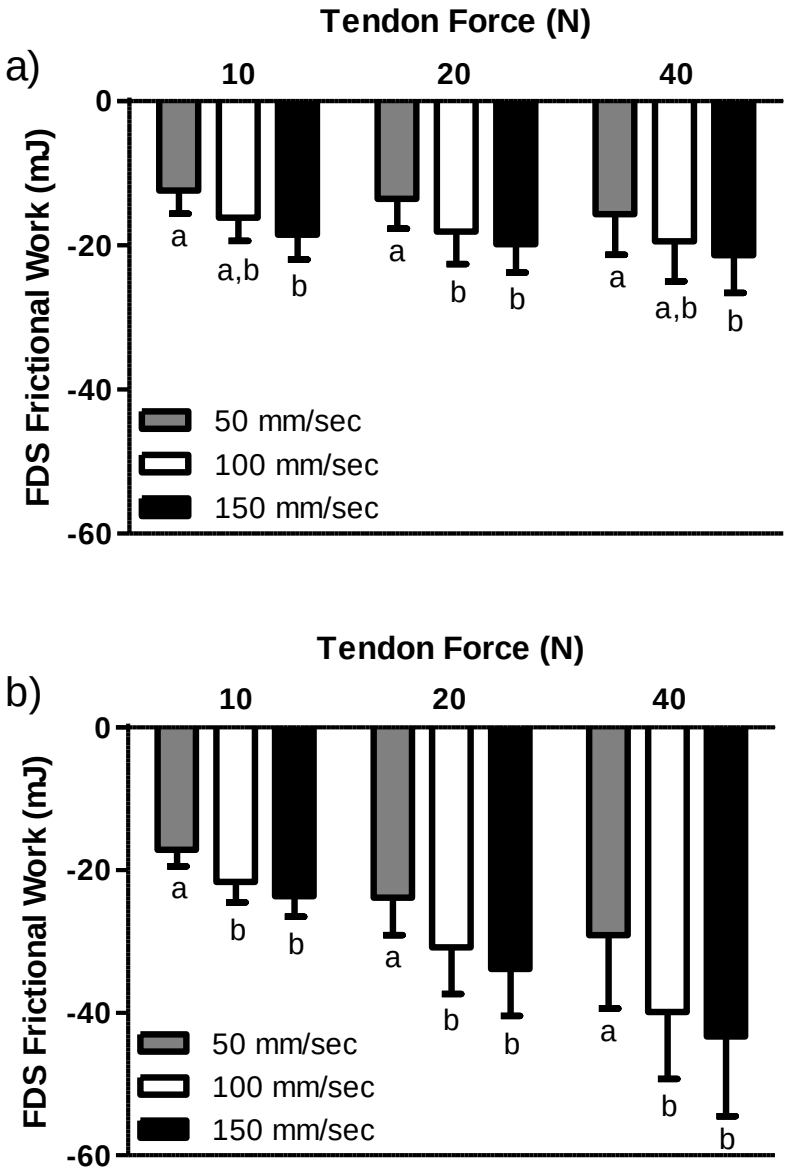

Figure 2.6. Mean (± standard error of the mean) tendon frictional work for distal tendon displacement in (a) 0° and (b) 30° wrist flexion. Letters indicate significant differences between the three tendon velocities (50, 100, 150 mm/sec) at each force (10, 20, 40 N).

2.5. Discussion

We evaluated the combined effects of wrist posture, tendon velocity, and force on tendon frictional work in cadaveric carpal tunnels. Concurrent exposure to several occupational risk factors multiplicatively increased tendon frictional work. During proximal tendon displacement (simulated finger flexion), wrist posture interacted with tendon force, while tendon velocity independently increased frictional work. During distal tendon displacement (simulated finger extension), there was an interaction between wrist posture, tendon velocity, and force, with frictional work being disproportionately greater for high magnitudes of all three biomechanical variables simultaneously. This was the first study to measure tendon gliding characteristics representative of repetitive and forceful work. Furthermore, our experiment included contact shear with adjacent anatomical structures and the viscoelastic SSCT.

Zhao et al. (2007) previously suggested that viscoelastic shear strain was the largest component of tendon gliding resistance, even for a non-physiological tendon velocity of 2 mm/sec and force of 2 N. We manipulated tendon velocity and tendon force in neutral and flexed wrist postures, and found high-order interactions between these three well-established biomechanical variables. Our results also suggest a linkage between contact and viscoelastic sources of friction (tendon velocity × tendon force interaction for distal tendon displacement). Overall, this study connects biomechanical risk factors with underlying mechanics. Our results provide mechanistic support for epidemiological studies, which indicate exposure to multiple physical work factors disproportionately increases injury risk for CTS (Bernard, 1997; Punnett and Wegman, 2004).

To provide context and a better visual, we re-addressed the main findings in a scalable model to calculate FDS tendon gliding resistance (Figure 2.7), which can be integrated to calculate tendon frictional work. A generic curve characterizes tendon gliding resistance as a function of tendon displacement for both proximal tendon displacement (finger flexion) and distal tendon displacement (finger extension). Gliding resistance is modulated by the biomechanical factors in this study (wrist posture, tendon velocity, and force), which were modelled using least squares regression. The model also includes interaction terms to represent the multiplicative effect of combined biomechanical risk factors, typical of observation studies characterizing work-relatedness in CTS. Future research will assess the capability of the model to predict work-related musculoskeletal disorders of the wrist/hand.

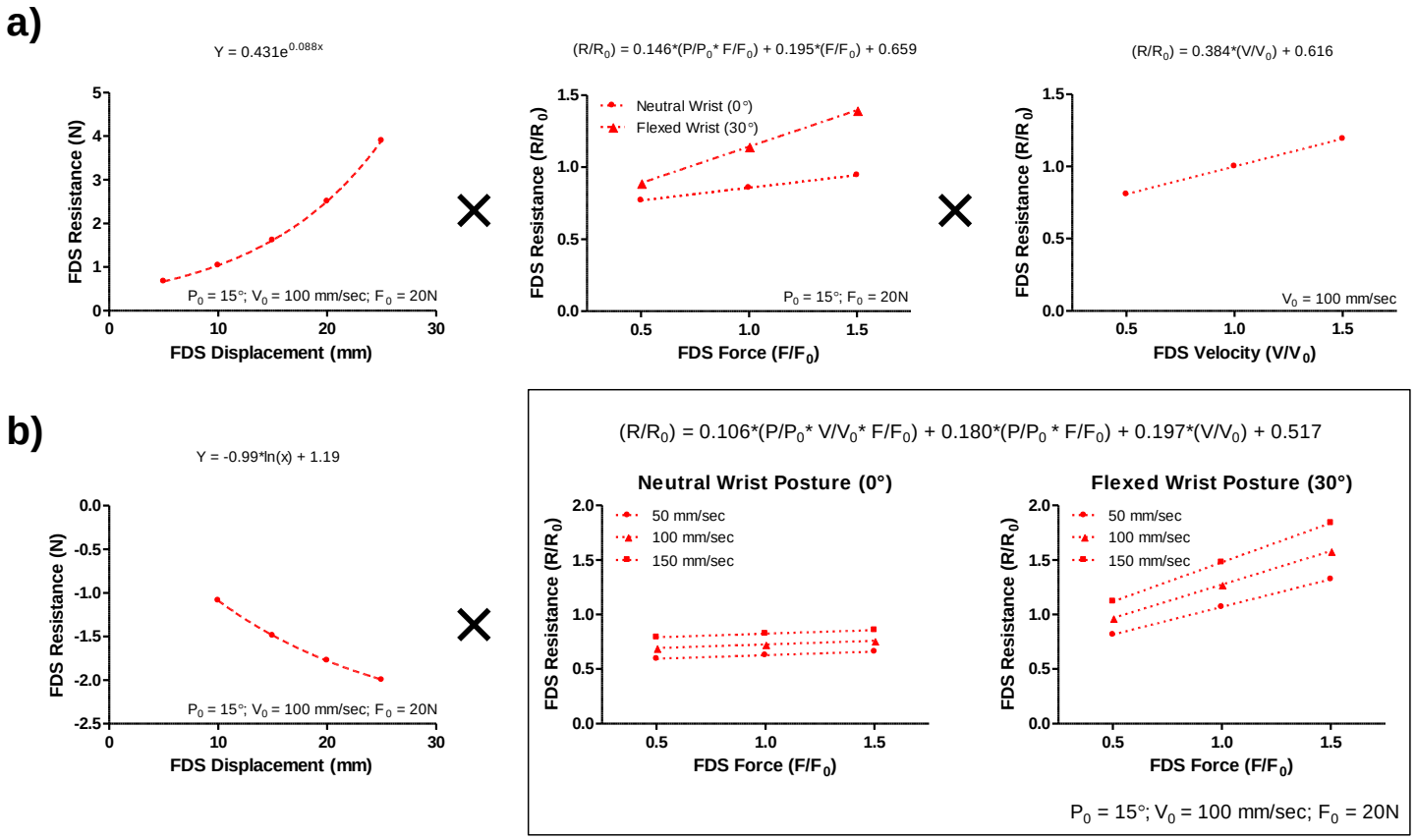

Figure 2.7. Middle finger FDS tendon gliding resistance during (a) proximal tendon displacement (simulated finger flexion) and (b) distal tendon displacement (simulated finger extension). Gliding resistance is calculated with an exponential model for proximal tendon displacement and a logarithmic model for distal tendon displacement. Gliding resistance computations are further scalable based on the biomechanical risk factors tested in this study, including wrist posture, tendon velocity, and force. R/R_0 represents scaling factors to modulate gliding resistance calculations. The model inputs P, V, and F are wrist posture (°), tendon velocity (mm/sec), and tendon force (N), respectively. $P_0 = 15°$; $V_0 = 100$ mm/sec; $F_0 = 20$ N.

Schweizer et al. (2003) indirectly quantified finger flexor tendon friction via the difference between maximum eccentric and concentric muscle contractions. Wrist and finger movements against a high load produced greater estimates than previous studies that directly measured gliding resistance with low loads between the FDS tendon and A2 pulley (An et al., 1992; Uchiyama et al., 1995). In this study, friction in the carpal tunnel was greater with high load, and this effect was magnified in wrist flexion. While friction between the finger flexor tendons and digital pulleys may enable higher fingertip forces than theoretically possible from musculotendon force transmission alone (Schweizer et al., 2009; Vigouroux et al., 2006), the broader mechanical implications of carpal tunnel friction are unknown. Anatomical characteristics of the digital pulley system, including transverse chiasma (or ridges) of FDP tendon and the A2 pulley, are ideally suited for a tendon compression mechanism, thus providing a means to decrease muscular force contributions (Walbeehm and McGrouther, 1995). However, the smaller arc of contact between flexor tendon and the transverse carpal ligament in wrist flexion as well as SSCT viscoelastic strain may limit any mechanical advantage of friction through the carpal tunnel.

Peak tendon gliding resistance in this study was remarkably high relative to the input force of 10 – 40 N, ranging from 2.68 ± 0.65 N to 6.49 ± 1.14 N. During wrist flexion, the finger flexor tendons migrate palmarly, generating friction with the transverse carpal ligament (Keir and Wells, 1999). Lee and Kamper (2009) demonstrated the importance of digital pulleys and passive joint characteristics on spatial coordination of finger joint kinematics in a biomechanical model of the musculoskeletal system. Tendon

resistance in the carpal tunnel, including both synovial and extrasynovial friction, represents another important consideration in musculoskeletal models used to investigate motor control, injury mechanisms, surgical procedures, and rehabilitation protocols (Holzbaur et al., 2005; Sancho-Bru et al., 2001; Wu et al., 2008; Valero-Cuevas, 2005).

Using a similar setup, Zhao et al. (2007) found that peak tendon gliding resistance increased from 1.15 N to 1.85 N from 0° to 30° wrist flexion. We obtained higher peak gliding resistance with 3.84 ± 0.85 N (0°) to 4.75 ± 0.85 N (30° wrist flexion). While both studies found similar trends, magnitude differences were anticipated due to the specific test conditions in each experiment, including higher tendon velocities (50 mm/sec – 150 mm/sec) and forces (10 N – 40 N) in the current study to replicate *in vivo* conditions (Dennerlein, 2005; Tat et al., 2013). Smutz et al. (1994) showed that friction increased over time using a high-repetition, low-force cadaveric model; however, their *in vivo* protocol with rhesus monkeys found no histological evidence of inflammation or fibrosis. Together these results further highlight the importance of multiple biomechanical risk factors on finger flexor tendon gliding resistance and frictional work.

In the current study, the relationship between tendon force and tendon frictional work was dependent on wrist posture during proximal tendon displacement. Changing tendon force from 10 N to 40 N increased tendon frictional work by 33.5% and 93.0% in the neutral (0°) and flexed (30°) wrist postures, respectively. Keir and Wells (1999) showed the radius of flexor tendon curvature decreased with wrist flexion and tendon force, and thus increased contact stress on surrounding structures, including the median nerve. Representing these geometrical changes in the belt-pulley wrist model

qualitatively match the posture by force interaction observed in our study. FDS tendon velocity also influenced frictional work during finger flexion, presumably due to viscoelastic strain in adjacent layers of the SSCT (Osamura et al., 2007). While strain rate in viscoelastic tissue is by definition velocity dependent, gliding resistance between two adjacent structures (such as the finger flexor tendon and transverse carpal ligament) is velocity independent (assuming constant velocity and force). Our results underscore the importance of accounting for both synovial and extrasynovial sources of gliding resistance in the determination of flexor tendon frictional work.

There were a few limitations to this study. We measured tendon frictional work in fresh frozen cadavers, which required anatomical dissection proximal and distal to the carpal tunnel. SSCT damage may arise due to the formation of ice crystals as well as repetitive cyclical loading during testing (Filius et al., 2014). To minimize tissue damage, the cadavers were thawed slowly in a cold room at 5°C. We also pre-conditioned each specimen and block-randomized the experimental conditions to mitigate potential order effects due to tissue degradation. We generated a uniform tendon displacement of 30 mm without considering individual anthropometrics. However, it is unlikely that we exceeded the SSCT viscoelastic threshold, as tendon displacements for combined wrist and finger flexion are of considerably higher magnitude (~ 5 to 8 cm). Finally, we did not validate the regression equations due to the limited number of specimens available for model development. However, our data showed a multiplicative effect of combined biomechanical risk factors, in general agreement with odds ratios from epidemiology

(Bernard, 1997). Furthermore, additional research is planned to test the predictive capabilities of the model in the workplace.

2.6. Conclusions

Concurrent exposure to several biomechanical risk factors including wrist posture, tendon velocity, and force, multiplicatively increased tendon frictional work in the carpal tunnel. We found a wrist posture × tendon force interaction during proximal tendon displacement (simulated finger flexion), demonstrating that greater tendon force increased tendon frictional work, especially in wrist flexion. Tendon velocity independently increased tendon frictional work for proximal tendon displacement. During distal tendon displacement (simulated finger extension), we identified a three-way interaction between wrist posture, tendon velocity, and force, showing disproportionately greater frictional work with high magnitudes for all three biomechanical risk factors simultaneously. The current results demonstrate the mechanistic link between physical exposure and carpal tunnel mechanics, thus providing further insight into the pathogenesis of wrist/hand tendinopathies and CTS. Additionally, our study provides the basic framework for an etiological method to predict tendon frictional work and injury risk during repetitive wrist and finger flexion/extension movements in the workplace.

Conflict of interest statement: There are no conflicts of interest.

Acknowledgements: This study was funded by NSERC (Discovery Grant # 217382-09). Thanks to Bruce Wainman and Glen Oomen for accommodating this research project in lab space for the Education Program in Anatomy.

2.7. References

An, K.N., Berglund, L., Uchiyama, S., Coert, J.H., 1992. Measurement of friction between pulley and flexor tendon. Biomedical Sciences Instrumentation 29 (1), 1–7.

Armstrong, T.J., Chaffin, D.B., 1978. An investigation of the relationship between displacements of the finger and wrist joints and the extrinsic finger flexor tendons. Journal of Biomechanics 11 (3), 119–128.

Armstrong, T.J., Chaffin, D.B., 1979. Some biomechanical aspects of the carpal tunnel. Journal of Biomechanics 12 (7), 567–570.

Barr, A.E., Barbe, M.F., Clark, B.D., 2004. Work-related musculoskeletal disorders of the hand and wrist: epidemiology, pathophysiology, and sensorimotor changes. Journal of Orthopaedic & Sports Physical Therapy 34 (10), 610–627.

Bernard, B.P., 1997. Musculoskeletal disorders and workplace factors: A critical review of epidemiologic evidence for work-related musculoskeletal disorders of the neck, upper extremity, and low back (Publication # 97-141). Cincinnati, OH: National Institute for Occupational Safety and Health (Department of Health and Human Services).

Dennerlein, J.T., 2005. Finger flexor tendon forces are a complex function of finger joint motions and fingertip forces. Journal of Hand Therapy 18 (2), 120–127.

Ettema, A.M., Amadio, P.C., Zhao, C., Wold, L.E., O'Byrne, M.M., Moran, S.L., An, K.N., 2006. Changes in the functional structure of the tenosynovium in idiopathic carpal tunnel syndrome: A scanning electron microscope study. Journal of Plastic & Reconstructive Surgery 118 (6), 1413–1422.

Filius, A., Thoreson, A.R., Yang, T.H., Vanhees, M., An, K.N., Zhao, C., Amadio, P.C., 2014. The effect of low- and high-velocity tendon excursion on the mechanical properties of human cadaver subsynovial connective tissue. Journal of Orthopaedic Research 32 (1), 123–128.

Guimberteau, J.C., Delage, J.P., McGrouther, D.A., Wong, J.K.F., 2010. The microvacuolar system: how connective tissue sliding works. Journal of Hand Surgery 35E (8): 614–622.

Holzbaur, K.R., Murray, W.M., Delp, S.L., 2005. A model of the upper extremity for simulating musculoskeletal surgery and analyzing neuromuscular control. Annals of Biomedical Engineering 33 (6), 829–840.

Jinrok, O., Zhao, C., Amadio, P.C., An, K.N., Zobitz, M.E., Wold, L.E., 2004. Vascular pathological changes in the flexor tenosynovium (subsynovial connective tissue) in idiopathic carpal tunnel syndrome. Journal of Orthopaedic Research 22 (6), 1310–1315.

Keir, P.J., Wells, R.P., 1999. Changes in geometry of the finger flexor tendons in the carpal tunnel with wrist posture and tendon load: an MRI study on normal wrists. Clinical Biomechanics 14 (9), 635–645.

Kociolek, A.M., Keir, P.J., 2013. Assessing flexor tendon and subsynovial connective tissue excursion with colour Doppler ultrasound. In proceedings of XXIV Congress of the International Society of Biomechanics. Natal, RN.

Lee, S.W., Kamper, D.G., 2009. Modeling of multiarticular muscles: importance of inclusion of tendon–pulley interactions in the finger. IEEE Transactions on Biomedical Engineering 56 (9), 2253–2262.

Moore, A., Wells, R., Ranney, D., 1991. Quantifying exposure in occupational manual tasks with cumulative trauma disorder potential. Ergonomics 34 (12), 1433–1453.

Osamura, N., Zhao, C., Zobitz, M.E., An, K.N., Amadio, P.C., 2007. Evaluation of the material properties of the subsynovial connective tissue in carpal tunnel syndrome. Clinical Biomechanics 22 (9), 999–1003.

Punnett, L., Wegman, D.H., 2004. Work-related musculoskeletal disorders: the epidemiologic evidence and the debate. Journal of Electromyography and Kinesiology 14 (1), 13–23.

Sancho-Bru, J.L., Perez-Gonzalez, A., Vergara-Monedero, M., Giurintano, D., 2001. A 3-D dynamic model of human finger for studying free movements. Journal of Biomechanics 34 (11), 1491–1500.

Schuind, F., Ventura, M., Pasteels, J.L., 1990. Idiopathic carpal tunnel syndrome: histologic study of the flexor synovium. Journal of Hand Surgery 15A (3), 497–503.

Schweizer, A., Frank, O., Ochsner, P.E., Jacob, H.A.C., 2003. Friction between human finger flexor tendons and pulleys at high loads. Journal of Biomechanics 36 (1), 63–71.

Schweizer, A., Moor, B.K., Nagy, L., Snedecker, J.G., 2009. Static and dynamic human flexor tendon–pulley interaction. Journal of Biomechanics 42 (12), 1856–1861.

Smutz, W.P., Miller, S.C., Eaton, C.J., Bloswick, D.S., France, E.P., 1994. Investigation of low-force high-frequency activities on the development of carpal-tunnel syndrome. Clinical Biomechanics 9 (1), 15–20.

Staal, J.B., de Bie, R.A., Hendriks, E.J.M., 2007. Aetiology and management of work-related upper extremity disorders. Best Practice & Research Clinical Rheumatology 21 (1), 123–133.

Tanaka, S., McGlothlin, J.D., 1993. A conceptual quantitative model for prevention of work-related carpal tunnel syndrome (CTS). International Journal of Industrial Ergonomics 11 (3), 181–193.

Tat, J., Kociolek, A.M., Keir, P.J., 2013. Repetitive differential motion increases shear strain between the flexor tendon and subsynovial connective tissue. Journal of Orthopaedic Research 31 (10), 1533–1539.

Uchiyama, S., Amadio, P.C., Ishikawa, J.I., An, K.N., 1997. Boundary lubrication between the tendon and the pulley in the finger. Journal of Bone and Joint Surgery 79A (2), 213–218.

Uchiyama, S., Coert, J.H., Berglund, L., Amadio, P.C., An, K.N., 1995. Method for the measurement of friction between tendon and pulley. Journal of Orthopaedic Research 13 (1), 83–89.

Valero-Cuevas, F.J., 2005. An integrative approach to the biomechanical function and neuromuscular control of the fingers. Journal of Biomechanics 38 (4), 673–684.

Vigouroux, L., Quaine, F., Labarre-Vila, A., Moutet, F., 2006. Estimation of finger muscle tendon tensions and pulley forces during specific sport-climbing grip techniques. Journal of Biomechanics 39 (14), 2583–2592.

Walbeehm, E.T., McGrouther, D.A., 1995. An anatomical study of the mechanical interactions of flexor digitorum superficialis and profundus and the flexor tendon sheath in zone 2. Journal of Hand Surgery 20B (3), 269–280.

Williams, R.B., Fisher, C.D., Gallon, J.C., 2013. Practical considerations for using constant force springs in space-based mechanisms. In proceedings of 54th AIAA/ASME/ASCE/AHS/ASC Structures, Structural Dynamics, and Materials Conference. Boston, MA.

Wu, J.Z., An, K.N., Cutlip, R.G., Krajnak, K., Welcome, D., Dong, R.G., 2008. Analysis of musculoskeletal loading in an index finger during tapping. Journal of Biomechanics 41 (3), 668–676.

Zhao, C., Ettema, A.M., Osamura, N., Berglund, L.J., An, K.N., Amadio, P.C., 2007. Gliding characteristics between flexor tendons and surrounding tissues in the carpal tunnel: A biomechanical cadaver study. Journal of Orthopaedic Research 25 (2), 185–190.

CHAPTER THREE

Development of a Kinematic Model to Predict Finger Flexor Tendon and Subsynovial Connective Tissue Displacement in the Carpal Tunnel

Aaron M. Kociolek and Peter J. Keir

Department of Kinesiology, McMaster University, Hamilton, Ontario, Canada

Kociolek, A.M., Keir, P.J., 2015. Development of a kinematic model to predict finger flexor tendon and subsynovial connective tissue displacement in the carpal tunnel. Ergonomics, Accepted, January 20, 2015. http://dx.doi.org/10.1080/00140139.2015.1013575

3.1. Abstract

Finger flexor tendinopathies and carpal tunnel syndrome are histologically characterized by non-inflammatory fibrosis of the subsynovial connective tissue (SSCT) in the carpal tunnel, which is indicative of excessive and repetitive shear forces between the finger flexor tendons and SSCT. We assessed flexor digitorum superficialis (FDS) tendon and adjacent SSCT displacements with colour Doppler ultrasound as sixteen healthy participants completed long finger flexion/extension movements captured by a motion capture system. FDS tendon displacements fit a second-order regression model based on metacarpophalangeal and proximal interphalangeal joint flexion angles (R^2 = 0.92 ± 0.01). SSCT displacements were 33.6 ± 1.7% smaller than FDS tendon displacements and also fit a second-order regression model (R^2 = 0.89 ± 0.01). FDS tendon and SSCT displacement both correlated with finger joint thickness, enabling participant-specific anthropometric scaling. We propose the current regression models as an ergonomic method to determine relative displacements between the finger flexor tendons and SSCT.

Practitioner Summary

Relative displacements between the finger flexor tendons and SSCT provide insight into gliding and friction in the carpal tunnel. Our regression models represent a move towards mechanistic-based ergonomic risk assessment of the wrist/hand. This is a natural evolution of ergonomic methods based on tendon-joint interaction.

Keywords: Finger; repetitive motion; relative displacement; tendon travel; shear injury

3.2. Introduction

Carpal tunnel syndrome (CTS) is the most common peripheral entrapment neuropathy of the upper limb (Tapedia et al. 2010). Claim rates are generally higher in industrial sectors with widespread exposure to repetitive wrist and/or hand motion (Zakaria et al. 2004). Temporal trends in CTS show increasing diagnosis rates, especially in individuals over the age of 45, which may have profound economic implications due to the aging workforce (Bongers et al. 2007; Gelfman et al. 2009). The costs associated with occupational carpal tunnel syndrome are particularly high since most cases require surgical intervention and rehabilitation, resulting in extended time off work (Manktelow et al. 2004).

While it is well-known that carpal tunnel syndrome is caused by mechanical compression of the median nerve, there are likely several underlying pathophysiological mechanisms involved in injury development (Barr et al. 2004). Histological changes in patients with flexor tendinopathies and CTS include non-inflammatory fibrosis and thickening of the subsynovial connective tissue (SSCT), a complex microvacuolar system comprised of multiple collagen layers surrounding the flexor tendons in the carpal tunnel (Ettema et al. 2006a; Guimberteau et al. 2010). Although the SSCT facilitates tendon gliding, excessive shear owing to relative tendon-SSCT motion may damage the SSCT. This injury mechanism is supported by a scanning electron microscope study showing that fibrosis is exacerbated in the tenosynovial layers directly bordering the flexor tendons (Ettema et al. 2006a). Thus, excessive shear may initiate a series of mechanical events, including altered stiffness and permeability of the SSCT (Osamura et al. 2007a, b),

increased volume of the carpal tunnel contents (Ettema et al. 2006a), elevated carpal tunnel pressures (Zhao et al. 2011), ischemia, and compression of the median nerve (Keir and Rempel 2005).

SSCT fibrosis also affects finger flexor tendon gliding in the carpal tunnel. Cadavers with a history of CTS showed either increased adherence or increased dissociation between tendon and SSCT in comparison to cadavers without a history of CTS (Ettema et al. 2008). Another study found greater relative motion between the finger flexor tendons and SSCT as well as the median nerve and SSCT in CTS patients than healthy controls (van Doesburg et al. 2012). Changes in the CTS patients were due to increased tendon and median nerve displacements as well as decreased displacements of the SSCT. These pathological changes may increase tendon-SSCT shear even further, resulting in further tissue degradation.

Several researchers have quantified finger flexor tendon displacements *in vitro* (An et al. 1983; Armstrong and Chaffin 1978; Brand et al. 1975; Horii et al. 1992; Franko et al. 2011; Yamaguchi et al. 2008). Armstrong and Chaffin (1978) measured flexor digitorum profundus (FDP) and flexor digitorum superficialis (FDS) tendon displacements with a micrometer gauge while simultaneously photographing wrist and finger joint postures. Linear regression equations were then developed to calculate tendon displacements based on wrist and finger joint flexion angles as well as the thickness of the finger joints to account for anthropometry. These well-established regression equations have been used in ergonomic assessments to calculate tendon travel

(cumulative displacement) and predict injury risk (Moore et al. 1991; Nelson et al. 2000; Treaster and Marras 2000; Ugbolue and Nicol 2010).

An et al. (1983) quantified tendon displacements and moment arms of the index finger and found that finger flexor (FDP and FDS) tendon displacements increased nonlinearly with the flexion angle of each finger joint. Although these nonlinearities were relatively small, curvilinear tendon displacements also influenced moment arm calculations, and thus mechanical function of the finger. The instantaneous moment arm is represented as the slope of the tendon displacement versus joint angle curve (Landsmeer 1961). Therefore, nonlinear tendon displacements also predict moment arms that increase with finger joint flexion angle (An et al. 1983). Since geometric models of tendon-joint interaction are often used in biomechanical models in addition to ergonomic risk assessments, it is important that any kinematic model of tendon displacement include even small nonlinearities (Franko et al. 2011).

Researchers are utilizing sonography more frequently in recent years to evaluate finger flexor tendon dynamics (Ettema et al. 2006b; Korstanje et al. 2010; Lopes et al. 2011; Oh et al. 2007; Peolsson et al. 2010; van Doesburg et al. 2012; Yoshii et al. 2009a). Due to advances in image resolution, current methods enable simultaneous assessment of the finger flexor tendons and the adjacent SSCT. Thus, ultrasound provides the means to quantify relative displacement between tendon and SSCT. Oh et al. (2007) used colour Doppler imaging (CDI) to show that relative motion between the flexor tendons and adjacent SSCT increased with tendon velocities ranging from 2.5 – 10 cm/sec. Relative tendon-SSCT motion is also influenced by other occupational risk

factors, including wrist posture (Kociolek and Keir 2013), repetitive work (Yoshii et al. 2011), single-digit finger movement (Yoshii et al. 2009b), and task duration (Tat, Kociolek, and Keir 2013). However, there remains a need to assess both finger flexor tendon and SSCT displacements as a function of finger joint flexion angles.

The objectives of this study were to revisit traditional cadaveric models of tendon-joint interaction and determine a similar model for the adjacent SSCT. We assessed flexor tendon displacements with ultrasonography and finger joint angles with optical motion capture as sixteen healthy participants completed metacarpophalangeal and interphalangeal joint flexion/extension movements, individually and concurrently. We believe that the ability to estimate both tendon and SSCT displacements simultaneously will improve upon ergonomic risk assessments that only consider cumulative tendon displacement as a measure of shear potential. Estimating relative tendon-SSCT displacement may prove to be a better predictor of shear-related injuries, including flexor tendinopathies and CTS.

3.3. Methods

3.3.1. Participants

Sixteen healthy participants (8 males and 8 females) between 21 − 31 years of age (mean ± standard deviation: 24.7 ± 2.5) provided written informed consent prior to participating in the study, which was approved by the Hamilton Integrated Research Ethics Board. Each participant completed a brief questionnaire to screen for health conditions that may influence tendon gliding in the carpal tunnel. Exclusion criteria included degenerative joint disease, arthritis, gout, hemodialysis, sarcoidosis,

amyloidosis, hypothyroidism, diabetes mellitus, acute injury of the upper extremity, wrist tendinopathy, peripheral nerve disease, and pain, tingling, or numbness of the hand.

3.3.2. Experimental Protocol

Participants were seated at a table, which was adjusted to maintain approximately 120° of elbow joint flexion with the right arm at the side (~ 0° of shoulder abduction). The forearm was immobilized in a mid-prone posture using a thermoplastic splint (Figure 3.1a). A custom handgrip composed of polyvinyl chloride piping (outer diameter = 3.5 cm) fixed the index, ring, and little fingers in a mid-flexed position, allowing only the long finger to move freely. The handgrip also interconnected with the testing apparatus to keep the wrist joint in a neutral posture.

FDS tendon and SSCT displacements were assessed with ultrasound as the participants performed three long finger movements: (i) flexion/extension (F/E) of the metacarpophalangeal (MCP) joint, (ii) F/E of the proximal and distal interphalangeal (PIP + DIP) joints together, (iii) combined motions (i) and (ii), or full finger flexion (FF). Participants rehearsed the finger movements with the investigator prior to data collection to minimize potential learning effects. Each finger motion was performed cyclically for 10 seconds at a self-selected pace. The three finger movements were randomized to mitigate potential order effects.

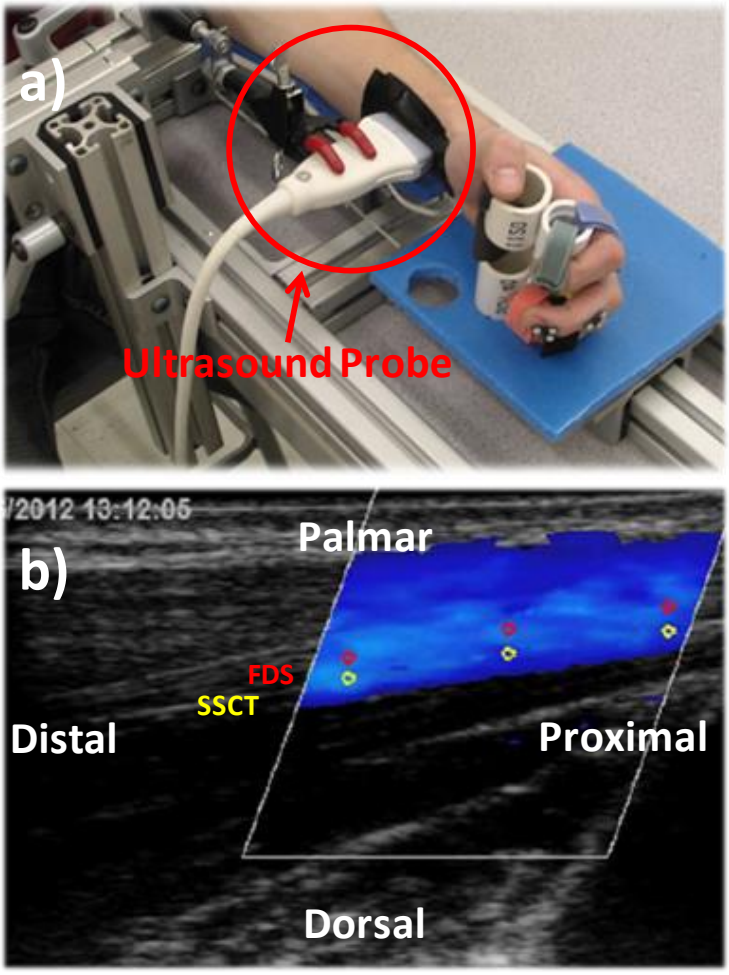

Figure 3.1. (a) Testing apparatus to perform long finger movements with the ultrasound probe positioned proximal to the wrist crease. (b) Grayscale images of the proximal wrist superimposed with CDI. Circular markers are depicted along the FDS tendon (red circles) and SSCT (yellow circles), and we obtained velocities at distal (left), centre, and proximal (right) locations.

3.3.3. Colour Doppler Imaging

An ultrasound system (Vivid Q, General Electric Healthcare Ltd., Milwaukee, WI) equipped with a high-frequency probe (12L-RS) was used to image the proximal wrist. The probe was positioned approximately 2 cm proximal to the wrist crease with a custom holding device. The FDS tendon of the long finger was easily identified based on the characteristic striated pattern of musculotendinous structures (due to acoustic speckles), whereas the adjacent subsynovial connective tissue was hyperechoic in appearance (Figure 3.1b). To ensure the correct flexor tendon was examined, we passively flexed and extended the fingers while observing tendon motion with CDI.

FDS tendon and SSCT velocities were represented by colour maps superimposed on grey-scale ultrasound. In colour flow imaging, a series of pulses (the pulse train) is transmitted and returned with a coinciding time-lag dependent on the tissue velocity. This is used to determine the phase shift and Doppler frequency (f_d), which is the basis of Doppler ultrasound methods, including CDI (Equation 3.1):

$$f_d = (2 \cdot v \cdot f_t \cdot \cos\theta) / c, \quad (3.1)$$

where v is velocity of scatter (relative to transmitter), f_t is the transmitted frequency, θ is angle of insonation (between scatter and beam), and c the speed of sound in tissue. Red colour maps represented finger flexion while blue color maps represented finger extension. Brighter colours corresponded to higher velocities of the FDS tendon and SSCT (Figure 3.1b).

The colour map selection pane on the ultrasound system was positioned near the proximal border of the carpal tunnel. Sonographic settings were optimized for musculotendinous tissue, including an acquisition frequency of 13 MHz. The colour Doppler scale was ± 11.0 cm/s, coinciding with the high-range of FDS tendon velocity during full finger flexion/extension (before correcting for the insonation angle). We also set a low velocity reject of 1.3 cm/s to reduce motion artefact. The steering angle of the probe was maximized at 20° and further supplemented with a gel wedge (Aquaflex Gel Pad, Parker Laboratories Inc., Fairfield, NJ), which reduced the angle of insonation to approximately 60°. Ten-second video clips of each finger motion were recorded at 29.5 frames per second.

Grey-scale images with superimposed colour maps were analyzed off-line using dedicated software (EchoPAC, General Electric Healthcare Ltd., Milwaukee, WI). The quantitative analysis toolkit (Q-Analysis) was used to position circular regions of interest (diameter = 0.5 mm) within the colour map selection pane and obtain velocity-time data. Three markers were placed along the FDS tendon (FDS_{Distal}, FDS_{Centre}, $FDS_{Proximal}$) while three adjacent markers were placed on the SSCT ($SSCT_{Distal}$, $SSCT_{Centre}$, $SSCT_{Proximal}$). Each circular marker maintained a fixed position throughout the 10-second video clip, and was visually inspected to ensure tracking of the correct anatomical structure (Tat et al. 2014). The ensuing velocity profiles were exported for further analysis. Velocity-time data of the 3 FDS tendon and 3 SSCT markers were ensemble averaged, and dual low-pass filtered at 6.0 Hz (MatLab 7.6, The Mathworks Inc., Natick, MA), consistent with a previous study of similar finger movements (Tat et al. 2014). FDS tendon and SSCT

velocity profiles were corrected for the angle of insonation (cosθ), and integrated to obtain displacement-time data.

3.3.4. Joint Kinematics

Wrist and long finger joint kinematics were obtained with 12 Raptor-4 cameras (Motion Analysis Corp., Santa Rosa, CA). Twenty-six reflective hemispherical markers (diameter = 4 mm) were attached to the distal forearm, hand, and long finger (Figure 3.2). Marker trajectories were collected at 120 Hz (Cortex 1.3, Motion Analysis Corp., Santa Rosa, CA). A digital trigger marked the start of each trial for both motion capture and ultrasound, which was used to synchronize the two datasets in post-processing.

Marker data were fed into a kinematic hand model to obtain long finger joint thicknesses and flexion/extension angles (Keir et al. 2013). Briefly, the model defined the metacarpals and the finger phalanges with unconstrained movement capabilities in 6 degrees of freedom. The metacarpals were modelled as elliptical cylinders using the palmar and dorsal wrist markers as well as the palmar and dorsal metacarpophalangeal joints markers. The finger phalanges were represented by frusta of circular cones based on markers affixed to the palmar and dorsal surfaces of the finger joints and the fingertips.

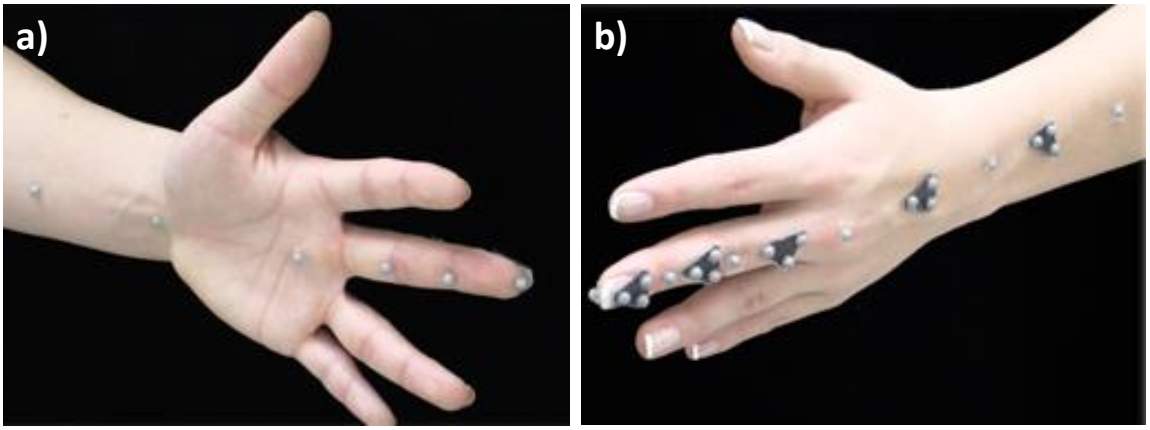

Figure 3.2. Reflective markers on the palmar (left) and dorsal (right) surfaces of the distal forearm, hand, and long finger. Segment definition markers on anatomical landmarks were used to model the hand in a neutral posture and were removed for the subsequent finger movement trials. Triad marker clusters on the dorsal hand, and long finger tracked finger movement throughout the experimental protocol.

A static calibration trial, with all twenty-six reflective markers, was applied to a model template to represent participant-specific anthropometrics. Metacarpophalangeal (MCP), proximal interphalangeal (PIP), and distal interphalangeal (DIP) joint thicknesses were calculated as the distance between the palmar and dorsal calibration markers for each joint. Mean finger joint thicknesses are presented in Table 3.1. However, the DIP joint was excluded from further analysis since the FDS tendon does not cross the DIP joint.

Table 3.1. Mean (± standard error of the mean) finger joint depths obtained from motion capture (mm).

Joint	Females (n = 8)	Males (n = 8)	Total (n = 16)
MCP	26.06 ± 0.71	29.85 ± 0.27	27.95 ± 0.61
PIP	15.33 ± 0.49	17.71 ± 0.24	16.52 ± 0.41
DIP	11.60 ± 0.39	13.88 ± 0.16	12.74 ± 0.36

Note: MCP, metacarpophalangeal joint; PIP, proximal interphalangeal joint; DIP, distal interphalangeal joint.

Definition markers on anatomical landmarks were removed after the static calibration trial, and marker triads on the dorsal metacarpals and phalanges tracked the positions of the finger segments for the following finger movement trials (Keir et al. 2013). For the long finger, MCP and PIP joint kinematics were calculated using an x-y-z Cardan sequence (anatomically equivalent to flexion/extension - abduction/adduction -

pronation/supination) based on guidelines by the International Society of Biomechanics (Wu et al. 2005).

Since the motion capture and ultrasound datasets were recorded on indivisible time scales (120 Hz versus 29.5 Hz, respectively), down-sampling the finger joint kinematics was not a feasible solution, as this would lead to a propagation of synchronization errors throughout the 10-second trial. Rather, we used a cubic spline to predict the corresponding finger joint flexion angle at each time-point of the FDS tendon / SSCT displacement profiles. This strategy had no discernible effect on the finger joint kinematics, and provided a means to combine the two datasets for further evaluation.

3.3.5. Regression Modelling

FDS tendon and SSCT displacements were modelled using least squares regression. The predictor variables included metacarpophalangeal joint and proximal interphalangeal joint flexion angles. Prior to regression analysis, a global correction factor was applied to FDS tendon and SSCT displacements based on in-house validation of CDI, which previously showed flexor tendon displacements were underrepresented by 9.4% for similar tendon velocities (Tat et al. 2014). A second-order (nonlinear) model was fit to the complete data set of each participant. The nonlinear model assumes flexor tendon bowstringing with finger joint flexion (Keir and Wells 1999; Landsmeer 1961), in accordance with previous observations (An et al. 1983). We used a forced-entry regression method to ensure that the underlying anatomical assumptions of the tendon paths were satisfied.

Developing individualized regression equations for each participant enabled anthropometric evaluation of the modelled results. We used the regression models to predict FDS tendon and SSCT displacements associated with each metacarpophalangeal joint and proximal interphalangeal joint flexion (in isolation). The ensuing tendon and SSCT displacements were correlated against MCP and PIP finger joint thicknesses. We pooled results for the metacarpophalangeal joint and proximal interphalangeal joint owing to the low anthropometric variability of each joint separately (An et al. 1983). The mean FDS tendon and SSCT regression equations were adjusted to represent a 50^{th} percentile male based on the current correlation analysis and previous anthropometric measurements of the hand (Garrett 1970; Greiner 1991). We also derived anthropometric equations to scale the 50^{th} percentile model predictions based on individual finger joint thicknesses for males and females.

3.4. Results

3.4.1. Finger Joint Kinematics

Participants successfully performed the experimental protocol, as demonstrated by the distinct kinematic patterns of all three long finger movements (Table 3.2). PIP + DIP joint F/E produced large changes to proximal interphalangeal joint flexion angles with very small changes to metacarpophalangeal joint flexion angles. MCP joint F/E proved to be a more challenging task. While the largest kinematic changes occurred at the metacarpophalangeal joint, there were also considerable proximal interphalangeal joint rotations of 20.9° ± 3.0°. Not surprisingly, full finger flexion (FF) resulted in substantial

changes to both the metacarpophalangeal and proximal interphalangeal joint flexion angles (Table 3.2).

Table 3.2. Mean (± standard error of the mean) changes in metacarpophalangeal (MCP) and proximal interphalangeal (PIP) joint flexion angles during active long finger motions (°).

Finger Motion	Finger Joint	
	PIP (°)	**MCP (°)**
PIP + DIP	90.1 ± 3.7	1.8 ± 2.5
MCP	20.9 ± 3.0	52.7 ± 3.0
FF	105.7 ± 2.3	38.7 ± 2.9

Note: PIP + DIP, proximal and distal interphalangeal joint flexion/extension; MCP, metacarpophalangeal joint flexion/extension; FF, full finger flexion.

3.4.2. Tendon-Joint and SSCT-Joint Interaction

Cyclical long finger flexion/extension movements produced bell-shaped FDS tendon and SSCT displacement profiles (Figure 3.3). Proximal tendon displacement increased with MCP and/or PIP joint flexion and distal tendon displacement increased with joint extension. SSCT displacement produced a similar profile in relation to finger joint flexion/extension. However, SSCT displacements were 33.6% ± 1.7% smaller than FDS tendon displacements.

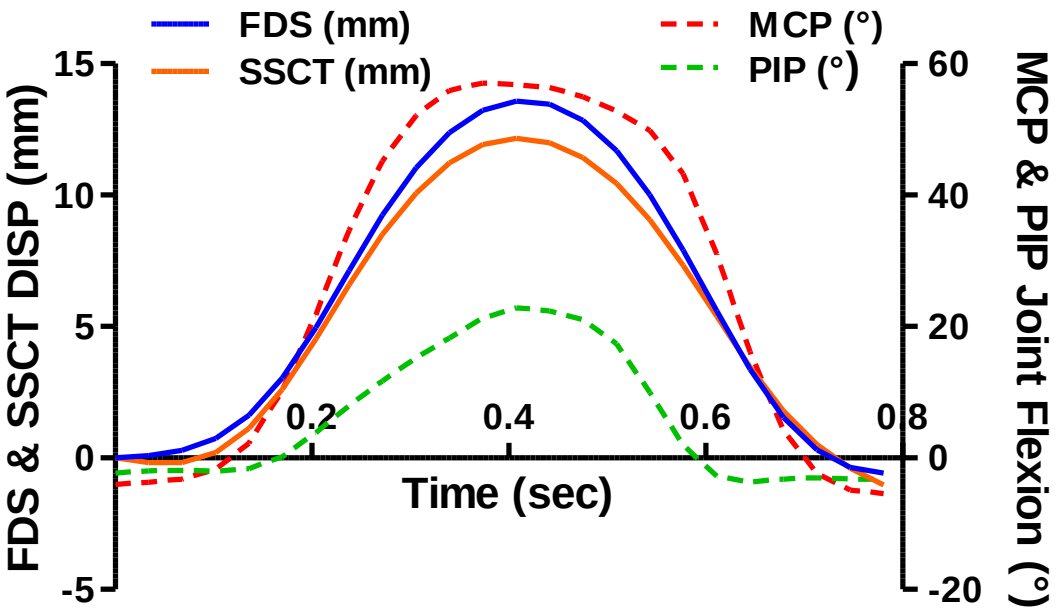

Figure 3.3. Typical data for a MCP joint F/E trial. FDS tendon and SSCT displacements are on the left vertical axis against time on the horizontal axis. MCP and PIP joint flexion angles are on the right vertical axis. The largest kinematic changes occurred at the MCP joint, although there were also smaller accessory joint rotations at the PIP joint.

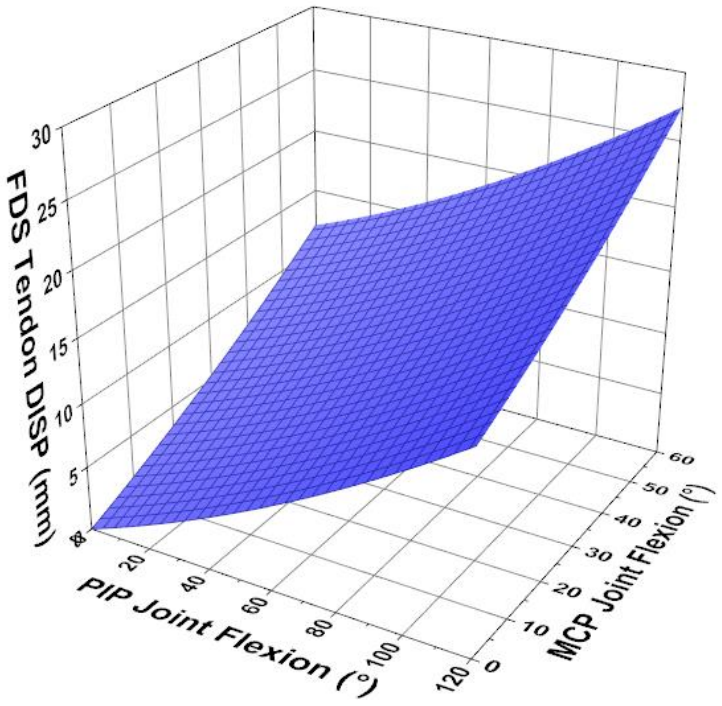

Figure 3.4. Mean second-order (nonlinear) regression of FDS tendon displacement based on MCP and PIP joint flexion angles.

A second-order (nonlinear) regression model of FDS tendon displacement based on MCP and PIP joint flexion angles resulted in an R^2 of 0.92 ± 0.01 and a RMSE of 1.8 ± 0.1 mm (Figure 3.4). A second-order regression model of the SSCT produced an R^2 of 0.89 ± 0.01 and RMSE of 1.5 ± 0.1 mm. We also evaluated the relationship between FDS tendon and SSCT displacements and anthropometrics. Flexor tendon displacement increased linearly with finger joint thickness (Figure 3.5), and this relationship was strong (r = 0.83). SSCT displacement versus finger joint thickness produced a moderate correlation of 0.66. FDS tendon and SSCT nonlinear regression equations were adjusted to represent a 50^{th} percentile male, which are embedded in Figure 3.6. Model predictions are further scalable based on individual measurement of MCP and PIP finger joint thicknesses for males and females using the equations in Figure 3.7.

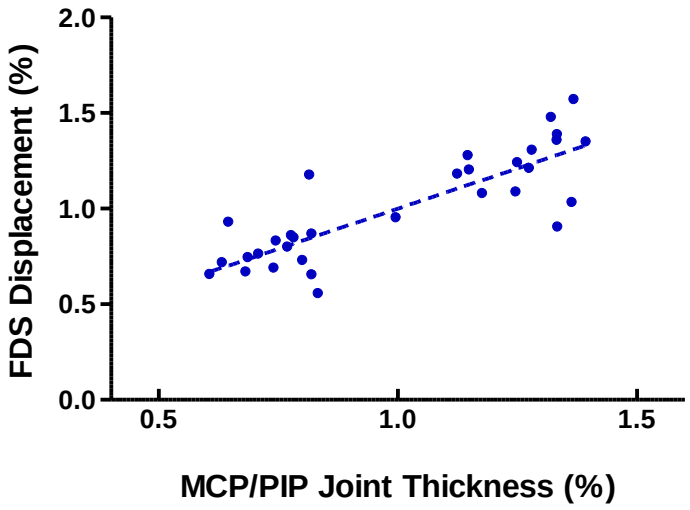

Figure 3.5. FDS tendon displacement versus MCP and PIP finger joint thickness. FDS tendon displacements are normalized to the mean tendon displacement for all 16 participants while MCP and PIP joint thicknesses are normalized the mean joint thickness (pooled across both joints).

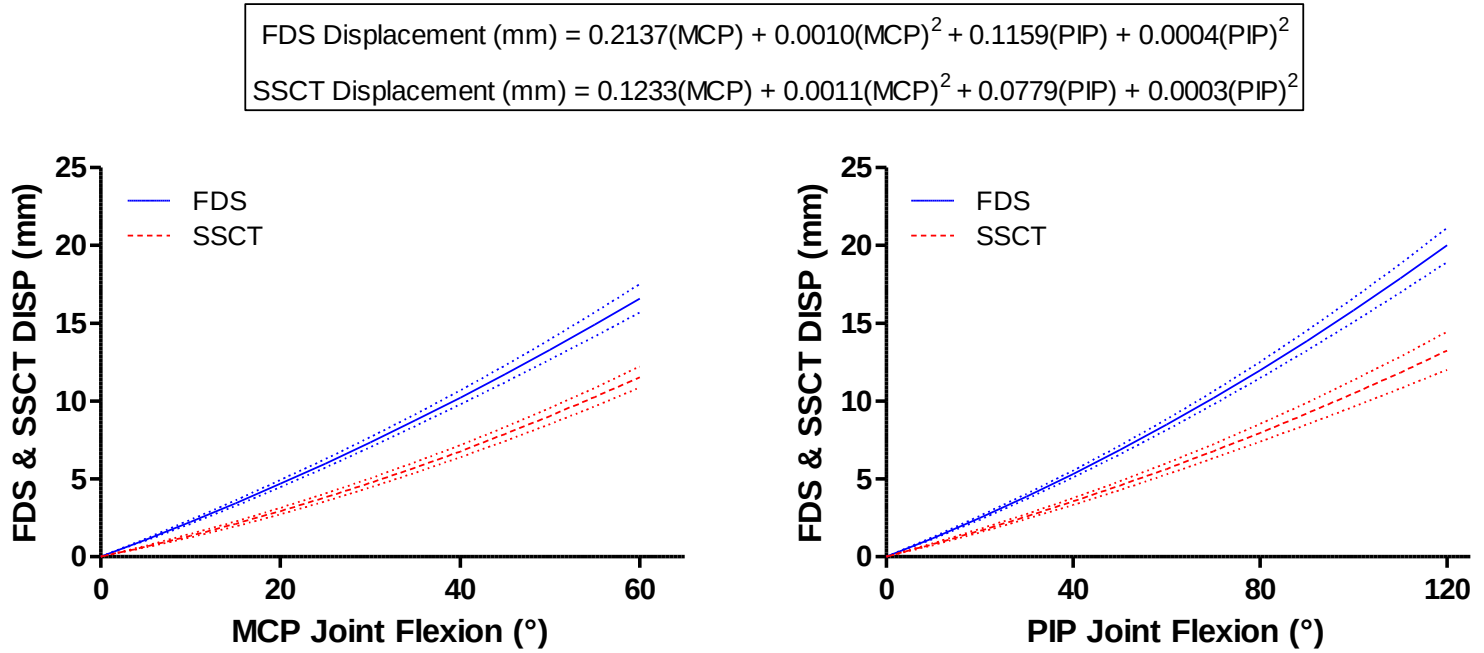

Figure 3.6. FDS tendon and SSCT displacements versus MCP (left) and PIP (right) joint flexion angles from the embedded nonlinear regression models (representative of a 50th percentile male). The solid line represents the FDS tendon and the dashed line represents the SSCT while the dotted lines are standard errors. Inputs in the regression equations: MCP, metacarpophalangeal joint flexion (°); PIP, proximal interphalangeal joint flexion (°).

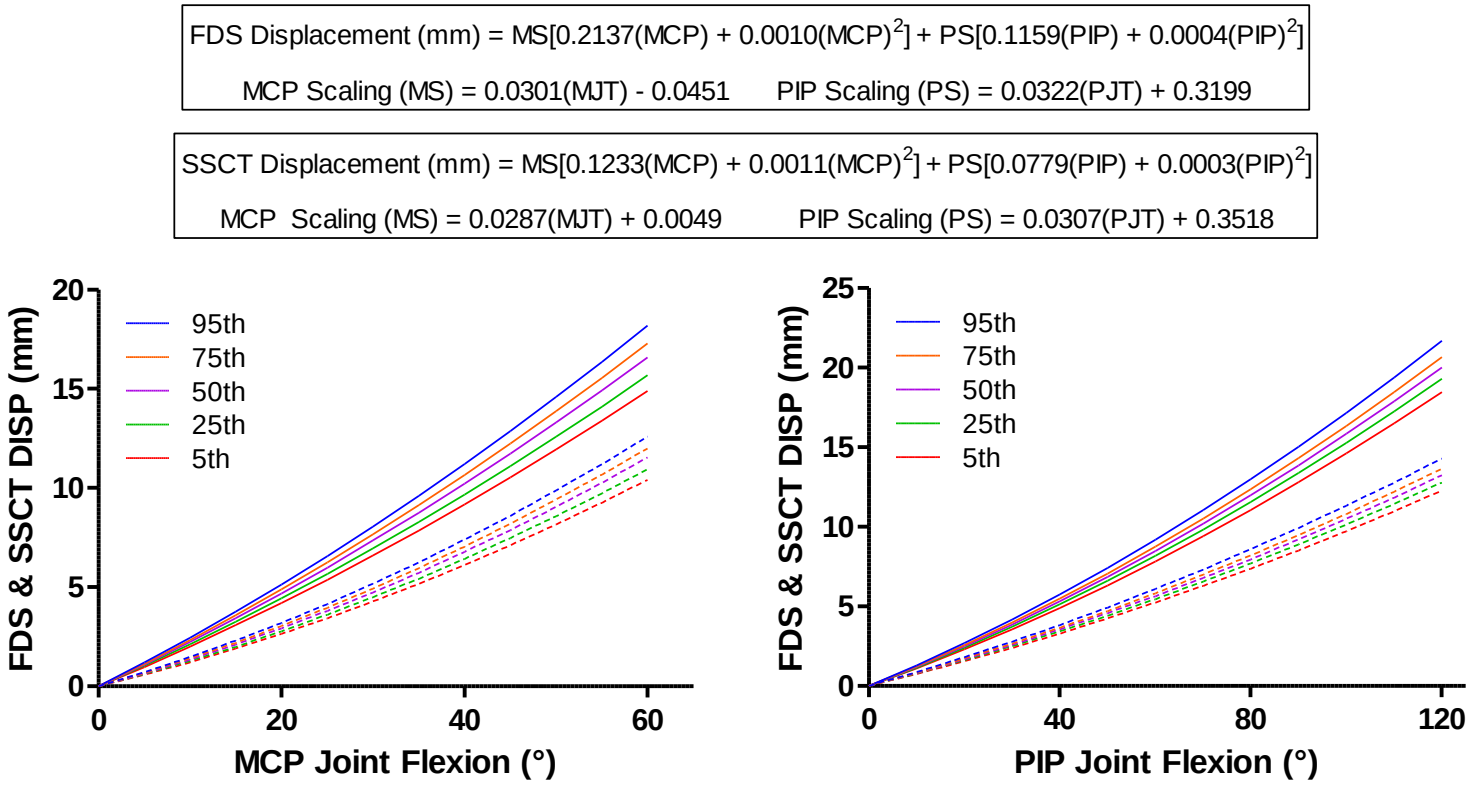

Figure 3.7. FDS tendon and SSCT displacements versus MCP (left) and PIP (right) joint flexion angles with anthropometric scaling. The solid lines are 5th to 95th percentile FDS tendon displacements and the dashed lines are 5th to 95th percentile SSCT displacements. The embedded anthropometric regression equations enable individualized model predictions based on finger joint thicknesses. Inputs in the regression equations: MCP, metacarpophalangeal joint flexion (°); PIP, proximal interphalangeal joint flexion (°); MJT, metacarpophalangeal joint thickness (mm); PJT, proximal interphalangeal joint thickness (mm).

3.5. Discussion

We developed nonlinear regression equations to predict both FDS tendon and SSCT displacements for use in ergonomic risk assessments. The current regression equations provide the means to predict relative displacement between FDS tendon and SSCT. This is an important step towards mechanistic-based ergonomic risk assessments since this relative displacement measure (FDS tendon – SSCT) is closely related to shear strain at the tendon-SSCT interface in the carpal tunnel (Ettema et al. 2006a, 2006b; Oh et al. 2007). While fibrosis of the SSCT suggests that shear strain is involved in injury, the exact pathogenesis of flexor tendinopathies and CTS remain uncertain (Vanhees et al. 2012). Injury may be related to exceeding viscoelastic limits acutely and/or exceeding a shear strain threshold over time. Regardless of the precise origins, we believe the current model will be a useful ergonomic tool, and further studies will seek to validate its capacity to predict injury risk in the workplace.

FDS tendon velocities and displacements in this study were similar to previous sonographic assessments, including spectral Doppler ultrasound (Ettema et al. 2006b; Lopes et al. 2011), speckle tracking (Korstanje et al. 2010), and colour Doppler imaging (Oh et al. 2007; Tat et al. 2013, 2014). Generally, full finger flexion produces 20 – 30 mm of FDS tendon displacement, depending on the ultrasound method. Uncorrected tendon displacements in our study were 21.1 ± 1.0 mm for full finger movements. However, we employed a 10% correction based on in-house validation of CDI (Tat et al. 2014), which increased our full finger tendon displacements to 23.2 ± 1.1 mm. The custom handgrip used to restrain the non-test fingers also impeded long finger motion

near the end range of motion to some degree. This small distinction may slightly decrease tendon displacements relative to similar experimental protocols with no end range restrictions (Lopes et al. 2011; Tat et al. 2013).

In the cadaver-based linear regression model developed by Armstrong and Chaffin (1978), full finger flexion for a 50th percentile male produced 27.0 mm of FDS tendon displacement. Remarkably, our nonlinear model estimated 27.1 mm of FDS tendon displacement using the same kinematic and anthropometric inputs (MCP joint flexion – 40°; PIP joint flexion – 105°; MCP joint depth – 34.7 mm; PIP joint depth – 21.1 mm). However, for smaller finger joint angles, our nonlinear model predicted lower flexor tendon displacements compared to Armstrong and Chaffin (1978). Even these model differences were relatively modest (~ 0.5 to 1.5 mm).

We found that FDS tendon and SSCT displacement versus finger joint thickness were linearly correlated. However, this correlation was higher for the FDS tendon ($r = 0.83$) compared to the SSCT ($r = 0.66$). An et al. (1983) also showed a similar relationship between tendon displacement and joint thickness in cadaveric specimens, with correlation coefficients for each muscle of the index finger ranging from 0.85 to 0.92. Armstrong and Chaffin (1978) included joint thickness in their linear regression equations and determined that FDS tendon displacements were 6% lower for a 5th percentile male and 6% higher for a 95th percentile male compared to a 50th percentile male. In the current nonlinear regression model, tendon displacements were 9% lower for a 5th percentile male and 9% higher for a 95th percentile male (than a 50th percentile male). Anthropometric scaling in this study also better matched a musculoskeletal model

of the hand (Kociolek and Keir 2011), which showed that FDS tendon displacements and moment arms were more sensitive to the finger dimensions than previously predicted by Armstrong and Chaffin (1978).

The nonlinear regression equations from our study have important implications for musculoskeletal models, which often calculate musculotendon moment arms using the partial velocity method (Delp et al. 2007). This approach is equivalent to the change in musculotendon length relative to the change in joint angle. Musculotendinous moment arms derived from our nonlinear regression equations increased with the finger joint angles (Figure 3.8). For a 50th percentile male, the FDS moment arm at the PIP joint increased from 6.9 mm to 11.5 mm between 0° and 105° of PIP joint flexion (representative of full finger flexion). Likewise, the FDS moment arm at the MCP joint ranged from 12.5 mm to 16.8 mm with 0° to 40° of MCP joint flexion. Conversely, a linear model of tendon displacement versus joint rotation does not predict a mechanical advantage in flexed finger postures (Figure 3.8). We also found that a nonlinear model better fit the data compared to a linear model, resulting in higher R^2 and lower RMSE. The improved fit of a nonlinear model combined with tendon bowstringing during finger flexion suggests that a second-order model is better suited for quantifying tendon displacements and moment arms.

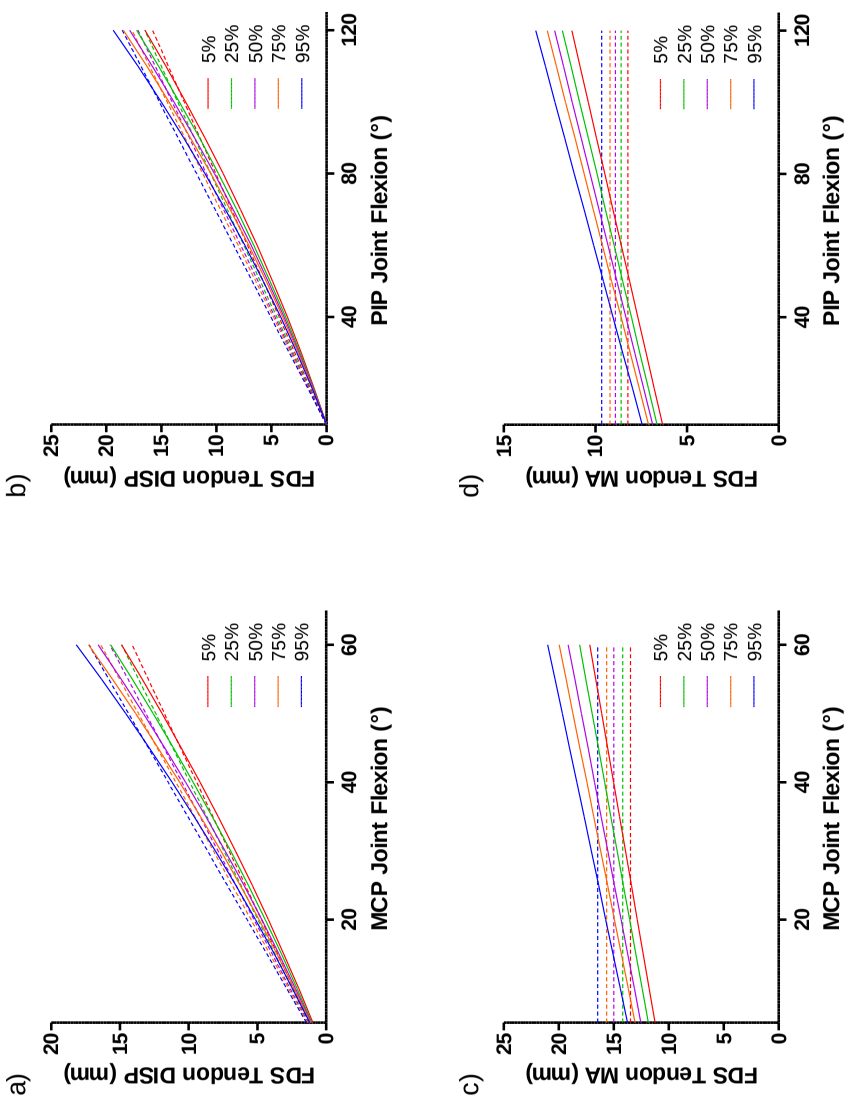

Figure 3.8. FDS tendon displacements versus (a) MCP joint and (b) PIP joint flexion, and FDS tendon moment arms against (c) MCP joint and (d) PIP joint flexion with anthropometric scaling for 5th, 25th, 50th 75th, and 95th percentile males. The solid lines represent a second-order (nonlinear) regression model and the dashed lines are a first-order (linear) regression model.

Relative tendon-SSCT displacement predictions are important to further investigate the pathophysiological mechanisms of injury development. We quantified FDS tendon and SSCT displacements from the regression equations in this study, and further calculated the relative displacement (FDS tendon – SSCT). For full finger flexion, relative displacement increased with MCP and PIP flexion (Figure 3.9). This finding highlights the significance of deviated finger posture as an occupational risk factor. Relative displacements between FDS tendon and SSCT are also influenced by other risk factors, including deviated wrist posture (Kociolek and Keir 2013), high-velocity tendon motion (Yoshii et al. 2011), single-digit finger movement (Yoshii et al. 2009b), and task duration (Tat et al. 2013). Thus, it is possible to account for these additional risk factors using the regression equations in this study as the base. We present two examples of relative tendon-SSCT displacements during full finger flexion in either a neutral or flexed wrist posture as a proof of principle in Figure 3.9 (Kociolek and Keir, 2013). Ultimately, the ability to predict relative displacement will improve our understanding of tenosynovial loading and forward ergonomic risk assessments, using a mechanistic approach.

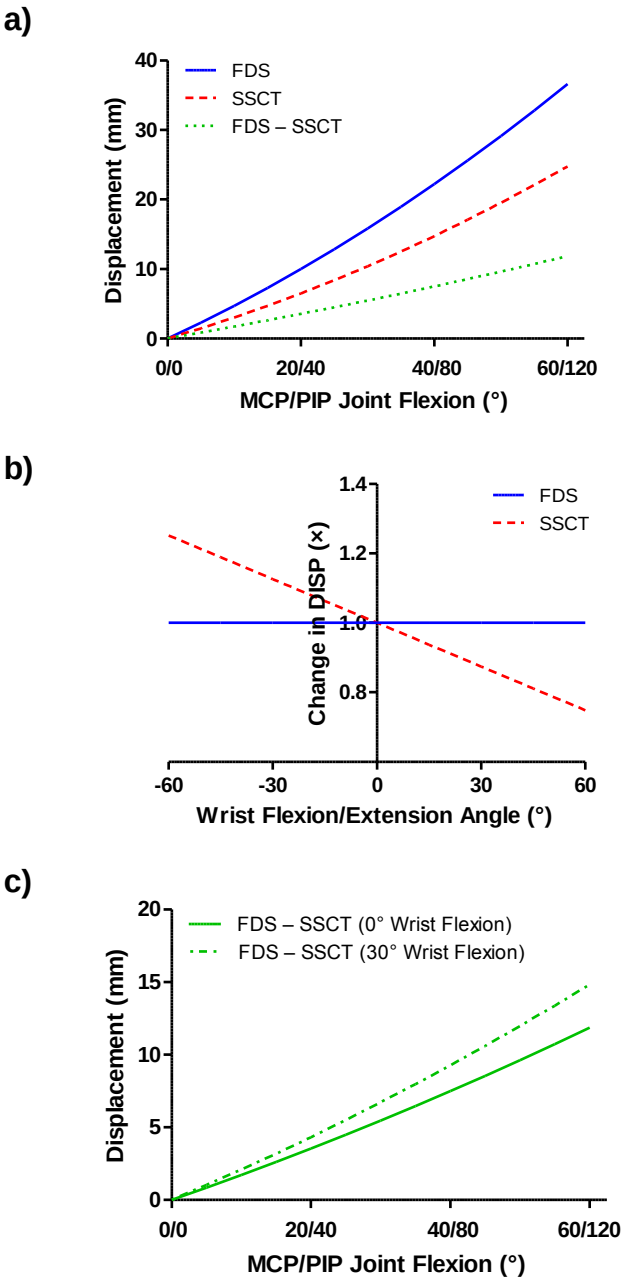

Figure 3.9. (A) FDS tendon, SSCT, and relative (FDS – SSCT) displacement versus combined MCP and PIP joint flexion for a 50th percentile male. (B) Change in FDS tendon and SSCT displacement against wrist angle. FDS tendon displacement is not influenced by wrist posture while SSCT displacement decreases with wrist flexion angle. (C) Relative (FDS – SSCT) displacement versus combined MCP and PIP joint flexion for both 0° (neutral) and 30° wrist flexion. Relative displacement is higher in 30° wrist flexion (due to lower SSCT displacement with no change in FDS tendon displacement). Note: data for wrist from Kociolek and Keir (2013).

There were a few limitations to this study. We evaluated FDS tendon and SSCT displacements of the long finger only, which may not be representative of the other fingers or multi-finger movements. While previous models of tendon-joint interaction do not make anatomical distinctions between different fingers of the hand (Armstrong and Chaffin, 1978), there is evidence that isolated versus concurrent finger movements increase relative displacements between FDS tendon and SSCT (Tat et al., 2013). Future iterations of the model will include terms for "isolated" or "concurrent" finger movements. The regression models may also benefit from a more detailed anthropometric analysis, including both joint thicknesses and digit lengths. Our current approach only considered finger joint thickness, based on the well-established geometric relationship between moment arm and tendon displacement (Landsmeer, 1961; Armstrong and Chaffin, 1978).

Doppler ultrasound methods are influenced by the angle of insonation. We used a standoff gel wedge and maximized the steering angle of the ultrasound beam, effectively reducing the angle of insonation to approximately 60°. Decreasing the angle between the beam and tissue to 45° – 60° minimizes potential angle correction errors (McDicken 1991). We performed in-house validation of CDI in eight fresh-frozen human cadavers and showed that our ultrasound method captured subtle differences in FDS tendon and SSCT movement during finger flexion versus finger extension, also confirmed in simultaneous direct measurements of frictional work (Kociolek et al. 2015; Tat et al. 2014). These findings link relative tendon-SSCT motion and shear strain. With respect to the kinematics, as with any optical marker-based system, skin motion artefact remains

a concern. However, Kuo et al. (2002) found similar thumb joint angles determined using skin-surface markers and fluoroscopy with an adjusted coefficient of multiple determination of 0.999 and 0.973 for interphalangeal and metacarpophalangeal joint flexion/extension, respectively.

3.6. Conclusions

We found that a second-order model of FDS tendon displacement versus MCP and PIP joint flexion resulted in a R^2 of 0.92 ± 0.01. SSCT displacements were similarly described with a second-order regression equation (R^2 = 0.89 ± 0.01). FDS tendon and SSCT displacements correlated with finger joint thicknesses, enabling anthropometric scaling to represent both male and female participants. SSCT displacements were smaller than FDS tendon displacements by 33.6% ± 1.7%. The current FDS tendon and SSCT regression models provide the means to calculate relative displacement between FDS tendon and SSCT, which is related to shear strain in the carpal tunnel (Ettema et al. 2006a, b). Relative tendon-SSCT displacement may improve upon ergonomic risk assessments that only consider cumulative tendon displacement (Nelson et al. 2000; Treaster and Marras 2000), although future studies are needed to validate relative displacement as a predictor of occupational injury risk.

Conflict of interest statement: There are no conflicts of interest.

Acknowledgements: Thanks to Katherine Wilson and Jimmy Tat for their assistance with ultrasound during data collection as well as Calvin Tse and Michael Rizzuto for their assistance with motion capture. This work was supported by the Centre of Research

Expertise for the Prevention of Musculoskeletal Disorders and the Natural Sciences and Engineering Research Council of Canada under Discovery Grant # 217382-09.

3.7. References

An, K.N., Ueba, Y., Chao, E.Y., Cooney, W.P., Linscheid, R.L., 1983. Tendon excursion and moment arm of index finger muscles. Journal of Biomechanics 16 (6), 419–425.

Armstrong, T.J., Chaffin, D.B., 1978. An investigation of the relationship between displacements of the finger and wrist joints and the extrinsic finger flexor tendons. Journal of Biomechanics 11 (3), 119–128.

Barr, A.E., Barbe, M.F., Clark, B.D., 2004. Work-related musculoskeletal disorders of the hand and wrist: epidemiology, pathophysiology, and sensorimotor changes. Journal of Orthopaedic & Sports Physical Therapy 34 (10), 610–627.

Bongers, F.J., Schellevis, F.G., van den Bosch, W.J., van der Zee, J., 2007. Carpal tunnel syndrome in general practice (1987 and 2001): incidence and the role of occupational and non-occupational factors. British Journal of General Practice 57 (534), 36–39.

Brand, P.W., Cranor, K.C., Ellis, J.C., 1975. Tendon and pulleys at the metacarpophalangeal joint of a finger. Journal of Bone & Joint Surgery 57A (6), 779−784.

Delp, S.L., Anderson, F.C., Arnold, A.S., Loan, P., Habib, A., John, C.T., Guendelman, E., Thelen, D.G., 2007. OpenSim: open-source software to create and analyze dynamic simulations of movement. IEEE Transactions on Biomedical Engineering 54 (11), 1940–1950.

Ettema, A.M., Amadio, P.C., Zhao, C., Wold, L.E., O'Byrne, M.M., Moran, S.L., An, K.N. 2006a. Changes in the functional structure of the tenosynovium in idiopathic carpal tunnel syndrome: a scanning electron microscope study. Plastic and Reconstructive Surgery 118 (6), 1413–1422.

Ettema, A.M., An, K.N., Zhao, C., O'Byrne, M.M. Amadio, P.C. 2008. Flexor tendon and synovial gliding during simultaneous and single digit flexion in idiopathic carpal tunnel syndrome. Journal of Biomechanics 41 (2), 292–298.

Ettema, A.M., Belohlavek, M., Zhao, C., Oh, S.H., Amadio, P.C., An, K.N. 2006b. High-resolution ultrasound analysis of subsynovial connective tissue in human cadaver carpal tunnel. Journal of Orthopaedic Research 24 (10), 2011–2020.

Franko, O.I., Winters, T.M., Tirrell, T.F., Hentzen, E.R., Lieber, R.L., 2011. Moment arms of the human digital flexors. Journal of Biomechanics 44 (10), 1987–1990.

Garrett, J.W., 1970. *Anthropometry of the hands of male air force flight personnel*. Dayton: United States Air Force (Aerospace Medical Research Division).

Gelfman, R., Melton, L.J., Yawn, B.P., Wollan, P.C., Amadio, P.C., Stevens, J.C., 2009. Long-term trends in carpal tunnel syndrome. Neurology 72 (1), 33–41.

Greiner, T.M., 1991. *Hand anthropometry of U.S. army personnel*. Natick: United States Natick Research (Development and Engineering Center).

Guimberteau, J.C., Delage, J.P., McGrouther, D.A., Wong, J.K.F., 2010. The microvacuolar system: how connective tissue sliding works. Journal of Hand Surgery 35E (8), 614–622.

Horii, E., Lin, G.T., Cooney, W.P., Linscheid, R.L., An, K.N., 1992. Comparative flexor tendon excursion after passive mobilization: an in vitro study. Journal of Hand Surgery 17A (3), 559–566.

Keir, P.J., Cocchiarella, D.M., Kociolek, A.M., 2013. Development of a kinematic hand model with a realistic representation of the metacarpal arch. In proceedings of XXIV Congress of the International Society of Biomechanics. Natal, RN.

Keir, P.J., Rempel, D.M., 2005. Pathomechanics of peripheral nerve loading: evidence in carpal tunnel syndrome. Journal of Hand Therapy 18 (2), 259–269.

Keir, P.J., Wells, R.P., 1999. Changes in geometry of the finger flexor tendons in the carpal tunnel with wrist posture and tendon load: an MRI study on normal wrists. Clinical Biomechanics 14 (9), 635–645.

Kociolek, A.M., Keir, P.J., 2013. Assessing flexor tendon and subsynovial connective tissue excursion with colour Doppler ultrasound. In proceedings of XXIV Congress of the International Society of Biomechanics. Natal, RN.

Kociolek, A.M., Keir, P.J., 2011. Modelling tendon excursions and moment arms of the finger flexors: anatomic fidelity versus function. Journal of Biomechanics 44 (10), 1967–1973.

Kociolek, A.M., Tat, J., Keir, P.J., 2015. Biomechanical risk factors and flexor tendon frictional work in the cadaveric carpal tunnel. Journal of Biomechanics 48 (3), 449−455.

Korstanje, J.W.H., Schreuders, T.R., van der Sijde, J., Hovius, S.E., Bosch, J.G., Selles, R.W., 2010. Ultrasonographic assessment of long finger tendon excursion in zone v during passive and active tendon gliding exercises. Journal of Hand Surgery 35A (4), 559–565.

Kuo, L.C., Su, F.C., Chiu, H.Y., Yu, C.Y., 2002. Feasibility of using a video-based motion analysis system for measuring thumb kinematics. Journal of Biomechanics 35 (11), 1499–1506.

Landsmeer, J.M., 1961. Studies in the anatomy of articulation. I. The equilibrium of the intercalated bone. Acta Morphologica Neerlando-Scandinavica 3, 287–303.

Lopes, M.M., Lawson, W., Scott, T., Keir, P.J., 2011. Tendon and nerve excursion in the carpal tunnel in healthy and CTD wrists. Clinical Biomechanics 26 (9), 930–936.

Manktelow, R.T., Binhammer, P., Tomat, L.R., Bril, V., Szalai, J.P., 2004. Carpal tunnel syndrome: cross-sectional and outcome study in Ontario workers. Journal of Hand Surgery 29A (2), 307–317.

McDicken, W.N., 1991. *Diagnostic Ultrasonics: Principles and Use of Instruments.* Edinburgh: Churchill Livingstone.

Moore, A., Wells, R., Ranney, D., 1991. Quantifying exposure in occupational manual tasks with cumulative trauma disorder potential. Ergonomics 34 (12), 1433–1453.

Nelson, J.E., Treaster, D.E., Marras, W.S., 2000. Finger motion, wrist motion and tendon travel as a function of keyboard angles. Clinical Biomechanics 15 (7), 489–498.

Oh, S., Belohlavek, M., Zhao, C., Osamura, N., Zobitz, M.E., An, K.N., Amadio, P.C., 2007. Detection of differential gliding characteristics of the flexor digitorum superficialis tendon and subsynovial connective tissue using color Doppler sonographic imaging. Journal of Ultrasound in Medicine 26 (2), 149–155.

Osamura, N., Zhao, C., Zobitz, M.E., An, K.N., Amadio, P.C., 2007a. Evaluation of the material properties of the subsynovial connective tissue in carpal tunnel syndrome. Clinical Biomechanics 22 (9), 999–1003.

Osamura, N., Zhao, C., Zobitz, M.E., An, K.N., Amadio, P.C., 2007b. Permeability of the subsynovial connective tissue in the human carpal tunnel: a cadaver study. Clinical Biomechanics 22 (5), 524–528.

Peolsson, M., Löfstedt, T., Vogt, S., Stenlund, H., Arndt, A., Trygg, J., 2010. Modelling human musculoskeletal functional movements using ultrasound imaging. BMC Medical Imaging 10 (1), 9.

Tapadia, M., Mozaffar, T., Gupta, R., 2010. Compressive neuropathies of the upper extremity: update on pathophysiology, classification, and electrodiagnostic findings. Journal of Hand Surgery 35A (4), 668–677.

Tat, J., Kociolek, A.M., Keir, P.J., 2013. Repetitive differential finger motion increases shear strain between the flexor tendon and subsynovial connective tissue. Journal of Orthopaedic Research 31 (10), 1533–1539.

Tat, J., Kociolek, A.M., Keir, P.J., 2014. Validation of colour Doppler ultrasonography for evaluating relative displacement between flexor tendon and subsynovial connective tissue. Journal of Ultrasound in Medicine, Accepted, July 22, 2014.

Treaster, D.E., Marras, W.S., 2000. An assessment of alternate keyboards using finger motion, wrist motion and tendon travel. Clinical Biomechanics 15 (7), 499–503.

Ugbolue, U.C., Nicol, A.C., 2010. A comparison of two interventions designed to promote neutral wrist postures during simple computer operations. *Work: A Journal of Prevention, Assessment and Rehabilitation* 37 (4), 413–424.

van Doesburg, M.H., Yoshii, Y., Henderson, J., Villarraga, H.R., Moran, S.L., Amadio, P.C., 2012. Speckle-tracking sonographic assessment of longitudinal motion of the flexor tendon and subsynovial tissue in carpal tunnel syndrome. Journal of Ultrasound in Medicine 31 (7), 1091–1098.

Vanhees, M., Morizaki, Y., Thoreson, A.R., Larson, D., Zhao, C., An, K.N., Amadio, P.C., 2012. The effect of displacement on the mechanical properties of human cadaver subsynovial connective tissue. Journal of Orthopaedic Research 30 (11), 1732–1737.

Wu, G., van der Helm, F.C.T., Veeger, H.E.J., Makhsous, M., Van Roy, P., Anglin, C., Nagels, J., Karduna, A.R., McQuade, K., Wang, X., Werner, F.W., Buchholz, B., 2005. ISB recommendation on definitions of joint coordinate systems of various joints for the reporting of human joint motion – Part II: shoulder, elbow, wrist and hand. Journal of Biomechanics 38 (5), 981–992.

Yamaguchi, T., Osamura, N., Zhao, C., An, K.N., Amadio, P.C., 2008. Relative longitudinal motion of the finger flexors, subsynovial connective tissue, and median nerve before and after carpal tunnel release in a human cadaver model. Journal of Hand Surgery 33 (6), 888–892.

Yoshii, Y., Villarraga, H.R., Henderson, J., Zhao, C., An, K.N., Amadio, P. C., 2009a. Speckle tracking ultrasound for assessment of the relative motion of flexor tendon and

subsynovial connective tissue in the human carpal tunnel. Ultrasound in Medicine & Biology 35 (12), 1973–1981.

Yoshii, Y., Zhao, C., Henderson, J., Zhao, K.D., An, K.N., Amadio, P.C., 2009b. Shear strain and motion of the subsynovial connective tissue and median nerve during single-digit motion. Journal of Hand Surgery 34A (1), 65–73.

Yoshii, Y., Zhao, C., Henderson, J., Zhao, K.D., An, K.N., Amadio, P.C., 2011. Velocity-dependent changes in the relative motion of the subsynovial connective tissue in the human carpal tunnel. Journal of Orthopaedic Research 29 (1), 62–66.

Zakaria, D., Robertson, J., Koval, J., MacDermid, J., Hartford, K., 2004. Rates of claims for cumulative trauma disorder of the upper extremity in Ontario workers during 1997. Chronic Diseases and Injuries in Canada 25 (1), 22–31.

Zhao, C., Ettema, A.M., Berglund, L.J., An, K.N., Amadio, P.C., 2011. Gliding resistance of flexor tendon associated with carpal tunnel pressure: a biomechanical cadaver study. Journal of Orthopaedic Research 29 (1), 58–61.

CHAPTER FOUR

Relative Motion between the Flexor Digitorum Superficialis Tendon and Subsynovial Connective Tissue Increases with Wrist Flexion Angle

Aaron M. Kociolek and Peter J. Keir*

Department of Kinesiology, McMaster University, Hamilton, Ontario, Canada

*Corresponding Author:
Peter J. Keir, PhD
Department of Kinesiology
McMaster University
1280 Main Street West
Hamilton, ON L8S 4K1, Canada
Phone: (905) 525-9140 (x23543)
Fax: (905) 523-6011
Email: pjkeir@mcmaster.ca

Type: Original Article

Planned Journal Submission: *Journal of Orthopaedic Research*

4.1. Abstract

Carpal tunnel syndrome is histologically characterized by non-inflammatory fibrosis of the subsynovial connective tissue (SSCT), which likely arises from excessive shear between the finger flexor tendons and SSCT. We assessed relative motion between the flexor digitorum superficialis (FDS) tendon and adjacent SSCT using ultrasound as 16 healthy participants completed three long finger movements (metacarpophalangeal joint flexion, proximal and distal interphalangeal joint flexion, full finger flexion) in three wrist postures (30° extension, 0°, 30° flexion). While the type of finger movement did not influence relative displacement between FDS tendon and SSCT, relative displacement (as a percentage of overall tendon displacement) increased from 27.2 ± 1.9% in 30° wrist extension to 39.9 ± 2.1% in 30° wrist flexion ($p<0.001$). No kinematic differences were found in finger motion between the three wrist postures. These results suggest greater susceptibility to shear injury during repetitive finger movements, especially with the wrist flexed. While our findings generally agree with previous cadaveric research, FDS-SSCT relative displacements differed in wrist extension. This discrepancy may stem from strain-related changes of the SSCT owing to challenges in preserving carpal tunnel anatomy *in vitro*. Our results emphasize the importance of *in vivo*, participant-driven, research using imaging techniques such as ultrasound.

Keywords: posture, carpal tunnel, shear, strain, ultrasound

4.2. Introduction

Carpal tunnel syndrome (CTS) is a pressure-induced compression of the median nerve. Elevated pressures arise from changes in the size and shape of the carpal tunnel as well as the volume and material properties of its contents (Ettema et al., 2004). Increased volume of the contents within the carpal tunnel is thought to be an important factor since non-inflammatory fibrosis and thickening of the subsynovial connective tissue (SSCT) surrounding the finger flexor tendons are common in patients with CTS (Barr et al., 2004; Ettema et al., 2006a; Jinrok et al., 2004). These pathological changes are pronounced in the tenosynovial layers adjacent to the finger flexor tendons, likely due to shear between the tendons and SSCT (Ettema et al., 2006a; Schuind et al., 1990). Excessive and repetitive shear forces are thought to initiate a series of mechanical events, including altered stiffness and permeability of the SSCT (Osamura et al., 2007a, b), increased volume of the contents in the carpal tunnel (Ettema et al., 2006a; Jinrok et al., 2004), elevated pressures (Zhao et al., 2011), ischemia (Keir and Rempel, 2005), and compression of the median nerve. CTS patients show either increased adherence or increased dissociation between the finger flexor tendons and SSCT compared to healthy controls, which may increase shear forces even further (Ettema et al., 2008).

Over the past few years, ultrasound has been used to assess musculoskeletal dynamics due to advances in image resolution (Ettema et al., 2006b; Korstanje et al., 2010a; Lopes et al., 2011; Peolsson et al., 2010; Tat et al., 2013; van Doesburg et al., 2012; Yoshii et al., 2009a). Oh et al. (2007) used colour Doppler ultrasound to show that relative motion between flexor digitorum superficialis (FDS) tendon and adjacent SSCT

increased with tendon velocities from 2.5 − 10 cm/s. Tat et al. (2015) validated colour Doppler imaging for FDS tendon displacement, and also found that relative displacement between FDS tendon and SSCT increased with tendon velocity (between 5 and 15 cm/s). Furthermore, tenosynovial relative displacements are influenced by several workplace exposures that increase injury risk, including wrist posture (Yoshii et al., 2008), speed of work (Yoshii et al., 2011), single finger motion (Yoshii et al., 2009b), and task duration (Tat et al., 2013). These findings support an injury mechanism of tendon shear, and demonstrate the need to better understand the relationship between, occupational risk factors, relative motion of tendon-SSCT, and fibrosis in patients with CTS.

Assessing tendon displacement *in vivo* with spectral Doppler ultrasound, Lopes et al. (2011) found that concurrent wrist and finger flexion produced larger FDS displacements than the sum of tendon displacements from isolated joint movements. Disproportionately greater tendon displacements with combined non-neutral wrist and finger flexion angles are particularly important since tendon travel is related to shear in the carpal tunnel (Nelson et al., 2000; Treaster and Marras, 2000). However, there is a need to assess relative displacement between the FDS tendon and adjacent SSCT, which may be better related to the underlying injury mechanisms. Yoshii et al. (2008) demonstrated that relative displacement between the FDS tendon and SSCT increased with wrist flexion angle using fluoroscopy in upper limb cadavers. However, the finger flexor tendons were displaced with a motor to simulate finger flexion, presenting a challenge in fully elucidating the relationship between finger movement, wrist angle, and relative tenosynovial displacement.

The purpose of this study was to investigate relative motion between the third (long) finger FDS tendon and adjacent SSCT during individual and combined finger joint movements in different wrist positions. We tested metacarpophalangeal and interphalangeal joint flexion, individually and concurrently, in three wrist postures (30° flexion, 0°, 30° extension). Optical motion capture was used to determine and account for kinematic differences (if any) between the finger movements. We hypothesized that (a) combined metacarpophalangeal and interphalangeal joint flexion would result in greater tendon and SSCT motion than summing the individual movements, and (b) non-neutral wrist postures would increase relative motion between the FDS and SSCT.

4.3. Methods

4.3.1. Participants

Sixteen healthy participants (8 men and 8 women) provided written informed consent prior to completing this study, which was approved by the Hamilton Integrated Research Ethics Board. Participants completed a brief questionnaire to screen for health conditions that may influence tendon gliding in the carpal tunnel. Exclusion criteria included degenerative joint disease, arthritis, gout, hemodialysis, sarcoidosis, amyloidosis, hypothyroidism, diabetes mellitus, acute injury of the upper extremity, wrist tendinopathy, peripheral nerve disease, and pain, tingling, or numbness of the hand.

4.3.2. Experimental Protocol

Participants were seated at an adjustable table with their right arm at their side (~ 0° shoulder abduction) and elbow bent (~ 120° elbow flexion). The right forearm was immobilized in a mid-prone posture with a thermoplastic splint. A custom handgrip

(outer diameter 3.5 cm) fixed the index, ring, and little fingers in a mid-flexed position, permitting only the long finger to move freely (Figure 4.1). The handgrip was also connected with the testing apparatus to keep the wrist joint at different flexion/extension angles (30° flexion, 0°, 30° extension).

Figure 4.1. Testing apparatus for performing cyclical long finger movements. A custom handgrip fixed the index, ring, and little fingers, allowing only the long finger to move freely. The handgrip also interlocked with the apparatus to set the wrist joint in each test posture.

Participants performed three long finger movements: (i) metacarpophalangeal (MCP) joint flexion/extension (F/E), (ii) combined proximal and distal interphalangeal (PIP + DIP) joint F/E, (iii) concurrent performance of movements (i) and (ii), or F/E of the full finger (FF). All three finger movements were performed in three static wrist postures (30° flexion, 0°, 30° extension). Participants practiced the finger movements with the investigator before data collection to minimize potential learning effects. Each finger movement was performed for 10 seconds at a self-selected pace. The three finger movement conditions were randomized in each wrist posture, which were counter-balanced to mitigate order effects.

4.3.3. Colour Doppler Imaging

An ultrasound scanner (Vivid Q, General Electric Healthcare Ltd., Milwaukee, WI) equipped with a high-frequency probe (12L-RS) was used to image the proximal wrist. The probe was positioned longitudinally approximately 2 cm proximal to the distal wrist crease with a custom holding device. The flexor digitorum superficialis tendon of the long finger was identified based on its speckled pattern while the adjacent subsynovial connective tissue was hyperechoic in appearance.

FDS tendon and adjacent SSCT velocities were represented by colour Doppler imaging overlaid on grey-scale ultrasound (Figure 4.2). Sonographic settings were optimized for musculoskeletal tissue, in line with previous ultrasound assessments of the wrist using colour imaging (Tat et al., 2013, 2015). The greyscale image depth was set to 3.0 cm and transducer acquisition frequency was 13.0 MHz. The colour Doppler scale was ± 11.0 cm/s to coincide with the high-range of tendon velocity during full finger

flexion (before correcting for the insonation angle). We also set a low velocity reject of 1.3 cm/s to reduce motion artifact. The steering angle of the ultrasound probe was maximized at 20°, and supplemented with a stand-off gel wedge (Aquaflex Gel Pad, Parker Laboratories Inc., Fairfield, NJ), which reduced the angle of insonation to approximately 60°. Ten-second video clips of each finger movement were recorded at 29.5 frames per second.

Greyscale sonograms superimposed with colour imaging were processed off-line using dedicated software (EchoPAC, General Electric Healthcare Ltd., Milwaukee, WI). The quantitative analysis toolkit (Q-Analysis) was used to position circular regions of interest (diameter = 0.5 mm) in the colour Doppler window and obtain velocity-time series (Figure 4.2). Three markers were placed along the FDS tendon ($FDS_{Proximal}$, FDS_{Centre}, FDS_{Distal}) while three adjacent markers were placed in the SSCT ($SSCT_{Proximal}$, $SSCT_{Centre}$, $SSCT_{Distal}$). Each marker maintained fixed a position for the 10-second trial. The markers were visually inspected throughout the trial to confirm tracking of the correct anatomical structures. Velocity profiles from all six markers were exported as text files for further analysis.

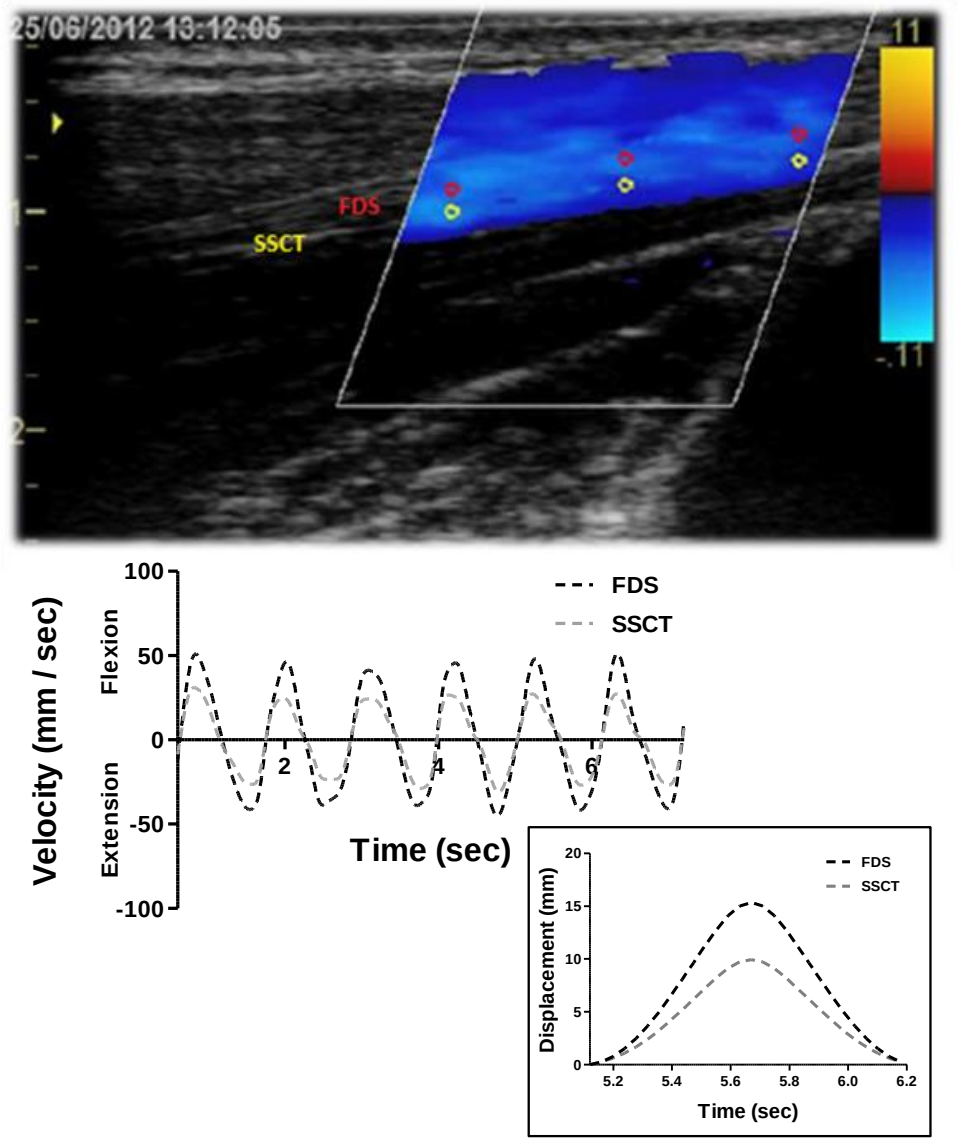

Figure 4.2. (Top) Grayscale image of the proximal wrist showing the long finger FDS tendon and adjacent SSCT. The superimposed colour map represents velocity of the underlying anatomical structures. Circular regions of interest depict FDS tendon (red) and SSCT (yellow) locations selected for further analysis. (Bottom) FDS tendon and SSCT velocity-time data during a cyclical long finger movement. The inset displays a displacement profile for one finger flexion/extension cycle.

Velocity-time profiles for the three FDS tendon markers and three adjacent SSCT markers were ensemble averaged, and dual low-pass filtered at 6.0 Hz (MatLab 7.6, The Mathworks Inc., Natick, MA). FDS tendon and SSCT velocities were corrected for the angle of insonation ($\cos\theta$), and integrated to obtain displacement-time series. Relative motion between the FDS tendon and SSCT were assessed using two measures, including a ratio of the maximum velocities between the two structures in equation 4.1 as well as a measure of relative displacements during both finger flexion and finger extension in equation 4.2 (Yoshii et al., 2008).

$$MVR = SSCT_{MaxVel} / FDS_{MaxVel} \cdot 100\%, \quad (4.1)$$

where MVR is the maximum velocity ratio (%), $SSCT_{MaxVel}$ is SSCT peak velocity (mm/sec), and FDS_{MaxVel} is FDS tendon peak velocity (mm/sec).

$$RDI = (FDS_{Disp} - SSCT_{Disp}) / FDS_{Disp} \cdot 100\%, \quad (4.2)$$

where RDI is the relative displacement index (%), $SSCT_{Disp}$ is SSCT displacement (mm), and FDS_{Disp} is FDS tendon displacement (mm).

4.3.4. Joint Kinematics

Wrist and long finger joint kinematics were obtained with 12 digital cameras (Raptor-4, Motion Analysis Corp., Santa Rosa, CA). Twenty-six hemispherical markers (diameter = 4 mm) were affixed to the forearm, hand, and long finger (Figure 4.3). Marker coordinates were collected at 120 Hz (Cortex 1.3, Motion Analysis Corp., Santa Rosa, CA). A digital trigger marked the beginning of each trial for both motion capture and ultrasound to synchronize the data in post-processing. Marker coordinates were fed into a kinematic hand model to calculate long finger joint flexion angles. The hand model is fully described in Keir et al. (2013). The model defined the metacarpals and the finger phalanges as independent segments with unconstrained movement in 6 degrees of freedom (Figure 4.3). The metacarpals were modelled as elliptical cylinders using reflective markers on the palmar and dorsal wrist crease and the palmar and dorsal metacarpophalangeal joints. The finger phalanges were represented by truncated cones from markers on the palmar and dorsal finger joints (at the joint creases) and the fingertips.

Figure 4.3. Reflective markers affixed to the palmar (top) and dorsal (bottom) surfaces of the forearm, hand, and long finger. Calibration markers over anatomical landmarks were used to model the hand in a neutral pose and were removed for subsequent trials. Triad marker clusters were used to track finger movement throughout the experimental protocol, which fed into a kinematic hand model (inset).

A static calibration trial, with all twenty-six reflective markers, was applied to the model template to represent participant-specific anthropometrics. Calibration markers on anatomical landmarks were removed for subsequent finger movement trials, and marker triads on the dorsal metacarpal and phalanges of the long finger tracked the segments in six degrees of freedom (Keir et al., 2013). Long finger joint kinematics were calculated using an x-y-z Cardan sequence (anatomically equivalent to flexion/extension - abduction/adduction - pronation/supination) according to the International Society of Biomechanics (Wu et al., 2005).

4.3.5. Statistical Analyses

The maximum velocity ratio (MVR) and relative displacement index (RDI) were calculated for both the finger flexion and finger extension phase of each cyclical finger movement performed during the 10-second trials. Mean scores of all cycles were tabulated for each trial. MVR and RDI means (± standard errors of the means) were reported for each experimental condition (n = 16). Three-way repeated measures analysis-of-variance models tested the effects of finger movement (MCP F/E, PIP + DIP F/E, FF F/E), wrist posture (30° flexion, 0°, 30° extension), and finger direction (finger flexion versus finger extension) on FDS tendon and SSCT velocities and displacements, the MVR and RDI, and long finger joint kinematics (from motion capture). Significant main effects and interactions were followed up with Tukey's HSD ($\alpha = 0.05$).

4.4. Results

4.4.1. Joint Kinematics

There was a significant main effect of finger movement on the change in MCP joint flexion ($F_{2,30} = 154.1$, $p < 0.001$) and PIP joint flexion ($F_{2,30} = 262.0$, $p < 0.001$). Across all wrist postures, PIP + DIP joint F/E produced large changes in PIP joint flexion with only slight changes to MCP joint flexion (Table 4.1). MCP joint F/E produced 53.7° ± 3.2° of MCP joint flexion and 19.7° ± 3.4° of unintended PIP joint flexion. As was expected, FF F/E produced large changes to both MCP and PIP joint flexion (Table 4.1). Across all three long finger movements, wrist posture did not influence the change in MCP joint flexion ($F_{2,30} = 1.4$, $p = 0.265$) and PIP joint flexion ($F_{2,30} = 0.6$, $p = 0.582$).

Table 4.1. Mean (± standard error of the mean) changes in metacarpophalangeal and proximal interphalangeal joint flexion angles during three active long finger motions in three different wrist postures. Lower case letters indicate significant differences between the different finger movements.

Finger Motion	**Wrist Posture**		
	30° Flexion	**0°**	**30° Extension**
	Metacarpophalangeal joint flexion angles		
MCP	52.4° ± 2.7° *c*	52.7° ± 3.0° *c*	55.9° ± 2.7° *c*
PIP + DIP	0.6° ± 2.8° *a*	1.8° ± 2.5° *a*	4.2° ± 2.5° *a*
FF	37.2° ± 4.0° *b*	38.7° ± 2.9° *b*	38.1° ± 3.7° *b*
	Proximal interphalangeal joint flexion angles		
MCP	16.1° ± 3.3° *a*	20.9° ± 3.0° *a*	22.2° ± 4.0° *a*
PIP + DIP	87.8° ± 4.2° *b*	90.1° ± 3.7° *b*	89.4° ± 4.5° *b*
FF	105.8° ± 3.3° *c*	105.7° ± 2.3° *c*	104.1° ± 3.6° *c*

MCP – Metacarpophalangeal joint flexion/extension; PIP + DIP – Proximal and distal interphalangeal joint flexion/extension; FF – Full finger flexion/extension.

4.4.2. FDS Tendon and SSCT Velocity

FDS tendon velocity was affected by finger movement ($F_{2,30} = 51.2$, $p < 0.001$). FF F/E produced the highest peak tendon velocity, followed by MCP joint F/E and PIP + DIP joint F/E (Figure 4.4a). There was a significant main effect of finger direction ($F_{1,15} = 27.9$, $p < 0.001$), with higher peak tendon velocities during finger extension (52.1 ± 2.5 mm/sec) than finger flexion (46.1 ± 2.3 mm/sec). FDS tendon velocity was not influenced by wrist posture.

There was a main effect of finger movement on SSCT velocity ($F_{2,30} = 36.0$, $p < 0.001$). FF F/E produced higher peak SSCT velocities than MCP joint F/E, which were higher than PIP + DIP joint F/E (Figure 4.4b). Wrist posture also influenced peak SSCT velocity, with a 27.3% increase from 30° wrist flexion to 30° wrist extension ($F_{2,30} = 9.8$, $p < 0.001$). Higher peak SSCT velocities were observed for finger extension (34.0 ± 1.9 mm/sec) compared to finger flexion (30.7 ± 1.7 mm/sec) ($F_{1,15} = 23.2$, $p < 0.001$).

While finger movement did not affect the MVR, there was a significant main effect of wrist posture on the MVR ($F_{2,30} = 15.6$, $p < 0.001$). MVR decreased from 72.2% ± 1.9% at 30° wrist extension to 59.8% ± 1.8% at 30° wrist flexion, indicating a greater difference between SSCT velocity and FDS tendon velocity when the wrist was flexed (Figure 4.4c). There was also a small but significant main effect of movement direction on the MRV, with a lower MRV during finger extension (65.7% ± 1.67%) than finger flexion (67.4% ± 1.53%) ($F_{1,15} = 5.3$, $p = 0.036$).

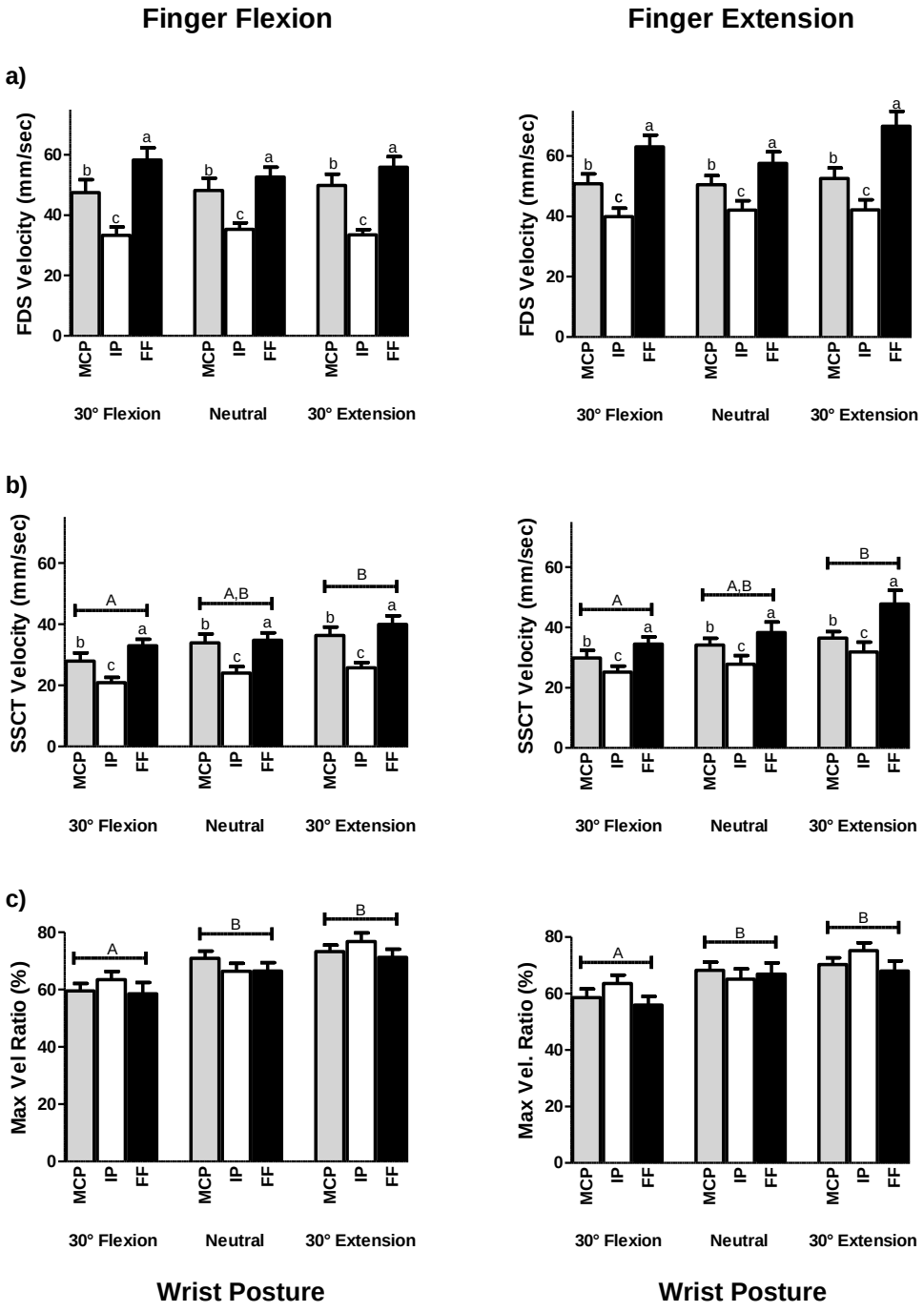

Figure 4.4. Peak velocity of the (a) FDS tendon and (b) SSCT as well as the (c) MVR during finger flexion (left) and finger extension (right). MCP – Metacarpophalangeal joint flexion/extension; IP – Proximal and distal interphalangeal joint flexion/extension; FF – full finger flexion/extension. Lower case letters indicate significant differences for type of finger movements while upper case letters are significant differences for wrist postures.

4.4.3. FDS Tendon and SSCT Displacement

FDS tendon displacements were similar for all three wrist postures (Figure 4.5a). However, there was a significant main effect of finger movement ($F_{2,30} = 71.6$, $p < 0.001$), with the largest FDS tendon displacement during FF F/E, followed by MCP joint F/E and PIP + DIP joint F/E. SSCT displacements displayed a similar main effect for the three finger movements (Figure 4.5b). Furthermore, wrist posture influenced displacements of the SSCT, which increased 29.4% from 30° wrist flexion to 30° wrist extension ($F_{2,30} = 10.8$, $p < 0.001$). There was a main effect of wrist posture on the relative displacement between FDS tendon and adjacent SSCT ($F_{2,30} = 41.7$, $p < 0.001$). The lowest RDI occurred in 30° wrist extension (27.2% ± 1.9%) and increased in 30° wrist flexion (39.9% ± 2.1%). There were no significant differences between the three finger movements on the RDI (Figure 4.5c).

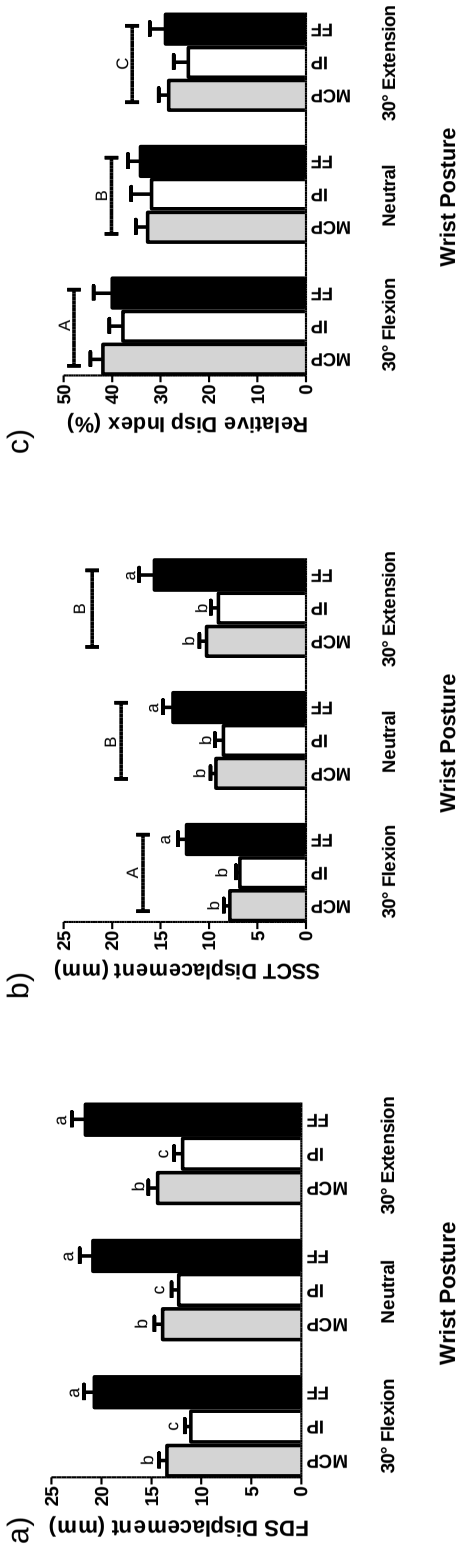

Figure 4.5. Longitudinal displacement of the (a) FDS tendon and (b) SSCT as well as the (c) RDI. MCP – Metacarpophalangeal joint flexion/extension; IP – Proximal and distal interphalangeal joint flexion/extension; FF – full finger flexion/extension. Lower case letters indicate significant differences for type of finger movements while upper case letters are significant differences for wrist postures.

4.5. Discussion

We investigated the effect of wrist posture on relative motion between FDS tendon and the adjacent SSCT as 16 healthy participants completed active long finger movements. Compared to the neutral wrist (0°), FDS-SSCT relative displacement increased with 30° wrist flexion and decreased with 30° wrist extension. While tendon velocity and displacement were not affected by wrist posture, SSCT velocity and displacement both decreased from 30° wrist extension to 30° wrist flexion, leading to increased relative motion assessed by the MVR (maximum velocity ratio) and RDI (relative displacement index). Motion capture showed similar finger joint kinematics between the three wrist postures, further suggesting that the characteristics of the SSCT were responsible for changes in the MVR and RDI. Our results indicate a greater likelihood of a shear injury during repetitive movements when the wrist is flexed.

Yoshii et al. (2008) also demonstrated that relative motion between FDS tendon and SSCT increased with wrist flexion angle using fluoroscopy in cadaver limbs. Furthermore, the absolute change in RDI from 0° to 30° wrist flexion was comparable between the current study (+7.0%) and Yoshii et al. (+5.0%). We also found a significant 5.7% decrease in relative displacement from 0° to 30° wrist extension while Yoshii and colleagues (2008) found similar relative displacements for 0°, 30°, and 60° wrist extension. Testing the effect of wrist posture on FDS-SSCT relative motion and shear in a cadaveric model is particularly challenging since the flexor tendons are often detached from both the proximal and distal attachment sites (Kociolek et al., 2015; Smutz et al., 1994; Tat et al., 2015; Yoshii et al., 2008, 2009, 2011). The finger flexor tendons and

connected SSCT move proximally during wrist flexion and distally during wrist extension, which may be difficult to represent in a cadaveric model. Strain-related changes of the SSCT during wrist motion influence its viscoelastic properties, which in turn affect relative motion between FDS tendon and adjacent SSCT.

Regardless of the differences in wrist extension, Yoshii et al. (2008) and the current study both showed greater relative displacements in wrist flexion. This suggests that tenosynovial strain and shear due to repetitive finger movement is greater with the wrist flexed while carpal tunnel pressure may have a larger role in the development of injury during wrist extension (Keir et al., 2007). However, the interplay between these two injury mechanisms is complicated by research showing that artificially manipulated carpal tunnel pressure increases tendon gliding resistance *in vitro* (Zhao et al., 2011). Additional studies are needed to shed further light on the potential relationship between injury mechanisms of CTS, including tenosynovial shear and carpal tunnel pressure. Admittedly, determining the interrelationships between different etiologies may prove challenging, even in cadaveric models with stringent controls.

We tested three finger flexion (F/E) movements including the MCP joint, PIP + DIP joints, and the full finger (FF). MCP joint F/E resulted in 13.9 ± 0.7 mm of FDS tendon displacement, and PIP + DIP joint F/E produced 11.7 ± 0.5 mm. Summing the two finger movements produced 25.6 ± 0.9 mm of tendon displacement for 55.9° ± 3.6° of MCP joint flexion and 108.9° ± 3.8° of PIP joint flexion. Conversely, FF F/E generated smaller tendon displacements of 21.1 ± 1.0 mm; however, finger joint flexion angles were also smaller (MCP – 38.0 ± 2.7 °; PIP – 105.2 ± 2.6 °). Qualitatively, the current results differ

from work by Lopes et al. (2011) showing that multi-joint movements produced larger tendon displacements than summing the individual joint movements (in isolation). Instead our results support traditional models of tendon-joint interaction that consider tendon displacement associated with each finger joint independently (An et al., 1983; Armstrong and Chaffin, 1978). We recently revisited geometric models of tendon-joint interaction, and our results lent further support of an additive model for multi-joint finger movements (Kociolek and Keir, 2015).

While type of finger movement did not significantly affect relative motion, there was a trend towards a lower MVR (greater relative motion) for finger movements with larger tendon velocities and displacements. Full finger F/E produced the lowest MVR of 64.2 ± 2.2 % while PIP + DIP joint F/E generated the highest at 68.2 ± 2.3%. This trend is consistent with cadaver studies that showed prescribed tendon velocity increased relative motion between the FDS tendon and SSCT (Oh et al., 2007; Tat et al., 2015; Yoshii et al., 2011).

The magnitudes of flexor tendon displacements in our study are similar to previous results using diagnostic imaging methods (Korstanje et al., 2010b, 2012; Lopes et al., 2011; Peolsson et al., 2010; Yoshii et al., 2009; Tat et al., 2013) as well as direct measurement techniques *in vitro* (An et al., 1983; Armstrong and Chaffin, 1978; Brand et al., 1975; Horii et al., 1992). Generally, full finger flexion produces 20 – 30 mm of FDS tendon displacement, depending on the method (21.1 ± 1.0 mm in the current study). While our tendon displacements are near the lower end of values in the literature, the handgrip impeded long finger motion near the end range of motion, which may have

decreased tendon displacements compared to similar experimental protocols without end range restrictions (Lopes et al., 2011; Tat et al., 2013). Our measurements of relative motion between FDS tendon and SSCT were also comparable to other colour ultrasound studies (Oh et al., 2007; Tat et al., 2013, 2015). While it is difficult to directly validate motion of the SSCT, we recently compared ultrasound assessment of relative motion (MVR and RDI) with direct measurement of flexor tendon frictional work in human cadavers (Tat et al. 2014). Ultrasound evaluation of relative motion captured subtle time-dependent changes in frictional work, including differences in finger flexion versus finger extension. Therefore, the current method is sensitive to changes in the SSCT.

There are a few limitations to this study. We evaluated FDS tendon and adjacent SSCT displacements for the long finger, which may not be applicable to the other fingers. However, traditional cadaver studies of tendon-joint interaction measured tendon displacements on all four fingers and did not find mechanical distinctions between the fingers. Second, colour Doppler imaging is sensitive to the angle of insonation. We steered the ultrasound beam 20° and used a gel stand-off, reducing the insonation angle to approximately 60° for improved accuracy (McDicken, 1991). Reflective markers were also placed on the hand to measure joint angles via optical motion capture, raising concerns that skin motion artifact may influence the results. However, the finger movements tested were the same for all three wrist postures, and thus any effect of skin motion artifact would be similar in different wrist positions. Kuo et al. (2002) also showed good agreement using skin-surface markers versus a fluoroscopy method with an

adjusted coefficient of multiple determination greater than 0.973 for metacarpophalangeal and interphalangeal joint flexion/extension of the thumb.

In summary, we showed that wrist position affected relative velocity and displacement of FDS tendon and SSCT during cyclical long finger movements *in vivo*. Finger movements during wrist flexion increased relative motion between the tissues, indicating greater tenosynovial shear, and further suggesting increased risk of injury to the SSCT. Furthermore, the use of motion capture ensured that our findings resulted from mechanical events and were not due to behavioral changes. Our results in wrist flexion also matched a previous fluoroscopy study in upper limb cadavers, although differences were noted in wrist extension (Yoshii et al., 2008). This discrepancy from the previous cadaver study highlights the importance of non-invasive imaging studies, *in vivo*, to preserve anatomic fidelity of the tendons and connected SSCT. We believe that determining how workplace exposures influence tenosynovial motion and shear will ultimately result in a better understanding of wrist/hand overuse disorders, and thus provide valuable information on reducing work-related musculoskeletal disorders and facilitating successful and safe return-to-work for injured workers.

Conflict of interest statement: There are no conflicts of interest.

Acknowledgements: Thanks to Katherine Wilson and Jimmy Tat for their assistance with ultrasound during data collection as well as Calvin Tse and Michael Rizzuto for their assistance with motion capture. This work was supported by the Centre of Research Expertise for the Prevention of Musculoskeletal Disorders, the Natural Sciences and

Engineering Research Council of Canada under Discovery Grant # 217382-09, and a doctoral Canada Graduate Scholarship to Aaron M. Kociolek.

4.6. References

An, K.N., Ueba, Y., Chao, E.Y., Cooney, W.P., Linscheid, R.L., 1983. Tendon excursion and moment arm of index finger muscles. Journal of Biomechanics 16 (6), 419−425.

Armstrong, T.J., Chaffin, D.B., 1978. An investigation of the relationship between displacements of the finger and wrist joints and the extrinsic finger flexor tendons. Journal of Biomechanics 11 (3), 119−128.

Barr, A.E., Barbe, M.F., Clark, B.D., 2004. Work-related musculoskeletal disorders of the hand and wrist: epidemiology, pathophysiology, and sensorimotor changes. Journal of Orthopaedic & Sports Physical Therapy 34 (10), 610−627.

Brand, P.W., Cranor, K.C., Ellis, J.C., 1975. Tendon and pulleys at the metacarpophalangeal joint of a finger. Journal of Bone and Joint Surgery 57 (6), 779−784.

Ettema, A.M., Amadio, P.C., Zhao, C., Wold, L.E., An, K.N., 2004. A histological and immunohistochemical study of the subsynovial connective tissue in idiopathic carpal tunnel syndrome. Journal of Bone & Joint Surgery 86 (7), 1458−1466.

Ettema, A.M., Amadio, P.C., Zhao, C., Wold, L.E., O'Byrne, M.M., Moran, S.L., An, K.N., 2006a. Changes in the functional structure of the tenosynovium in idiopathic carpal tunnel syndrome: A scanning electron microscope study. Journal of Plastic & Reconstructive Surgery 118 (6), 1413–1422.

Ettema, A.M., An, K.N., Zhao, C., O'Byrne, M.M., Amadio, P.C., 2008. Flexor tendon and synovial gliding during simultaneous and single digit flexion in idiopathic carpal tunnel syndrome. Journal of Biomechanics 41(2), 292−298.

Ettema, A.M., Belohlavek, M., Zhao, C., Oh, S.H., Amadio, P.C., An, K.N., 2006b. High-resolution ultrasound analysis of subsynovial connective tissue in human cadaver carpal tunnel. Journal of Orthopaedic Research 24 (10), 2011−2020.

Horii, E., Lin, G.T., Cooney, W.P., Linscheid, R.L., An, K.N., 1992. Comparative flexor tendon excursion after passive mobilization: an in vitro study. Journal of Hand Surgery 17A (3), 559−566.

Jinrok, O., Zhao, C., Amadio, P.C., An, K.N., Zobitz, M.E., Wold, L.E., 2004. Vascular pathological changes in the flexor tenosynovium (subsynovial connective tissue) in idiopathic carpal tunnel syndrome. Journal of Orthopaedic Research 22 (6), 1310−1315.

Keir, P.J., Bach, J.M., Hudes, M., Rempel, D.M., 2007. Guidelines for wrist posture based on carpal tunnel pressure thresholds. Human Factors 49 (1), 88−99.

Keir, P.J., Cocchiarella, D.M., Kociolek, A.M., 2013. Development of a kinematic hand model with a realistic representation of the metacarpal arch. In proceedings of XXIV Congress of the International Society of Biomechanics. Natal, RN.

Keir, P.J., Rempel, D.M., 2005. Pathomechanics of peripheral nerve loading: evidence in carpal tunnel syndrome. Journal of Hand Therapy 18 (2), 259–269.

Kociolek, A.M., Keir, P.J., 2015. Development of a kinematic model to predict finger flexor tendon and subsynovial connective tissue displacement in the carpal tunnel. Ergonomics, Accepted, January 20, 2015.

Korstanje, J.W.H., Schreuders, T.R., van der Sijde, J., Hovius, S.E., Bosch, J.G., Selles, R.W., 2010b. Ultrasonographic assessment of long finger tendon excursion in zone v during passive and active tendon gliding exercises. Journal of Hand Surgery 35A (4), 559−565.

Korstanje, J.W.H., Selles, R.W., Stam, H.J., Hovius, S.E.R., Bosch, J.G., 2010a. Development and validation of ultrasound speckle tracking to quantify tendon displacement. Journal of Biomechanics 43 (7), 1373−1379.

Korstanje, J.W.H., Soeters, J.N., Schreuders, T.A., Amadio, P.C., Hovius, S.E., Stam, H.J., Selles, R.W., 2012. Ultrasonographic assessment of flexor tendon mobilization: effect of different protocols on tendon excursion. Journal of Bone & Joint Surgery 94 (5), 394−402.

Kuo, L.C., Su, F.C., Chiu, H.Y., Yu, C.Y., 2002. Feasibility of using a video-based motion analysis system for measuring thumb kinematics. Journal of Biomechanics 35 (11), 1499–1506.

Lopes, M.M., Lawson, W., Scott, T., Keir, P.J., 2011. Tendon and nerve excursion in the carpal tunnel in healthy and CTD wrists. Clinical Biomechanics 26 (9), 930–936.

McDicken, W.N., 1991. Diagnostic ultrasonics: principles and use of instruments. Churchill Livingstone.

Nelson, J.E., Treaster, D.E., Marras, W.S., 2000. Finger motion, wrist motion and tendon travel as a function of keyboard angles. Clinical Biomechanics 15 (7), 489–498.

Oh, S., Belohlavek, M., Zhao, C., Osamura, N., Zobitz, M.E., An, K.N., Amadio, P.C., 2007. Detection of differential gliding characteristics of the flexor digitorum superficialis tendon and subsynovial connective tissue using color Doppler sonographic imaging. Journal of Ultrasound in Medicine 26 (2), 149−155.

Osamura, N., Zhao, C., Zobitz, M.E., An, K.N., Amadio, P.C., 2007a. Evaluation of the material properties of the subsynovial connective tissue in carpal tunnel syndrome. Clinical Biomechanics 22 (9), 999–1003.

Osamura, N., Zhao, C., Zobitz, M.E., An, K.N., Amadio, P.C., 2007b. Permeability of the subsynovial connective tissue in the human carpal tunnel: a cadaver study. Clinical Biomechanics 22 (5), 524–528.

Peolsson, M., Löfstedt, T., Vogt, S., Stenlund, H., Arndt, A., Trygg, J., 2010. Modelling human musculoskeletal functional movements using ultrasound imaging. BMC Medical Imaging 10 (1), 9.

Schuind, F., Ventura, M., Pasteels, J.L., 1990. Idiopathic carpal tunnel syndrome: histologic study of the flexor synovium. Journal of Hand Surgery 15A (3), 497–503.

Smutz, W.P., Miller, S.C., Eaton, C.J., Bloswick, D.S., France, E.P., 1994. Investigation of low-force high-frequency activities on the development of carpal-tunnel syndrome. Clinical Biomechanics 9 (1), 15–20.

Tat, J., Kociolek, A.M., Keir, P.J., 2013. Repetitive differential finger motion increases shear strain between the flexor tendon and subsynovial connective tissue. Journal of Orthopaedic Research 31 (10), 1533−1539.

Tat, J., Kociolek, A.M., Keir, P.J., 2014. Tendon shear is only partially represented by ultrasound shear. 7th World Congress of Biomechanics, Boston, MA.

Tat, J., Kociolek, A.M., Keir, P.J., 2015. Validation of colour Doppler ultrasonography for evaluating relative displacement between flexor tendon and subsynovial connective tissue. Journal of Ultrasound in Medicine 34 (4), 679−687.

Treaster, D.E., Marras, W.S., 2000. An assessment of alternate keyboards using finger motion, wrist motion and tendon travel. Clinical Biomechanics 15 (7), 499–503.

van Doesburg, M.H., Yoshii, Y., Henderson, J., Villarraga, H.R., Moran, S.L., Amadio, P.C., 2012. Speckle-tracking sonographic assessment of longitudinal motion of the

flexor tendon and subsynovial tissue in carpal tunnel syndrome. Journal of Ultrasound in Medicine 31 (7), 1091−1098.

Wu, G., van der Helm, F.C.T., Veeger, H.E.J., Makhsous, M., Van Roy, P., Anglin, C., Nagels, J., Karduna, A.R., McQuade, K., Wang, X., Werner, F.W., Buchholz, B., 2005. ISB recommendation on definitions of joint coordinate systems of various joints for the reporting of human joint motion – Part II: shoulder, elbow, wrist and hand. Journal of Biomechanics 38 (5), 981–992.

Yoshii, Y., Villarraga, H.R., Henderson, J., Zhao, C., An, K.N., Amadio, P.C., 2009a. Speckle tracking ultrasound for assessment of the relative motion of flexor tendon and subsynovial connective tissue in the human carpal tunnel. Ultrasound in Medicine & Biology 35 (12), 1973−1981.

Yoshii, Y., Zhao, C., Henderson, J., Zhao, K.D., An, K.N., Amadio, P.C., 2009b. Shear strain and motion of the subsynovial connective tissue and median nerve during single-digit motion. Journal of Hand Surgery 34 (1), 65−73.

Yoshii, Y., Zhao, C., Henderson, J., Zhao, K.D., An, K.N., Amadio, P.C., 2011. Velocity-dependent changes in the relative motion of the subsynovial connective tissue in the human carpal tunnel. Journal of Orthopaedic Research 29 (1), 62−66.

Yoshii, Y., Zhao, C., Zhao, K.D., Zobitz, M.E., An, K.N., Amadio, P.C., 2008. The effect of wrist position on the relative motion of tendon, nerve, and subsynovial connective tissue within the carpal tunnel in a human cadaver model. Journal of Orthopaedic Research 26 (8), 1153−1158.

Zhao, C., Ettema, A.M., Berglund, L.J., An, K.N., Amadio, P.C., 2011. Gliding resistance of flexor tendon associated with carpal tunnel pressure: a biomechanical cadaver study. Journal of Orthopaedic Research 29 (1), 58−61.

CHAPTER FIVE

Relative Displacement between Flexor Tendon and Subsynovial Connective Tissue Increases with Movement Frequency and Finger Force

Aaron M. Kociolek and Peter J. Keir*

Department of Kinesiology, McMaster University, Hamilton, Ontario, Canada

*Corresponding Author:
Peter J. Keir, PhD
Department of Kinesiology
McMaster University
1280 Main Street West
Hamilton, ON L8S 4K1, Canada
Phone: (905) 525-9140 (x23543)
Fax: (905) 523-6011
Email: pjkeir@mcmaster.ca

Type: Original Article

Planned Journal Submission: *Journal of Biomechanics*

5.1. Abstract

Carpal tunnel syndrome is characterized by non-inflammatory fibrosis of the subsynovial connective tissue (SSCT), suggesting that excessive shear forces during finger flexor tendon displacements are involved in injury development. We tested two well-known biomechanical predictors of injury, frequency and force, using ultrasound assessment of relative displacement between flexor digitorum superficialis (FDS) tendon and the SSCT. Twelve healthy participants performed metacarpophalangeal joint flexion/extension movements using three movement frequencies (0.75, 1.00, 1.25 Hz) and two finger forces (4, 8 N). FDS-SSCT relative displacement expressed as a percentage of overall tendon displacement was lowest at 0.75 Hz (22.5 ± 3.2 %), and increased at 1.00 Hz (32.2 ± 2.9 %) and 1.25 Hz (32.5 ± 2.8 %). While the effect of finger force was considerably smaller than movement frequency, relative displacement also increased with force exertion, from 26.6 ± 3.0 % (4 N) to 31.6 ± 3.0 % (8 N). MCP and PIP joint kinematics measured via electrogoniometry were not influenced by frequency or force, suggesting that changes were due to carpal tunnel mechanics. Since relative displacement is often considered a proxy for friction, we calculated tendon frictional work using a recently published model and fine-wire EMG. Ultrasound assessment of the relative distance travelled between the FDS and SSCT was more sensitive to changes in frequency and force than model predictions of FDS tendon frictional work. The ability to indirectly assess relative displacement using ultrasound may prove fruitful in further elucidating the link between pathomechanics, biomechanical risk factors, and severity of work-related injury.

Keywords: Exertion; repetition; ultrasound; shear; strain

5.2. Introduction

Carpal tunnel syndrome (CTS) is the most common entrapment neuropathy of the upper limb (Barr et al., 2004). CTS prevalence in the general population is 3% (Atroshi et al., 1999); however, the prevalence is substantially higher in industries with exposure to repetitive wrist and finger movements (Davis et al., 2001; Silverstein et al., 1998; Zakaria et al., 2004). Epidemiological studies also support movement frequency and force as physical risk factors for wrist/hand tendinitis, tenosynovitis, and CTS (Frost et al., 1998; Silverstein et al., 1987; Thomsen et al., 2002).

Although it is well known that CTS is caused by compression of the median nerve, the underlying pathomechanics are complex and most likely multi-factorial (Staal et al., 2007). Finger flexor tendinitis and tenosynovitis are often considered precursors to CTS, which may result in elevated carpal tunnel pressure due to inflammation and edema (Barr et al., 2004). Smutz et al. (1994) suggested that tendinitis was caused by mechanical abrasion due to relative motion with other carpal tunnel structures, including adjacent tendons and the median nerve. This pathogenesis is supported by a belt-pulley mechanism (Armstrong and Chaffin, 1979), which provides a conceptual basis to predict tendon friction inside the carpal tunnel (Moore et al., 1991; Tanaka et al., 1993). Moore et al. (1991) quantified tendon displacement and friction using the belt-pulley mechanism, and found that frictional work was a strong predictor of wrist/hand musculoskeletal disorders, including CTS.

More recently, we quantified tendon frictional work through the carpal tunnel *in vitro*, which increased with tendon velocity and tendon force, especially when the wrist was flexed (Kociolek et al., 2015). Direct cadaveric measurement of friction includes contact stress with adjacent carpal tunnel structures as well as viscoelastic gliding resistance of the subsynovial connective tissue or SSCT (Filius et al., 2014; Zhao et al., 2007). This loose connective tissue consists of collagen bundles organized in adjacent layers that are interconnected by small perpendicular fibrils, and attaches the tendons and nerve to the visceral synovium in the carpal tunnel (Guimberteau et al., 1993). During tendon displacement, the SSCT is gradually strained, with layers closest to tendon lengthening first (Guimberteau et al., 2010). Cadaver studies reveal an exponential relationship between tendon displacement and gliding resistance (Kociolek et al., 2015; Zhao et al., 2007), presumably due to the viscoelastic behavior of the SSCT (Osamura et al., 2007a, 2007b). Furthermore, our research indicates strain-dependent characteristics of the SSCT make up the greatest contribution to overall tendon gliding resistance in the carpal tunnel (Tat et al., 2014).

Given that tendon gliding characteristics cannot be directly measured *in vivo*, ultrasound is used to evaluate tendon strain and shear in the carpal tunnel (Kociolek and Keir, 2015; Korstanje et al., 2012; Oh et al., 2007; Tat et al., 2013, Yoshii et al., 2009a). Ultrasound quantifies relative motion between the finger flexor tendons and SSCT. Tendon-SSCT relative motion is influenced by several biomechanical work factors, including single-finger movement (Yoshii et al., 2009b), wrist position (Kociolek and Keir, 2015; Yoshii et al., 2008), speed of work (Yoshii et al., 2011; Tat et al., 2015a), and

task duration (Tat et al., 2013). We recently found that tendon velocity and force each act independently to increase relative displacement between tendon and SSCT inside the cadaveric carpal tunnel (Tat et al., 2014). However, relative displacements may differ in participants than cadavers (Kociolek and Keir, 2015), underscoring the need to test repetitive and forceful motions *in vivo*. Furthermore, there remains a need to better understand how ultrasound measures of relative motion between tendon and the SSCT relate to frictional loss inside the carpal tunnel.

The purpose of this study was to investigate two well-known physical workplace factors, frequency and force of work, on ultrasound assessment of FDS-SSCT relative displacement in 12 healthy participants, and to compare ultrasound with an analytical model of FDS tendon friction in the carpal tunnel (Kociolek et al., 2015). We hypothesized that ultrasound would capture velocity dependent changes associated with the viscous characteristics of tenosynovial gliding, while force would not affect relative displacement between tendon and the SSCT.

5.3. Methods

5.3.1. Participants

Twelve participants provided written informed consent prior to completing the study, which was approved by the Hamilton Integrated Research Ethics Board. A survey was administered to screen for health conditions known to influence tendon gliding in the carpal tunnel. Exclusion criteria were degenerative joint disease, arthritis, gout, hemodialysis, sarcoidosis, amyloidosis, hypothyroidism, diabetes mellitus, acute injury of

the upper limb, peripheral neuropathy, tendinopathy, and pain, tingling, or numbness of the hand.

5.3.2. Anthropometrics

Forearm and hand anthropometrics were measured using the standard by Greiner (1991). Forearm length (olecranon to wrist crease), hand length (wrist crease to middle fingertip) and hand breadth (at the metacarpophalangeal joints) were determined with a measuring tape. Metacarpophalangeal (MCP), proximal interphalangeal (PIP), and distal interphalangeal (DIP) joint thicknesses (at the joint creases) were measured with a digital caliper set. Participant anthropometrics are presented in Table 5.1.

Table 5.1. Anthropometrics of the forearm, hand, and middle finger.

	Mean	**S.D.**
Forearm & hand (cm)		
Forearm length	26.6	1.6
Hand length	18.1	0.9
Hand breadth	7.7	0.5
Middle finger (mm)		
MCP joint thickness	25.5	1.7
PIP joint thickness	16.4	1.2
DIP joint thickness	12.2	0.9

5.3.3. Protocol

Participants were seated at the test apparatus and chair height was adjusted to maintain 120° of right elbow flexion with the arm at the side (0° of shoulder abduction). The forearm was supinated and immobilized with a thermoplastic splint. A custom

handgrip (diameter – 3.5 cm) fixed the index, ring, and little fingers in a mid-flexed posture, allowing only the middle finger (3rd digit) to move freely (Figure 5.1). Velcro strapping attached to the apparatus kept the handgrip in a set position and the wrist joint near neutral (0°).

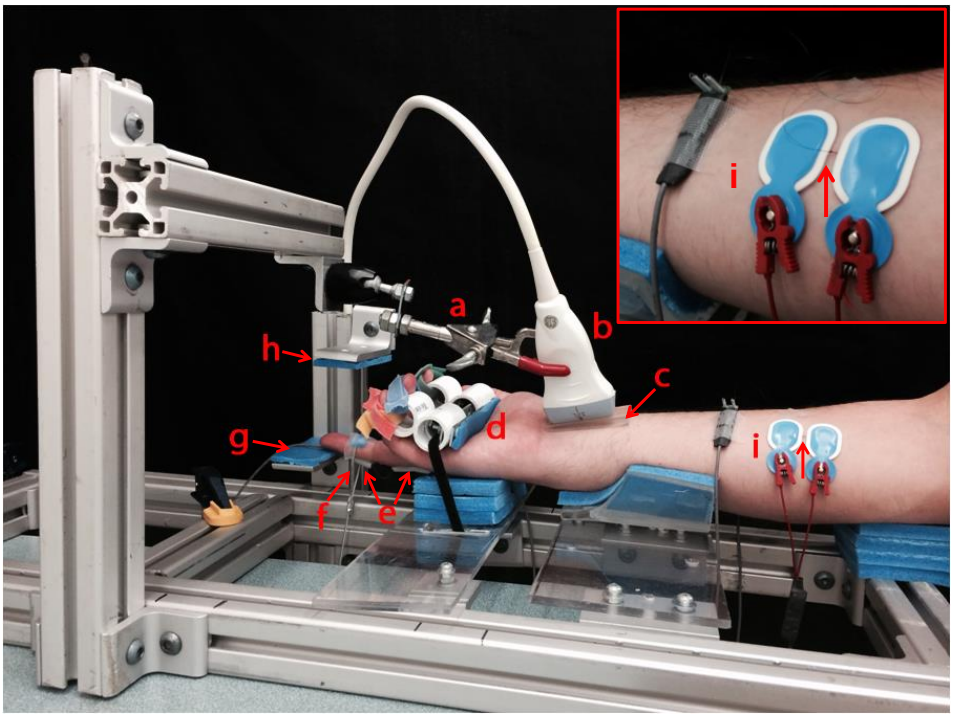

Figure 5.1. Testing apparatus for performing middle finger MCP joint F/E. (a) Probe holder; (b) ultrasound probe; (c) gel wedge standoff; (d) handgrip; (e) electrogoniometers; (f) padded finger ring (attached to constant force spring); (g) extension end range target; (h) flexion end range target; (i) Wire and surface electrodes on FDS.

Each participant performed MCP joint flexion/extension (F/E) with the middle finger in six test conditions, including a combination of three movement frequencies (0.75 Hz, 1 Hz, 1.25 Hz) and two finger forces (4 N and 8 N). Movements were performed cyclically and continuously in 10-second trials. Participants were instructed to bend at the MCP joint while keeping the middle finger straight (PIP and DIP joint flexion ~ 0°). End range of motion targets restricted MCP joint F/E to approximately 45°. Force was applied to the middle phalanx with a cable-pulley system and a constant force spring (N-series, Vulcan Spring Co, Telford, PA), and the applied force was measured with a light-weight uniaxial s-beam load cell in line with the constant force spring (LCM-200, Futek Inc., Irvine, CA). A web-based metronome was sounded at the movement end ranges to achieve each repetition frequency (www.webmetronome.com). Participants rehearsed the finger movements with the investigator prior to data collection. The repetition frequencies were counter-balanced within each counter-balanced fingertip force to mitigate order effects.

5.3.4. Data Collection

FDS tendon and SSCT velocities were obtained with high-frequency ultrasound (Vivid Q, General Electric Healthcare Ltd., Milwaukee, WI). A linear probe (12L-RS) was aligned with the middle finger FDS tendon 2 cm proximal to the distal wrist crease (Figure 5.2). Finger flexor tendon is characterized by hypoechoic striations while the adjacent SSCT is highly hyperechoic (Tat et al., 2015a). Passive flexion/extension of the middle finger ensured the correct tendon was identified before the probe was set in a custom holding device. Tissue velocities were detected using colour Doppler imaging

(CDI). System settings were optimized for musculoskeletal tissue, including an acquisition frequency of 13.0 MHz, colour Doppler scale of ± 11.0 cm/s, and low velocity reject of 1.3 cm/s (Tat et al., 2015a). A combination of beam steering (20° maximum) and a gel standoff wedge (Gel Pad, Parker Laboratories Inc., Fairfield, NJ) reduced the angle of insonation to approximately 60°. CDI video clips were recorded at 29.5 fps.

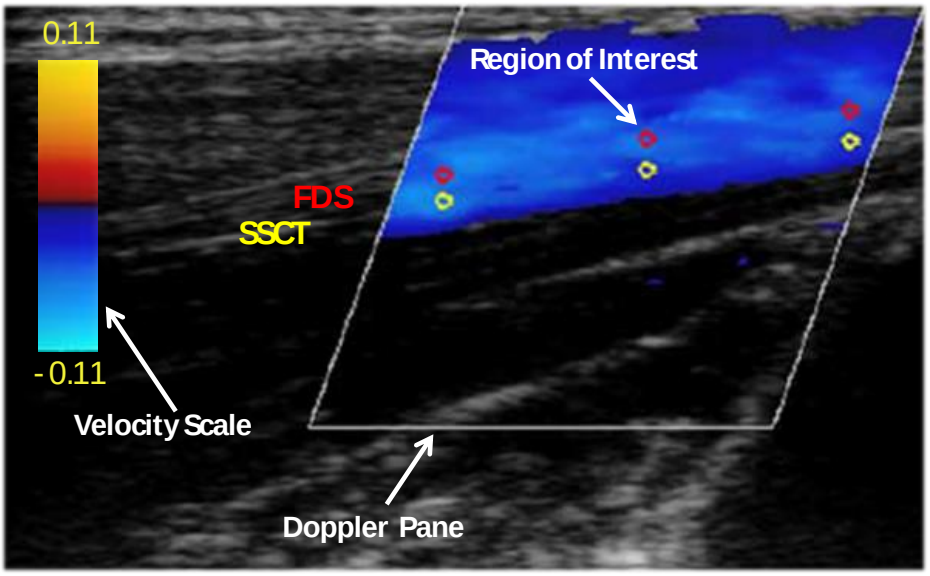

Figure 5.2. Grayscale ultrasound of the proximal wrist superimposed with CDI. Brighter colours correspond to higher velocities of underlying anatomical structures. FDS tendon and SSCT velocities were sampled in circular regions of interest for further analysis.

Middle finger FDS and extensor digitorum (ED) muscle activities were recorded with intramuscular electromyography (EMG). Bipolar nickel-chromium alloy wire electrodes (50 μm diameter) were inserted with a 25-guage hypodermic needle (Chalgren Enterprises Inc., Gilroy, CA). Electrode insertion followed placement guidelines for intramuscular EMG (Perotto and Delagi, 2004). Briefly, the FDS electrode was inserted in the distal one-third of the forearm in line with the lateral humeral condyle and the third metacarpal at a depth of 1-3 cm while the ED electrode was inserted in the distal forearm in line with the medial humeral condyle and the third metacarpal at a depth of 0.5-1.5 cm. B-mode ultrasound was used to guide electrode insertions for the FDS and ED muscle compartments of the middle finger.

Each participant placed their right forearm on a table in a mid-prone position, and a 60-second quiet trial was collected to de-bias EMG. To ensure signal quality and normalize EMG, participants performed a series of maximal voluntary efforts (MVEs). The investigator provided resistance against the middle finger, allowing the participant to slowly overcome the resistance, during maximal finger flexion (FDS MVE) and maximal finger extension (ED MVE) at the MCP joint throughout the full range of motion. Each participant completed 3 FDS trials and 3 ED trials to verify the wire electrodes were set in the muscle bellies, and produce genuine MVEs. The mean of a 50 ms window centered on peak EMG represented each MVE. EMG recordings for the MVEs and the experimental protocol were amplified and band-pass filtered between 10 − 2000 Hz (AMT-8, Bortec Biomedical Ltd., Calgary, AB; Z_I = 10 GΩ; CMRR > 115 dB @ 60 Hz).

Note: FDS and ED muscle activities were also recorded with surface electromyography for future comparison; however this paper focuses on results from fine-wire EMG.

Finger force was determined from the load cell in line with the constant force spring while MCP and PIP joint flexion angles were evaluated with two small electrogoniometers on the dorsal middle finger (F35, Biometrics Ltd., Gwent, U.K.). Force and posture recordings were amplified with a multi-channel conditioning system (RDP-600, RDP Electrosense Inc., Pottstown, PA). Finger force, MCP and PIP joint F/E, and EMG were sampled at 4096 Hz (LabView 8.5, USB-6229 A/D converter, National Instruments Corp., Austin TX).

5.3.5. Data Analysis

5.3.5.1. Colour Doppler Imaging

Colour ultrasound images were processed offline with dedicated software (EchoPAC, General Electric Healthcare Ltd., Milwaukee, WI). Similar to Kociolek and Keir (2015), velocity-time data were obtained from six regions of interest (each 0.5 mm diameter), including three on the FDS (FDS_{Distal}, FDS_{Centre}, $FDS_{Proximal}$) and three on the adjacent SSCT ($SSCT_{Distal}$, $SSCT_{Centre}$, $SSCT_{Proximal}$). Each region of interest maintained a fixed position, and was visually inspected throughout the trial to ensure tracking of the correct anatomical structure. Velocity-time profiles for the three FDS markers and three SSCT markers were ensemble averaged and smoothed with a 6^{th} order dual low-pass critically damped filter at 3 Hz (MatLab 7.6, Mathworks Inc., Natick, MA). FDS tendon and SSCT velocities were corrected for the angle of insonation ($\cos\theta$), and integrated to determine displacements over time. Tendon-SSCT relative displacement was calculated

for finger flexion and extension in each 10 second trial. The mean displacement of all cycles was determined for each trial. Flexion and extension scores were also averaged, as our previous work indicated no difference with direction (Kociolek and Keir, 2015; Tat et al., 2013). Mean (± standard error of the mean) displacements were reported for each experimental condition.

5.3.5.2. Approximating Muscle Force

EMG was de-biased, full-wave rectified, and dual low-pass filtered (critically damped, 6^{th} order, 3Hz cutoff). EMG signals were offset 70 ms to represent the electromechanical delay (Hug, 2011), and normalized to MVEs. FDS and ED musculotendon force was estimated with the distribution moment approximation (DMA), originating from Huxley's (1957) mathematical formulation of cross bridge dynamics (Cashaback et al. 2013). Huxley's kinetic model is based directly on physiology of muscle contraction; however, computations for even simple experiments on isolated muscle fibres are complicated. Zahalak (1981) proposed the DMA as a macroscopic (lumped-parameter) surrogate model to estimate the proportion of bound cross-bridges, $n(x,t)$, with displacement, x, and time, t, using a Gaussian distribution. The model included three coupled differential equations to calculate stiffness, force, and energy (Zahalak and Ma, 1991). Cashaback et al. (2013) added a fourth equation to account for musculotendon length, and updated the DMA to include muscle and tendon properties from Thelen (2003).

Muscle force-generating characteristics include physiological cross-sectional area, optimal fibre length, tendon slack length, and penetration angle, which were obtained

from modelling literature (Hale et al., 2011; Holzbaur et al., 2005). Muscle parameters were scaled to better represent our study participants. Physiological cross-sectional area was scaled with a regression equation based on the product of hand length and breadth (Sancho-Bru et al., 2008). Musculotendon length linearly scaled with combined forearm and hand length, and the ratio of optimal fibre length to tendon slack length was preserved (Hale et al., 2011). The model also uses a series of rate parameters to specify cross-bridge bonding and unbonding, which were derived from Oomens et al. (2003). DMA model inputs were muscle activation and musculotendon velocity normalized to optimal fibre length. FDS and ED muscle activations were determined from fine-wire EMG, and musculotendon velocities were based on models of tendon-joint interaction (An et al., 1983; Kociolek and Keir, 2015).

5.3.5.3. Tendon Friction

FDS tendon gliding resistance and frictional work were calculated from the analytical model in Kociolek et al. (2015). Briefly, the friction model is based on direct cadaveric measurement of proximal (finger flexion) and distal (finger extension) tendon displacement in the carpal tunnel. The model is further scalable based on wrist posture, tendon velocity, and inline musculotendon force. The wrist was assumed to be fixed in a neutral position (0°). Tendon displacement and velocity were both derived from colour ultrasound. FDS musculotendon force was obtained from the DMA.

5.3.6. Statistics

Two-way repeated measures analysis-of-variance models tested the effects of movement frequency (0.75 Hz, 1 Hz, 1.25 Hz) and finger force (4 N, 8 N) on FDS, SSCT,

and FDS-SSCT relative displacement (as a percentage of the overall tendon displacement). Repeated measures ANOVAs also tested the change in MCP and PIP joint flexion, applied finger force as well as FDS and ED average and peak EMG. Significant effects were followed up with Tukey's range test ($\alpha = 0.05$).

Musclotendon force predictions were only performed with mean data due to high variability in the fine-wire EMG. The muscle model predicts a nonlinear relationship between muscle activation and force, and is highly sensitive to EMG. The mean data provided a stable solution and better represented inline musculotendon force. FDS tendon gliding resistance and frictional work are dependent on tendon force, and therefore analyses were also limited to descriptive statistics. Despite these limitations, modelling musculotendon force and tendon friction based on physiological data provides a valuable comparison with ultrasound-based measures of relative displacement. Since frictional work was calculated throughout the movement cycle, we calculated the relative distance travelled during both finger flexion and finger extension. FDS-SSCT relative distance, or relative travel, provided the best comparison to FDS tendon frictional work.

5.4. Results

5.4.1. Joint Kinematics

The flexion/extension motion in the experimental protocol produced MCP joint flexion angle changes of 33.7° ± 2.5° and accessory PIP joint flexion angle changes of 8.6° ± 1.4°. MCP joint flexion followed a symmetrical bell-shaped profile. PIP joint flexion curves were more variable, although the peak angle generally occurred at the

transition from flexion to extension (50% cycle time). Changes to MCP and PIP joint flexion angles were not affected by movement frequency or finger force (Table 5.2).

Table 5.2. Mean (± standard error of the mean) changes in metacarpophalangeal and proximal interphalangeal joint flexion angles during cyclical middle finger movements.

Fingertip Force	**Movement Rate**		
	0.75 Hz	**1.00 Hz**	**1.25 Hz**
	Metacarpophalangeal joint flexion angles (°)		
4 N	34.1° ± 3.0°	33.5° ± 2.7°	33.7° ± 3.0°
8 N	33.0° ± 2.4°	35.3° ± 2.2°	32.6° ± 2.5°
	Proximal interphalangeal joint flexion angles (°)		
4 N	9.1° ± 2.2°	8.0° ± 1.7°	7.6° ± 1.7°
8 N	9.5° ± 1.4°	8.4° ± 1.2°	9.0° ± 1.5°

5.4.2. FDS, SSCT and Relative Displacement

FDS tendon and SSCT displacements were bell-shaped with MCP joint F/E (Figure 5.3). Tendon displacement was 13.7 ± 0.3 mm (over all test conditions), and was not influenced by movement frequency and finger force. However, there was a significant main effect of movement frequency on displacement of the SSCT ($F_{2,22} = 11.1$, $p < 0.01$), with lower displacements at 1.00 Hz and 1.25 Hz compared to 0.75 Hz (Figure 5.4). SSCT displacement did not change with finger force magnitude.

There was a significant main effect of movement frequency on relative displacement between FDS tendon and adjacent SSCT ($F_{2,22} = 37.0$, $p < 0.01$; Figure 5.4). FDS-SSCT relative displacement normalized to overall tendon displacement was higher

at 1 Hz (32.2 ± 2.9 %) and 1.25 Hz (32.5 ± 2.8 %) than 0.75 Hz (22.5 ± 3.2 %). Relative displacement also increased with finger force magnitude from 26.6 ± 3.0 % at 4 N to 31.6 ± 3.0 % at 8 N ($F_{1,11} = 7.4$, $p = 0.02$; Figure 5.4).

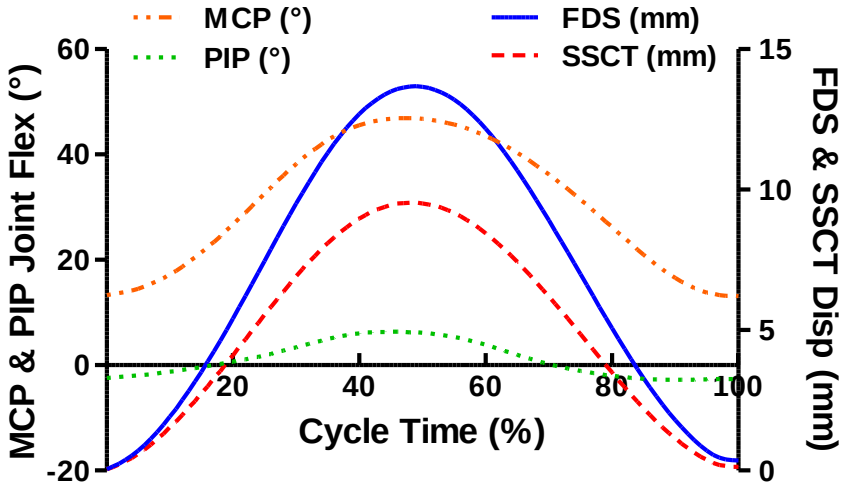

Figure 5.3. MCP and PIP joint flexion angles (left vertical axis) as well as FDS tendon and SSCT displacements (right vertical axis) versus MCP joint F/E cycle time (averaged over all test conditions).

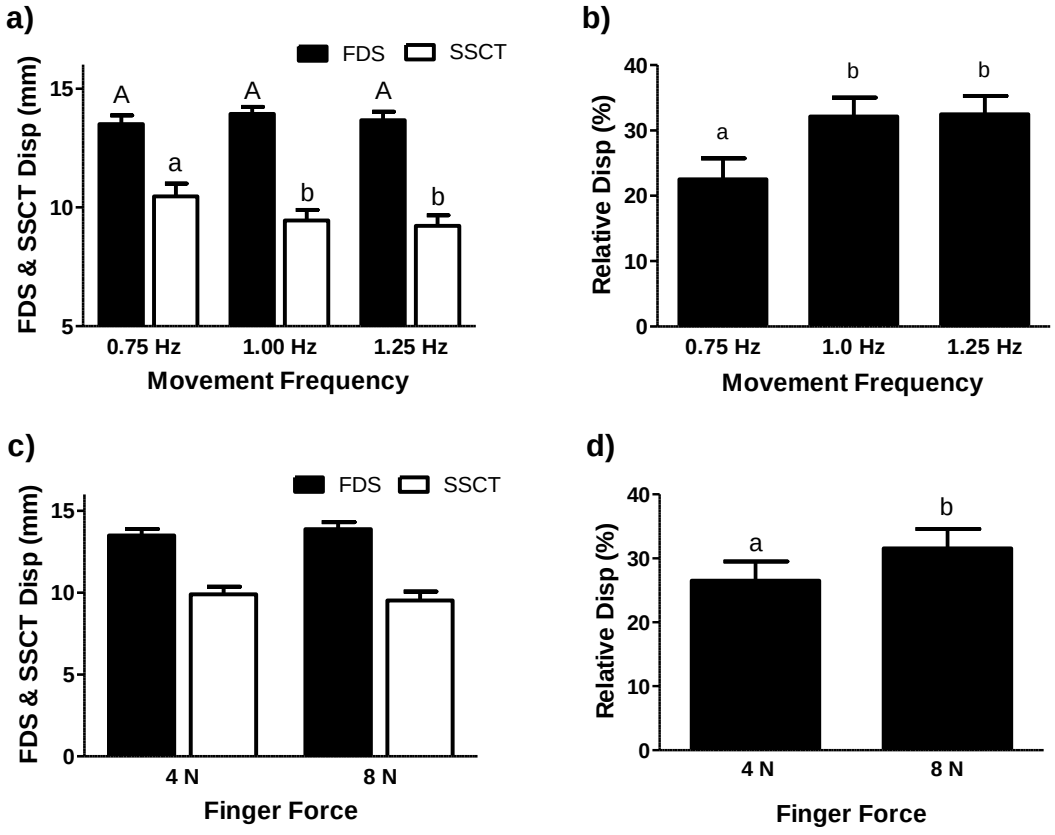

Figure 5.4. (a) FDS tendon and SSCT displacement, and (b) FDS-SSCT relative displacement versus movement frequency. (c) FDS tendon and SSCT displacement, and (d) FDS-SSCT relative displacement versus finger force. FDS-SSCT relative displacement is normalized as a percentage of FDS tendon displacement. All data are reported as the mean ± standard error of the mean.

5.4.3. Muscle Activity and Musculotendon Force

Finger flexor (FDS) and extensor (ED) muscle activity during MCP joint F/E is depicted in Figure 5.5. FDS activity resembled an inverted-U during finger flexion (0 – 50 % cycle time), followed by constant low-level activity in extension (50 – 100 % cycle time). ED activity was relatively low for the entire movement; however, activity increased slightly from 0% to 100% cycle time (Figure 5.5). FDS and ED aEMG throughout MCP joint F/E did not significantly change with movement frequency or finger force (Table 5.3). However, FDS aEMG trended towards higher activity levels with both movement frequency ($F_{2,22}$ = 2.0, p = 0.17) and finger force ($F_{1,11}$ = 4.5, p = 0.06). FDS peak EMG was significantly greater with a finger force of 8 N versus 4 N ($F_{1,11}$ = 5.1, p < 0.05), though movement frequency was not statistically significant ($F_{2,22}$ = 2.4, p = 0.11). ED peak EMG was similar over all test conditions (Table 5.3).

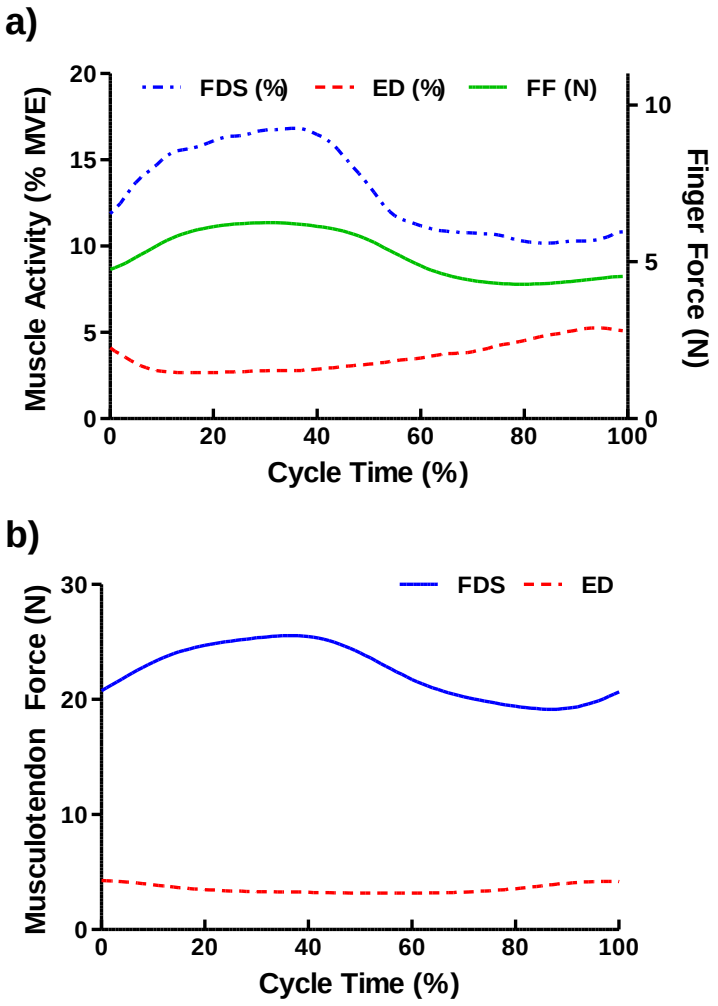

Figure 5.5. (a) FDS and ED muscle activity (left vertical axis) and finger force (right vertical axis) as well as (b) FDS and ED musculotendon force versus cycle time (averaged over all test conditions).

Table 5.3. Mean and peak FDS and ED muscle activity as a percentage of MVE throughout MCP joint F/E (mean ± standard error of the mean).

Fingertip Force	Movement Rate					
	0.75 Hz		1.00 Hz		1.25 Hz	
	Mean	Peak	Mean	Peak	Mean	Peak
	Flexor Digitorum Superficialis (% MVE)					
4 N	9.4 ± 3.2	13.1 ± 4.2	10.4 ± 3.8	15.0 ± 4.9	11.2 ± 3.5	17.5 ± 4.7
8 N	13.1 ± 3.6	20.3 ± 5.2	16.9 ± 7.1	25.3 ± 10.2	18.0 ± 7.2	27.9 ±10.6
	Extensor Digitorum (% MVE)					
4 N	3.1 ± 0.7	7.2 ± 1.7	2.4 ± 0.5	4.5 ± 0.8	3.3 ± 0.7	6.1 ± 1.4
8 N	3.2 ± 0.7	5.4 ± 1.0	3.1 ± 0.6	5.4 ± 1.0	3.1 ± 0.8	4.8 ± 1.2

Finger force across all participants and test conditions produced a sinosuidal curve during MCP joint F/E. FDS force versus cycle time mirrored the finger force, also resembling a sinusoid, with the highest force occurring at 36.5% cycle time and the lowest force at 87.0% cycle time (Figure 5.5). FDS force was 4.27 times the finger force over the full range of motion. FDS force averaged throughout the movement range increased from 18.8 N to 26.2 N with finger forces of 4 − 8 N. The average FDS force changed less with movement frequency, ranging from 20.7 N (0.75 Hz) to 24.1 N (1.25 Hz). Across all test conditions, ED force was low during MCP joint F/E (< 6.0 N).

5.4.4. Relative Travel versus Frictional Work

FDS-SSCT relative travel and FDS frictional work versus FDS tendon displacement are represented in Figure 5.6. While both relative travel and frictional work increased nonlinearly with tendon displacement during finger flexion, frictional work displayed a higher degree of nonlinearity. During finger extension, relative travel was linear while frictional work remained nonlinear (Figure 5.6). FDS-SSCT relative travel during MCP

joint F/E increased 32.3% from 0.75 Hz to 1.25 Hz (Figure 5.7). In contrast, frictional work increased 11.4% with repetition frequency (0.75 Hz − 1.25 Hz). Relative travel increased 13.6% while frictional work increased 8.2% with finger forces of 4 N − 8 N (Figure 5.7).

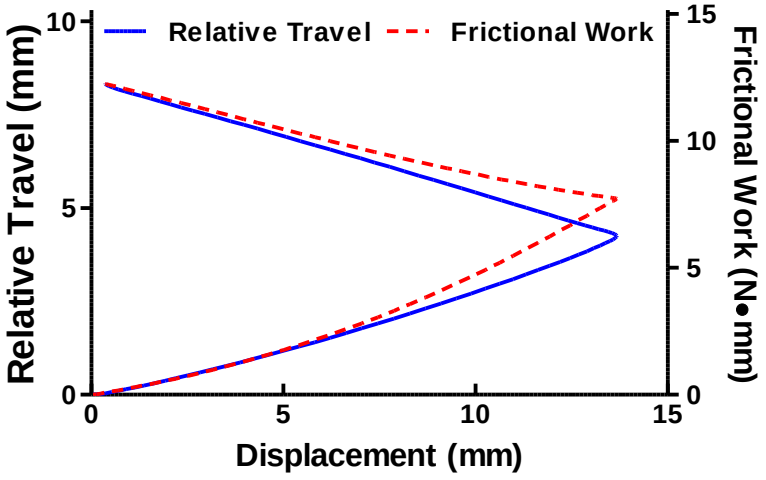

Figure 5.6. FDS-SSCT relative distance travelled (left vertical axis) and FDS tendon frictional work (right vertical axis) versus FDS tendon displacement (averaged over all test conditions).

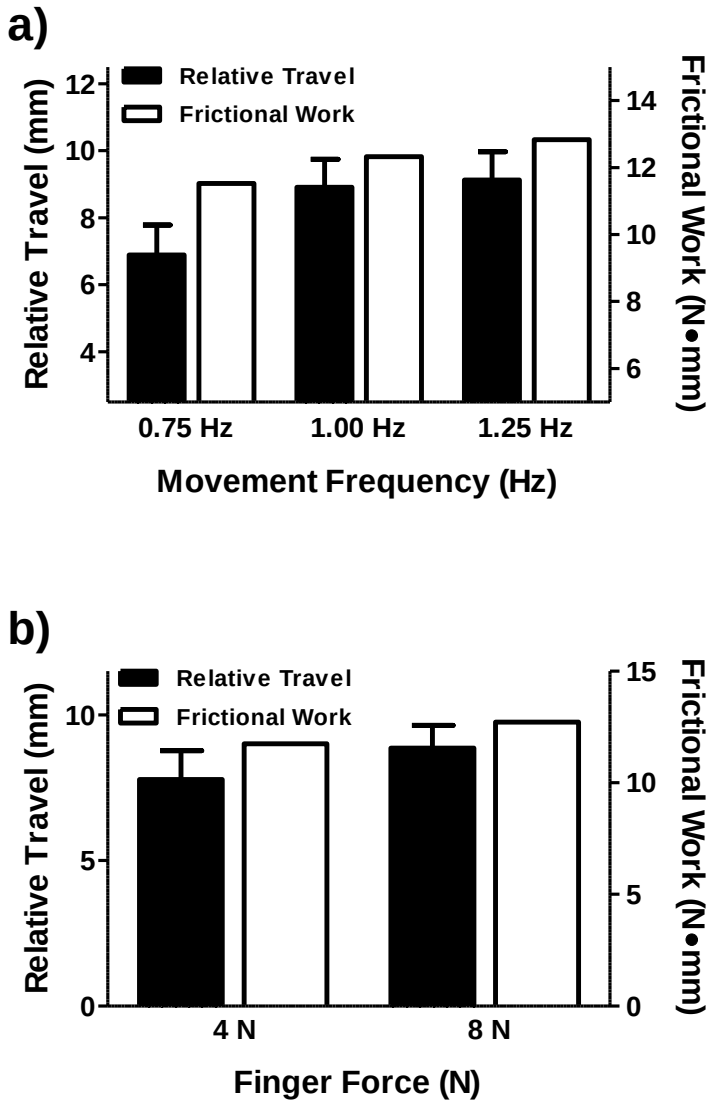

Figure 5.7. FDS-SSCT relative distance travelled (left vertical axis) and FDS tendon frictional work (right vertical axis) versus (a) movement frequency and (b) finger force. Relative travel is represented as the mean ± standard error of the mean while tendon frictional work is the mean.

5.5. Discussion

We investigated FDS tendon and SSCT displacement in 12 healthy participants performing repetitive middle finger MCP joint flexion/extension, and found that FDS-SSCT relative displacement increased with finger forces of 4 − 8 N and movement frequencies greater than 0.75 Hz. Greater relative displacement with higher movement frequencies (1.0 and 1.25 Hz) was primarily due to lower SSCT displacement, with no significant difference in tendon displacement. Interestingly, relative displacement increased significantly with finger force, even though the individual FDS tendon and SSCT displacements did not differ significantly between 4 and 8 N. MCP and PIP joint kinematics were not affected by frequency or force, suggesting that changes in relative displacement were influenced by local factors in the carpal tunnel. This is the first study to show velocity and force dependent changes of relative motion between tendon and the subsynovial connective tissue *in vivo*. Our results suggest greater risk of shear strain injury during repetitive and forceful finger movements, with repetition frequency having a greater effect than finger force.

Yoshii et al. (2011) used fluoroscopy to show that relative displacement increased with tendon velocity between 2.0 − 10.0 mm/sec in cadavers. In our study, FDS-SSCT relative displacement increased from 22.5 ± 3.2% at 0.75 Hz to 32.2 - 32.5% at 1.00 and 1.25 Hz. Tendon velocities ranged from 35.6 ± 1.1 mm/sec (0.75 Hz) to 59.8 ± 1.8 mm/sec (1.25 Hz). We propose the higher tendon velocities in our study captured a SSCT viscous limit, resulting in a relative displacement plateau above 1 Hz. Yoshii et al. (2011) showed that velocity dependent changes were exaggerated with greater tendon

displacements, which may reflect an interaction between the viscous and elastic components of the SSCT. Since our study evaluated MCP joint F/E in isolation, the tendon motion was relatively small (13.7 ± 0.3 mm). We anticipate that greater joint excursions and tendon displacements may exhibit a higher viscoelastic ceiling for the SSCT. Consistent with this hypothesis, a recent cadaver study found that relative displacement during full finger flexion (FDS tendon displacement = 25 mm) increased with tendon velocity up to 150 mm/sec (Tat et al., 2015a).

While finger force affected relative displacement, retrospective power analysis revealed that upwards of sixty participants were needed to achieve statistical significance for individual displacements of the FDS and SSCT. We advise interpreting these results with some caution, as the underlying mechanical factors for the significant force effect remains speculative. For example, Goldstein et al. (1987) showed that viscoelastic strain and creep increased 0.2 − 1.8% with tendon forces of 23 – 65 N in a cadaveric model, coinciding with small (non-significant) tendon displacement changes in this study. Ugbolue et al. (2005) recorded coincident longitudinal and dorsopalmar tendon displacements with a low tendon force of only 5 N. In our study, higher tendon forces (13.9 – 31.9 N) may further increase dorsopalmar tendon displacement, in turn affecting strain and load transferred to the SSCT. Regardless of the precise mechanism(s), we found that FDS-SSCT relative displacement increased independently with both movement frequency and finger force, suggesting a greater likelihood of shear injury during repetitive and forceful work.

FDS and ED musculotendon forces were predicted with fine-wire EMG as an input to a distribution-moment approximation (DMA). FDS force was 4.27 times the external finger force (across all experimental conditions). This ratio is similar to reported *in vivo* tendon to finger force ratios of 3.3 ± 1.4 during isometric pressing (Dennerlein et al., 1998a) and 5.2 ± 1.3 for key-switch tapping (Dennerlein et al., 1999) measured during carpal tunnel release surgery. FDS forces in musculoskeletal models vary between 1.2 and 5.0 times the external finger force (Chao et al., 1989; Dennerlein et al., 1998a, 1999; Harding et al., 1993, MacIntosh and Keir, 2014; Paclet and Quaine, 2012; Powell and Trail, 2004; Valero-Cuevas et al., 1998; Vigouroux et al., 2007). Differences are likely due to anatomical representation and solution methods as well as the simulated work task. ED force in the current study was relatively constant (3.15 N – 4.26 N) and low (16.0% of FDS) throughout MCP joint F/E (Figure 5.5). Dennerlein et al. (1998b) also showed very little extensor co-activation during the downswing (finger flexion) of a keystroke using fine-wire EMG. Together, these results suggest that the extrinsic extensors do not act antagonistically to the extrinsic flexors during finger movements, which differs considerably from isometric finger exertions (Sanei and Keir, 2013).

FDS force was also used to predict tendon frictional work, which displayed a greater degree of nonlinearity than FDS-SSCT relative travel throughout MCP joint F/E (Figure 5.6). This discrepancy likely represents a nonlinear relationship between the displacement and load transferred to the fibrillar paratenon due to sequential loading of the multi-layered SSCT (Guimberteau et al., 2010; Tat et al., 2015a). As additional layers of the SSCT are stretched, gliding resistance increases exponentially compared to

displacement (Kociolek and Keir, 2015). Interestingly, relative distance travelled between FDS tendon and SSCT was nonlinear during finger flexion and linear during finger extension. Tat et al. (2015a) observed a similar trend during proximal and distal tendon displacements in cadavers. Together, our results suggest that tendon dynamics differ with the direction of finger movement, which may arise from relaxation and creep of the viscoelastic SSCT (Goldstein et al., 1987).

We also found that the relative travel between the FDS tendon and SSCT increased 32.3% with a change in movement frequency from 0.75 to 1.25 Hz while frictional work only increased 11.4%. Similarly, increasing finger force from 4 to 8 N influenced relative distance travelled (13.7%) more than frictional work (8.2%). The greater sensitivity of relative travel to movement frequency likely reflects the viscous properties of the SSCT, which contains a gel-like interfibrillar matrix to provide boundary lubrication (Amadio, 2005; Guimberteau et al. 2010). Ultrasound assessment of relative motion may better capture these local characteristics of the tenosynovial gliding system whereas frictional work typifies friction globally within the carpal tunnel.

We tested relatively small joint excursions in our protocol (MCP joint flexion 33.7° ± 2.5°; PIP joint flexion 8.6° ± 1.4°), which produced FDS tendon friction in the lower range of the gliding resistance versus displacement exponential curve fit (Kociolek et al., 2015). In contrast, larger joint excursions and tendon displacements (e.g. full finger flexion) would produce disproportionately higher gliding resistance and frictional work. Thus, the displacement range has important consequences for friction, highlighting the difference between kinematic-based FDS-SSCT relative travel and kinetic prediction of

FDS frictional work. While these measures differ fundamentally, their implications for ergonomic use to predict injury risk in the workplace are not yet determined. The greater sensitivity of the relative distance travelled in a functional movement range as well as the clinical utility of colour Doppler ultrasound (Tat et al., 2015b) provide an intriguing option to link pathomechanics, physical work factors, and severity of injury and/or disability.

There were a few limitations of this study. Colour imaging is very sensitive to the angle of insonation between the ultrasound beam and the movement direction of anatomical structures (FDS tendon or SSCT). We steered the ultrasound beam 20° and applied a gel wedge to reduce the Doppler angle to approximately 60° (McDicken, 1991). Second, although the DMA comprised of a contractile element in series with a compliant tendon, a parallel elastic element was not included in the muscle model (Cashaback et al., 2013). However, the muscle model operated on the plateau region of the force-length curve, and thus the passive contributions of muscle force would be small (Thelen, 2003). These forces may be important in some postures beyond the scope of this study (Keir et al., 1996). FDS and ED forces were calculated in isolation, with no consideration for the other muscles of the middle finger. Admittedly, further research is needed for musculoskeletal models of the hand. However, our force predictions were well within the *in vivo* measurement range tested during surgery (Dennerlein, 2005).

In summary, we found that relative displacement between the FDS tendon and SSCT increased with movement frequency from 0.75 to 1.00 Hz, and plateaued from 1.00 − 1.25 Hz. Greater relative displacements with the higher movement frequencies suggest

an increased risk of a shear injury, while the plateau may represent the viscoelastic boundary of the SSCT. We also found relative displacement increased with finger force. To provide further comparison, FDS tendon frictional work was calculated using a previously published analytical model (Kociolek et al., 2015). Both movement frequency and finger force had a greater effect on ultrasound assessment of the relative distance travelled between the FDS tendon and SSCT compared to FDS tendon frictional work. Ultrasound assessment of relative displacement may better represent local properties of the paratenon gliding system. The ability to indirectly assess FDS-SSCT relative motion using ultrasound should prove fruitful in elucidating the link between pathomechanics, biomechanical risk factors, and injury in the workplace.

Conflict of interest statement: There are no conflicts of interest.

Acknowledgements: Thanks to Dr. Joshua G. Cashaback for use of his Distribution-Moment Model, and insights in muscle modelling. This work was supported by the Natural Sciences and Engineering Research Council of Canada under Discovery Grant # 217382-09.

5.6. References

Amadio, P.C., 2005. Friction of the gliding surface: implications for tendon surgery and rehabilitation. Journal of Hand Therapy 18 (2), 112–119.

An, K.N., Ueba, Y., Chao, E.Y., Cooney, W.P., Linscheid, R.L., 1983. Tendon excursion and moment arm of index finger muscles. Journal of Biomechanics 16 (6), 419−425.

Armstrong, T.J., Chaffin, D.B., 1979. Some biomechanical aspects of the carpal tunnel. Journal of Biomechanics 12 (7), 567−570.

Atroshi, I., Gummesson, C., Johnsson, R., Ornstein, E., Ranstam, J., Rosén, I., 1999. Prevalence of carpal tunnel syndrome in a general population. Journal of the American Medical Association 282 (2), 153−158.

Barr, A.E., Barbe, M.F., Clark, B.D., 2004. Work-related musculoskeletal disorders of the hand and wrist: epidemiology, pathophysiology, and sensorimotor changes. Journal of Orthopaedic & Sports Physical Therapy 34 (10), 610−627.

Cashaback, J.G., Potvin, J.R., Pierrynowski, M.R., 2013. On the derivation of a tensor to calculate six degree-of-freedom, musculotendon joint stiffness: implications for stability and impedance analyses. Journal of Biomechanics 46 (15), 2741−2744.

Chao, E.Y., An, K.N., Cooney, W.P., Linscheid, P.L., 1989. Biomechanics of the hand: a basic research study. World Scientific.

Davis, L., Wellman, H., Punnett, L., 2001. Surveillance of work-related carpal tunnel syndrome in Massachusetts, 1992–1997: A report from the Massachusetts sentinel event notification system for occupational risks (SENSOR). American Journal of Industrial Medicine 39 (1), 58−71.

Dennerlein, J.T., 2005. Finger flexor tendon forces are a complex function of finger joint motions and fingertip forces. Journal of Hand Therapy 18 (2), 120−127.

Dennerlein, J.T., Diao, E., Mote, C.D., Rempel, D.M., 1999. In vivo finger flexor tendon force while tapping on a keyswitch. Journal of Orthopaedic Research 17 (2), 178−184.

Dennerlein, J.T., Diao, E., Mote, C.D., Rempel, D.M., 1998a. Tensions of the flexor digitorum superficialis are higher than a current model predicts. Journal of Biomechanics 31 (4), 295−301.

Dennerlein, J.T., Mote, C.D., Rempel, D.M., 1998b. Control strategies for finger movement during touch typing: the role of the extrinsic muscles during a keystroke. Experimental Brain Research 121 (1), 1−6.

Filius, A., Thoreson, A.R., Yang, T.H., Vanhees, M., An, K.N., Zhao, C., Amadio, P.C., 2014. The effect of low- and high-velocity tendon excursion on the mechanical properties of human cadaver subsynovial connective tissue. Journal of Orthopaedic Research 32 (1), 123–128.

Frost, P., Andersen, J.H., Nielsen, V.K., 1998. Occurrence of carpal tunnel syndrome among slaughterhouse workers. Scandinavian Journal of Work, Environment & Health 24 (4), 285−292.

Greiner, T.M., 1991. Hand anthropometry of U.S. army personnel (Publication # Natick/TR−92/011). Natick, MA: United States Army Natick Research (Development and Engineering Center).

Goldstein, S.A., Armstrong, T.J., Chaffin, D.B., Matthews, L.S., 1987. Analysis of cumulative strain in tendons and tendon sheaths. Journal of Biomechanics 20 (1), 1−6.

Guimberteau, J.C., Delage, J.P., McGrouther, D.A., Wong, J.K.F., 2010. The microvacuolar system: how connective tissue sliding works. Journal of Hand Surgery 35E (8), 614–622.

Guimberteau, J.C., Panconi, B., Boileau, R. 1993. Mesovascularized island flexor tendon: new concepts and techniques for flexor tendon salvage surgery. Plastic and Reconstructive Surgery 92 (5), 888−903.

Hale, R., Dorman, D., Gonzalez, R.V., 2011. Individual muscle force parameters and fiber operating ranges for elbow flexion–extension and forearm pronation–supination. Journal of Biomechanics 44 (4), 650–656.

Harding, D.C., Brandt, K.D., Hillberry, B.M., 1993. Finger joint force minimization in pianists using optimization techniques. Journal of Biomechanics 26 (12), 1403−1412.

Holzbaur, K.R., Murray, W.M., Delp, S.L., 2005. A model of the upper extremity for simulating musculoskeletal surgery and analyzing neuromuscular control. Annals of Biomedical Engineering 33 (6), 829–840.

Hug, F., 2011. Can muscle coordination be precisely studied by surface electromyography? Journal of Electromyography and Kinesiology 21 (1), 1−12.

Huxley, A.F., 1957. Muscle structure and theories of contraction. Progress in Biophysics and Biophysical Chemistry 7, 257–318.

Keir, P.J., Wells, R.P., Ranney, D.A., 1996. Passive properties of the forearm musculature with reference to hand and finger postures. Clinical Biomechanics 11 (7), 401-409.

Kociolek, A.M., Keir, P.J., 2015. Development of a kinematic model to predict finger flexor tendon and subsynovial connective tissue displacement in the carpal tunnel. Ergonomics, Accepted, January 20, 2015.

Kociolek, A.M., Tat, J., Keir, P.J., 2015. Biomechanical risk factors and flexor tendon frictional work in the cadaveric carpal tunnel. Journal of Biomechanics 48 (3), 449-455.

Korstanje, J.W.H., Boer, M.S.D., Blok, J.H., Amadio, P.C., Hovius, S.E., Stam, H.J., Selles, R.W., 2012. Ultrasonographic assessment of longitudinal median nerve and hand flexor tendon dynamics in carpal tunnel syndrome. Muscle & Nerve 45 (5), 721−729.

Ma, S.P., Zahalak, G.L., 1991. A distribution-moment model of energetics in skeletal muscle. Journal of Biomechanics 24 (1), 21–35.

MacIntosh, A.R., Keir, P.J., 2014. Improving musculoskeletal hand modelling by incorporating intrinsic structures. 7th World Congress of Biomechanics, Boston, MA.

McDicken, W.N., 1991. Diagnostic ultrasonics: principles and use of instruments. Churchill Livingstone.

Moore, A., Wells, R., Ranney, D., 1991. Quantifying exposure in occupational manual tasks with cumulative trauma disorder potential. Ergonomics 34 (12), 1433−1453.

Oh, S., Belohlavek, M., Zhao, C., Osamura, N., Zobitz, M.E., An, K.N., Amadio, P.C., 2007. Detection of differential gliding characteristics of the flexor digitorum superficialis tendon and subsynovial connective tissue using color Doppler sonographic imaging. Journal of Ultrasound in Medicine 26 (2), 149−155.

Oomens, C.W.J., Maenhout, M., Van Oijen, C.H., Drost, M.R., Baaijens, F.P., 2003. Finite element modelling of contracting skeletal muscle. Philosophical Transactions of the Royal Society of London. Series B: Biological Sciences 358 (1437), 1453−1460.

Osamura, N., Zhao, C., Zobitz, M.E., An, K.N., Amadio, P.C., 2007a. Evaluation of the material properties of the subsynovial connective tissue in carpal tunnel syndrome. Clinical Biomechanics 22 (9), 999–1003.

Osamura, N., Zhao, C., Zobitz, M.E., An, K.N., Amadio, P.C., 2007b. Permeability of the subsynovial connective tissue in the human carpal tunnel: a cadaver study. Clinical Biomechanics 22 (5), 524–528.

Paclet, F., Quaine, F., 2012. Motor control theories improve biomechanical model of the hand for finger pressing tasks. Journal of Biomechanics 45 (7), 1246−1251.

Perotto, A., Delagi, E.F., 2005. Anatomical guide for the electromyographer: the limbs and trunk. Charles C Thomas.

Powell, E.S., Trail, I.A., 2004. Forces transmitted along human flexor tendons during passive and active movements of the fingers. Journal of Hand Surgery 29B (4), 386−389.

Sancho-Bru, J.L., Vergara, M., Rodríguez-Cervantes, P.J., Giurintano, D.J., Pérez-González, A., 2008. Scalability of the muscular action in a parametric 3D model of the index finger. Annals of Biomedical Engineering 36 (1), 102–107.

Sanei, K., Keir, P.J., 2013. Independence and control of the fingers depend on direction and contraction mode. Human Movement Science 32 (3), 457−471.

Silverstein, B.A., Fine, L.J., Armstrong, T.J., 1987. Occupational factors and carpal tunnel syndrome. American Journal of Industrial Medicine 11 (3), 343−358.

Silverstein, B., Welp, E., Nelson, N., Kalat, J., 1998. Claims incidence of work-related disorders of the upper extremities: Washington State, 1987 through 1995. American Journal of Public Health 88 (12), 1827−1833.

Smutz, W.P., Miller, S.C., Eaton, C.J., Bloswick, D.S., France, E.P., 1994. Investigation of low-force high-frequency activities on the development of carpal-tunnel syndrome. Clinical Biomechanics 9 (1), 15−20.

Staal, J.B., de Bie, R.A., Hendriks, E.J.M., 2007. Aetiology and management of work-related upper extremity disorders. Best Practice & Research Clinical Rheumatology 21 (1), 123−133.

Tanaka, S., McGlothlin, J.D., 1993. A conceptual quantitative model for prevention of work-related carpal tunnel syndrome (CTS). International Journal of Industrial Ergonomics 11 (3), 181−193.

Tat, J., Kociolek, A.M., Keir, P.J., 2013. Repetitive differential finger motion increases shear strain between the flexor tendon and subsynovial connective tissue. Journal of Orthopaedic Research 31 (10), 1533−1539.

Tat, J., Kociolek, A.M., Keir, P.J., 2014. Tendon shear is only partially represented by ultrasound shear. 7th World Congress of Biomechanics, Boston, MA.

Tat, J., Kociolek, A.M., Keir, P.J., 2015a. Validation of colour Doppler ultrasonography for evaluating relative displacement between flexor tendon and subsynovial connective tissue. Journal of Ultrasound in Medicine 34 (4), 679−687.

Tat, J., Wilson, K.E., Keir, P.J., 2015b. Pathological changes in the subsynovial connective tissue increase with severity of carpal tunnel syndrome symptoms. Clinical Biomechanics, Accepted, February 23, 2015.

Thelen D.G., 2003. Adjustment of muscle mechanics model parameters to simulate dynamic contractions in older adults. Journal of Biomechanical Engineering 125 (1), 70−77.

Thomsen, J.F., Hansson, G.Å., Mikkelsen, S., Lauritzen, M., 2002. Carpal tunnel syndrome in repetitive work: a follow-up study. American Journal of Industrial Medicine 42 (4), 344−353.

Ugbolue, U.C., Hsu, W.H., Goitz, R.J., Li, Z.M., 2005. Tendon and nerve displacement at the wrist during finger movements. Clinical Biomechanics 20 (1), 50−56.

Valero-Cuevas, F.J., Zajac, F.E., Burgar, C.G., 1998. Large index-fingertip forces are produced by subject-independent patterns of muscle excitation. Journal of Biomechanics 31 (8), 693−703.

Vigouroux, L., Quaine, F., Labarre-Vila, A., Amarantini, D., Moutet, F., 2007. Using emg data to constrain optimization procedure improves finger tendon tension estimations during static fingertip force production. Journal of Biomechanics 40 (13), 2846−2856.

Yoshii, Y., Villarraga, H.R., Henderson, J., Zhao, C., An, K.N., Amadio, P.C., 2009a. Speckle tracking ultrasound for assessment of the relative motion of flexor tendon and subsynovial connective tissue in the human carpal tunnel. Ultrasound in Medicine & Biology 35 (12), 1973−1981.

Yoshii, Y., Zhao, C., Henderson, J., Zhao, K.D., An, K.N., Amadio, P.C., 2009b. Shear strain and motion of the subsynovial connective tissue and median nerve during single-digit motion. Journal of Hand Surgery 34 (1), 65−73.

Yoshii, Y., Zhao, C., Henderson, J., Zhao, K.D., An, K.N., Amadio, P.C., 2011. Velocity-dependent changes in the relative motion of the subsynovial connective tissue in the human carpal tunnel. Journal of Orthopaedic Research 29 (1), 62−66.

Yoshii, Y., Zhao, C., Zhao, K.D., Zobitz, M.E., An, K.N., Amadio, P.C., 2008. The effect of wrist position on the relative motion of tendon, nerve, and subsynovial connective tissue within the carpal tunnel in a human cadaver model. Journal of Orthopaedic Research 26 (8), 1153−1158.

Zahalak, G.I., 1981. A distribution-moment approximation for kinetic theories of muscular contraction. Mathematical Biosciences, 55 (1), 89−114.

Zakaria, D., Robertson, J., Koval, J., MacDermid, J., Hartford, K., 2004. Rates of claims for cumulative trauma disorder of the upper extremity in Ontario workers during 1997. Chronic Diseases in Canada 25 (1), 22−31.

Zhao, C., Ettema, A.M., Osamura, N., Berglund, L.J., An, K.N., Amadio, P.C., 2007. Gliding characteristics between flexor tendons and surrounding tissues in the carpal

tunnel: A biomechanical cadaver study. Journal of Orthopaedic Research 25 (2), 185–90.

CHAPTER SIX: THESIS SUMMARY

6.1. Research Approach

In this thesis, I investigated work-related characteristics of flexor tendon motion and shear, and presented a mechanistic framework to assess wrist/hand musculoskeletal disorders in an occupational setting. While carpal tunnel syndrome (CTS) is caused by pressure-induced compression of the median nerve, the underlying pathomechanics are not well-defined. Histological changes, including non-inflammatory thickening and fibrosis of the subsynovial connective tissue (SSCT), are indicative of strain and/or shear injury between tendon and SSCT (Ettema et al., 2006a; Jinrok et al., 2004). Although exceeding the SSCT elastic threshold may cause acute injury, SSCT fibrosis is greatest adjacent to tendon, suggesting an injury mechanism of excessive shear due to repetitive wrist and finger motion (Ettema et al., 2006a; Schuind et al., 1990). A previous model of tendon friction was developed to predict work-related CTS (Moore et al., 1991). However, this method was based on the time honoured belt-pulley wrist model (Armstrong and Chaffin, 1979), which did not consider the viscoelastic SSCT (Guimberteau et al., 2010).

I used a combination of cadaveric dissection, ultrasound, motion capture, and fine-wire electromyography to characterize the relationship between physical exposures and flexor tendon motion and shear in the carpal tunnel. The association between biomechanical work factors, including non-neutral postures, speed of work, and forceful exertions, and wrist/hand musculoskeletal disorders is well-documented (Silverstein et al., 1986, 1987; Bernard, 1997; Harris-Adamson et al., 2014). Defining the relationship

between flexor tendon shear and the above risk factors is essential to understanding the development of tendinitis, tenosynovitis, and CTS. This thesis provides the means to calculate tendon motion and shear during repetitive and forceful work, thus presenting a set of powerful research tools to further elucidate injury pathways. As an occupational biomechanist, I believe that understanding the underlying mechanisms (or root causes) of injury will ultimately have the desired outcome of reducing wrist/hand musculoskeletal disorders. Determining the relationship between physical exposures and tendon shear represents an important step towards this pursuit.

6.2. Cadaveric Tendon Friction

A cadaveric model was used to measure finger flexor tendon gliding resistance and frictional work in the carpal tunnel during proximal tendon displacement to simulate finger flexion and distal tendon displacement to simulate finger extension (Chapter 2). The effects of wrist posture, tendon velocity, and force were evaluated in concert, which was the first study to measure tendon friction representative of physically demanding work. Tendon velocities between 50 and 150 mm/sec were tested, with the upper limit corresponding to repetitive finger flexion/extension movements performed at 1 Hz (Tat et al., 2013). Tendon forces ranged from 9.5 – 39.1 N for proximal tendon displacements (finger flexion) and 6.4 – 30.2 N for distal tendon displacements (finger extension). While tendon force is a complex function of fingertip force and muscle mechanics, unobstructed finger tapping on a keyswitch previously produced peak flexor tendon forces of 8 – 17 N (Dennerlein et al., 1999). However, a more physically demanding finger pressing task (9 − 15 N fingertip force) produced peak tendon force exceeding 40

N (Kursa et al., 2005). Therefore, flexor tendon forces in this cadaver study sufficiently represented a wide range of physical exertions.

The cadaveric model showed that concurrent exposure to multiple physical exposures disproportionately increased tendon frictional work within the carpal tunnel. During proximal tendon displacement, wrist posture interacted with tendon force to increase frictional work, indicative of friction with adjacent anatomical structures. A greater wrist flexion angle decreases the radius of tendon curvature, thereby increasing the normal stress and friction on the median nerve (Keir and Wells, 1999). While the wrist posture × tendon force interaction reflects these geometrical changes, strain-dependent characteristics of the SSCT may further influence frictional work in a flexed wrist posture. Pilot testing confirmed the effect of tenosynovial strain on tendon displacements representative of wrist flexion. Both origins of friction, contact with adjacent anatomical structures and elastic resistance of the SSCT, likely contribute to nonlinearities in overall friction measurement. While we found a multiplicative relationship between wrist posture and tendon force, there remains a need to systematically quantify nonlinearities associated with each frictional component.

During proximal tendon displacement, velocity independently affected frictional work. Since friction between tendon and adjacent anatomical structures is velocity-independent, increased frictional work was attributed to viscous properties of the SSCT. A gel-like interfibrillar matrix containing glycoproteins surrounds the collagen layers of the SSCT, providing boundary lubrication (Guimberteau et al. 2010). Thus, the fluid-permeated SSCT serves as a nutrient delivery system and facilitates smooth tendon

gliding inside the carpal tunnel (Amadio, 2005). Changes in permeability of the connective tissue may lead to edema and elevated hydrostatic pressure (Osamura et al., 2007a, b; Goetz and Barr, 2014). Thus, velocity-dependent friction reflects the condition of the SSCT, and the current study provides normative data for healthy wrists. Determining the relationship between SSCT stiffness and permeability, carpal tunnel hydrostatic pressure, and mechanical insult of the median nerve may be central to resolving the etiology of CTS.

Interestingly, during return distal tendon displacement, there was a three-way interaction involving tendon velocity, force, and wrist posture, with disproportionately greater frictional work for high magnitudes of all three physical exposures together. This interplay suggests the viscous contribution to overall gliding resistance is influenced by other frictional components within the carpal tunnel. Palmar migration of the flexor tendons against the transverse carpal ligament during wrist flexion may redistribute interstitial fluids, resulting in elevated carpal tunnel pressure and increased gliding resistance of the SSCT (Goetz and Barr, 2014).

Alternatively, or perhaps even synergistically, this high-order interaction may represent viscoelastic hysteresis during distal tendon displacement. Elastic materials strain in response to stress and return to their original state once the stress is removed, producing identical loading and unloading stress-strain curves. Conversely, viscous materials resist deformation in response to stress. Since viscoelastic materials have elastic and viscous properties, they also exhibit time-dependent strain. Hysteretic strain rate dependence is well-established for tendon (Taylor et al., 1990). However, viscous

energy dissipation may be even greater for tenosynovial gliding in the carpal tunnel, owing to the gel-like interfibrillar matrix of the SSCT. Differences in FDS tendon gliding resistance versus displacement during proximal tendon displacement (finger flexion) compared to return distal tendon displacement (finger extension) lend further support to hysteresis (Figure 2.3).

While quantifying friction in a cadaveric model provided further insight into tenosynovial gliding and the development of injury, the main contribution of this study was a model to predict tendon gliding resistance and frictional work based on biomechanical risk factors (Figure 6.1). Gliding resistance is defined as a function of tendon displacement, and the model is scalable based on wrist posture, tendon velocity, and force. The kinematic regression developed in Chapter 3 predicts tendon displacement from finger posture, and the first derivative of tendon displacement over time represents tendon velocity. Furthermore, the relationship between external finger force and internal tendon force is established in the literature, and was further tested in Chapter 5. Therefore, ergonomic assessment of wrist and finger posture and applied fingertip force satisfies the model inputs to calculate flexor tendon gliding resistance and frictional work. Future research will assess the capability of the friction model to predict work-related flexor tendinitis, tenosynovitis, and CTS.

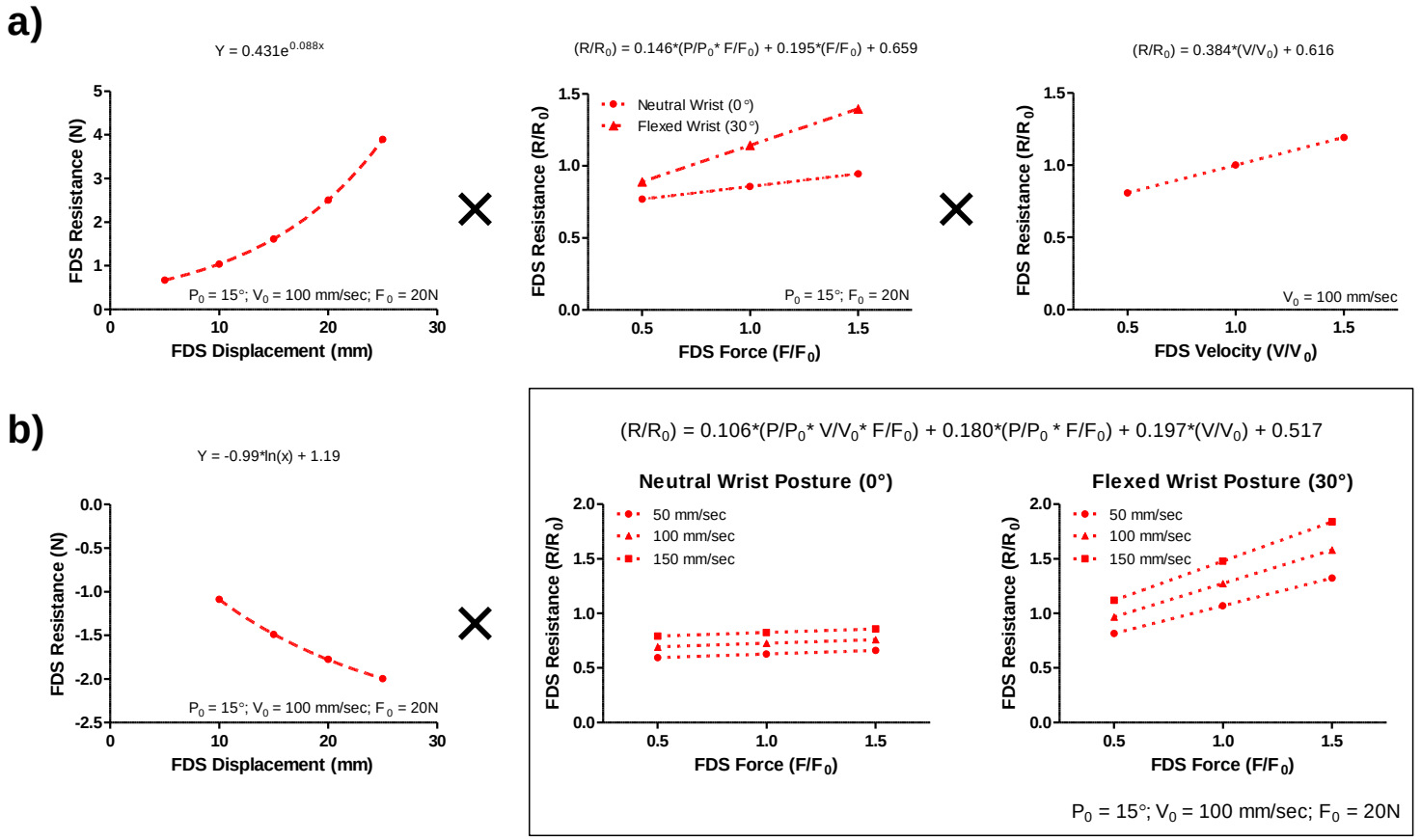

Figure 6.1. Middle finger FDS tendon gliding resistance during (a) proximal tendon displacement (simulated finger flexion) and (b) distal tendon displacement (simulated finger extension). Gliding resistance is calculated with an exponential model for proximal tendon displacement and a logarithmic model for distal tendon displacement. Gliding resistance computations are further scalable based on the biomechanical risk factors tested in this thesis, including wrist posture, tendon velocity, and force. R/R_0 represents scaling factors to modulate gliding resistance calculations. The model inputs P, V, and F are wrist posture (°), tendon velocity (mm/sec), and tendon force (N), respectively. $P_0 = 15°$; $V_0 = 100$ mm/sec; $F_0 = 20$ N. *Note: Reprinted from Chapter 2.*

6.3. Ultrasound Assessment of Tendon-SSCT Motion

Given that tendon friction cannot be directly measured *in vivo*, a series of studies were conducted to explore tendon gliding characteristics in healthy participants using colour Doppler imaging (CDI). Briefly, colour flow imaging computes the Doppler shift from scattered ultrasonic waves using serial correlation (Kukulski et al. 2000). CDI generates a colour-coded map overlaid on greyscale ultrasound, thus enabling assessment of relative motion between neighbouring anatomical structures. I quantified relative displacement between flexor tendon and adjacent connective tissue to determine gliding patterns during repetitive finger motions. Similar to the cadaveric study in Chapter 2, the aim was to determine the effects of physical exposures on tenosynovial function, including non-neutral wrist postures, speed of work, and forceful exertions.

I developed kinematic based models to calculate flexor tendon and adjacent SSCT displacements from metacarpophalangeal joint and proximal interphalangeal joint flexion angles (Chapter 3). A second-order model fit *in vivo* tendon displacements from CDI, and characterized important anatomical features including tendon bowstringing during finger flexion. Armstrong's and Chaffin's (1978) cadaver model of tendon wrapping assumed fixed geometry, therefore generating static moment arms. The updated model of tendon-joint interaction in Chapter 3 better matches the architecture of the digital pulley system, which will vastly improve computerized musculoskeletal simulations of forces in the hand (Kociolek and Keir, 2011; MacIntosh et al., 2014). Furthermore, anthropometric scaling in the current model will support the development and validation of musculoskeletal finger models through a more detailed examination of model topology

and parameterization (Valero-Cuevas et al., 2003). Validating biomechanical models over a range of anthropometric representations (instead of parameterizing one normative solution) will ultimately improve structure and function, as current models do not passably reproduce biological data (Valero-Cuevas et al., 2003).

SSCT displacement was also represented by a second-order model (in addition to FDS tendon), thus providing the means to calculate FDS-SSCT relative displacement. This thesis introduced the first series of kinematic models to calculate relative displacement, replacing ergonomic methods based on tendon displacement alone (Sommerich et al., 1998; Nester et al., 2000; Treaster and Marras, 2000; Ugbolue and Nicol, 2010, 2012). I also tested well-established ergonomic risk factors, including wrist posture, movement frequency, and applied finger force. While tendon displacements were not affected by these (above) risk factors, changes were observed to the adjacent SSCT. Displacements of the SSCT decreased with greater wrist flexion angles and finger movement frequencies, resulting in higher relative displacements between tendon and SSCT. Even though applied finger force did not influence FDS tendon or SSCT displacement (individually), the relative displacement between the two tissues increased with finger force.

Similar to tendon friction in Chapter 2, a scalable model to calculate relative displacement between FDS tendon and adjacent SSCT is presented in Figure 6.2. Relative tendon-SSCT displacement is calculated with the kinematic regressions first introduced in Chapter 3. Subsequently, relative displacement is scaled based on the biomechanical risk factors tested in this thesis (wrist posture, tendon velocity, and force).

The model includes cadaveric data from preliminary validation of CDI (Tat et al., 2015) as well as relative displacements in healthy participants from thesis chapters 3 – 5. Both the cadaver and participant based datasets were weighted equally in the final ergonomic model, which predicts an additive effect of combined biomechanical risk factors. Additional risk factors may be incorporated into the relative displacement model in future iterations, including isolated (single) versus concurrent (multiple) finger movement (Yoshii et al., 2009b; Zhao et al., 2007), and task duration (Tat et al., 2013). Further research will test the capability of the model to predict work-related injury and determine the dose-response relationship between relative displacement and tenosynovial damage.

This thesis also provided new insight into the normal function of the SSCT. Tendon-SSCT relative displacement increased in wrist flexion and decreased in wrist extension (relative to neutral posture) in Chapter 4, which differed from a cadaver study that manipulated wrist posture (Yoshii et al., 2008). SSCT strain owing to proximal (wrist flexion) and distal (wrist extension) tendon displacements influence subsequent displacement and elasticity of the SSCT. Relative displacements in different wrist postures reflect these strain-related changes, providing valuable information on normal tenosynovial function. While relative displacement between tendon and adjacent SSCT increased with finger movement frequency from 0.75 – 1.00 Hz, relative displacement was similar from 1.00 – 1.25 Hz (Chapter 5). These velocity-dependent changes likely characterize the viscoelastic limit of the SSCT, since relative displacement plateaued at the high movement frequencies. Yoshii et al. (2011) found greater relative displacement (*in vitro*) for high-velocity versus low-velocity tendon motion, only for tendon

displacements over 30 mm (representing full finger flexion). There is a need to evaluate the interplay between the elastic and viscous components of the SSCT, particularly for patients with CTS.

Applied finger force increased relative displacement between tendon and SSCT modestly, but significantly (Chapter 5). My colleagues and I found a similar force effect in cadaveric testing, although the underlying mechanics are not well understood (Tat et al., 2015). Higher finger force and tendon load may increase dorsopalmar tendon displacement, affecting strain of the SSCT (Ugbolue et al., 2005). Anecdotally, ultrasound probe adjustments were required to maintain an unobstructed view of the carpal tunnel contents between the different finger force levels (even though the test posture did not change). The emergence of ultrasound microscopy, with micrometer resolution, will enable dynamic assessment of the tenosynovial architecture, and shed further light on carpal tunnel mechanics.

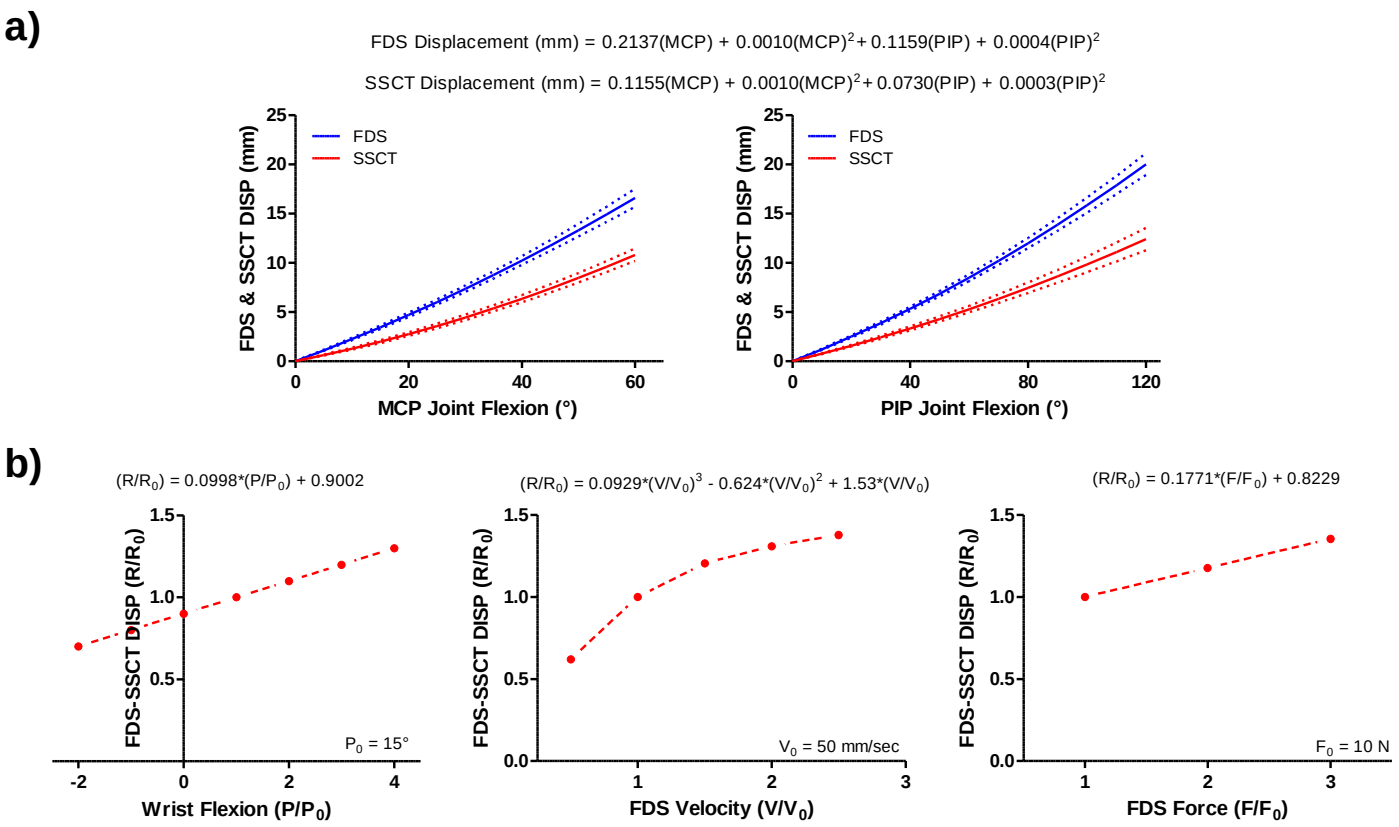

Figure 6.2. (a) FDS tendon and SSCT displacements versus MCP (left) and PIP (right) joint flexion angles from the embedded regression models (representative of a 50th percentile male). The solid lines are mean FDS tendon and SSCT displacements while the dashed lines are standard errors. Inputs in the regression equations: MCP – Metacarpophalangeal joint flexion (°); PIP – Proximal interphalangeal joint flexion (°). The equations are used to calculate tenosynovial relative displacement (FDS_{DISP} – $SSCT_{DISP}$ / FDS_{DISP} × 100%). (b) FDS-SSCT relative displacements are further scalable based on the biomechanical risk factors tested in this thesis, including wrist posture (left), tendon velocity (centre), and force (right). R/R_0 represents scaling factors to modulate relative displacement. The model inputs P, V, and F are wrist posture (°), tendon velocity (mm/sec), and tendon force (N), respectively. P_0 = 15°; V_0 = 50 mm/sec; F_0 = 10 N. *Note: Figure 6a was reprinted from Chapter 3.*

6.4. Work-relatedness of Tendon Motion and Friction

I developed two parallel models to determine FDS-SSCT relative displacement and FDS tendon gliding resistance during repetitive wrist/finger motion (Figures 6.1 and 6.2). The cadaveric friction model predicted a relatively modest effect of tendon velocity in a neutral wrist posture (0°). However, in a flexed wrist posture, both tendon velocity and force substantially increased tendon gliding resistance within the carpal tunnel. Integrating FDS tendon gliding resistance over displacement, FDS tendon frictional work was 122.0% higher with increased tendon velocities (50 to 150 mm/sec) and forces (10 to 30 N) when the wrist was flexed (30°). Likewise, relative displacement increased 101.0% for the same changes to the model inputs. However, the friction model predicted a multiplicative relationship whereas the relative displacement model predicted an additive relationship with wrist position, tendon velocity, and force (Figure 6.3). Thus, frictional work showed larger changes for high magnitudes of these physical exposures (especially in combination) while relative displacement showed larger changes for low magnitudes of wrist position, tendon velocity, and force (especially in isolation).

Although the relative displacement model and friction model both show promise as ergonomic methods, implications for the above-mentioned model differences with respect to injury prediction in the workplace remain uncertain. The relative displacement model is more responsive to lower physical exposures while the friction model ultimately produces greater changes overall (for higher exposures). Generally, epidemiological studies bear a likeness to the friction model, which demonstrated a multiplicative relationship with combined physical exposures. One classic study, with over 825

citations, showed disproportionately high injury odds ratios for CTS in combined high-repetition, high-force jobs (Silverstein et al., 1987). Caution is advised in directly comparing epidemiological outcomes with the relative displacement and friction models in this study since physical exposure definitions are not necessarily equivalent. However, in the interest of introspection, Figure 6.4 depicts the current model predictions alongside Silverstein et al. (1987). While the friction model best resembles epidemiological odds ratios, exactly how the current models relate to carpal tunnel syndrome is speculative. There is a need to test the relative displacement and friction models in occupational environments, and develop protective thresholds for injury prevention.

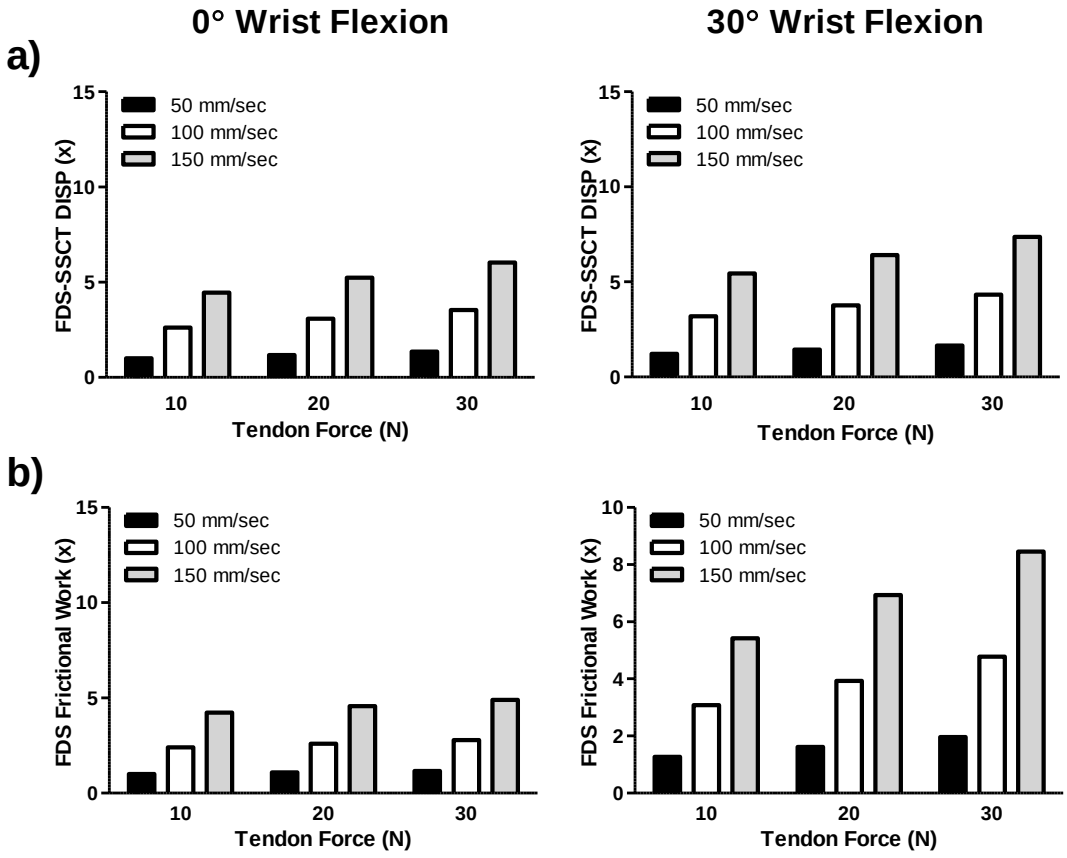

Figure 6.3. (a) FDS-SSCT relative displacement and (b) FDS tendon frictional work predictions in a (left) neutral wrist posture and (right) flexed wrist posture. Data normalized to: tendon displacement – 20 mm, wrist flexion − 0°, tendon velocity − 50 mm/sec, tendon force − 10 N.

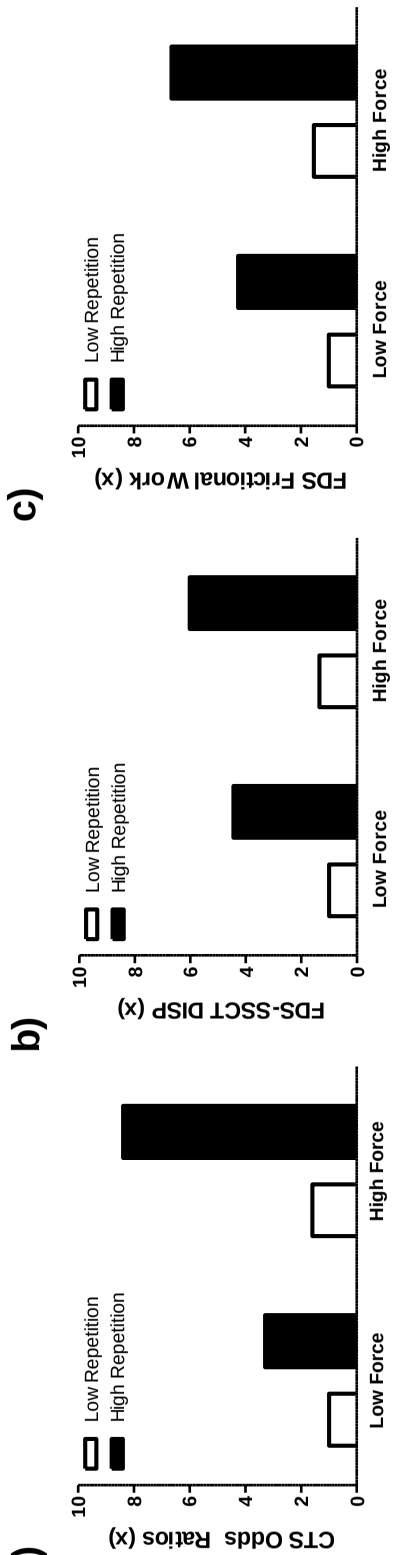

Figure 6.4. (a) CTS odds ratios for repetitive and forceful work (Silverstein et al., 1987). (b) FDS-SSCT relative displacement and (c) FDS tendon frictional work predictions. All data are normalized to the low repetition, low force work condition. Tendon velocities: 50 mm/sec (low repetition), 150 mm/sec (high repetition). Tendon forces: 10 N (low force), 30 N (high force). Model data represents 30° wrist flexion to best match Silverstein et al. (1987).

6.5. Research Directions

Future research directions broadly include (i) further investigation of the mixed tendon gliding system in the carpal tunnel, and (ii) validation of the proposed tendon models for use in ergonomic assessments. While this thesis provides valuable information on flexor tendon motion and shear, the origins of the documented gliding characteristics are still not fully understood. Cadaveric dissection enabled direct measurement of tendon gliding resistance through the carpal tunnel, however, this methodology did not allow for a distinction between synovial and extra-synovial (paratenon-like) components of friction. Although testing the effects of different physical exposures provided new insight into the likely contributions of the gliding sub-systems, there remains a need to better understand underlying mechanics for each frictional component. Ultrasound assessment of relative displacement between tendon and SSCT provided a better understanding of extra-synovial tendon gliding. However, ultrasound resolution is not sufficient for a detailed assessment of tenosynovial strain, and this method does not directly measure gliding resistance owing to tenosynovial relative displacement. Improved imaging technology, including the emergence of ultrasound microscopy and elastography, will enable dynamic assessment of tenosynovial function. Advanced imaging technologies will also assist in determining the complex relationship between SSCT stiffness and permeability, tendon shear, and carpal tunnel pressure, potentially unifying these 'separate' mechanisms of CTS. To lend support in this future pursuit, a theoretical model linking physical work factors with pathomechanics is depicted in Figure 6.5.

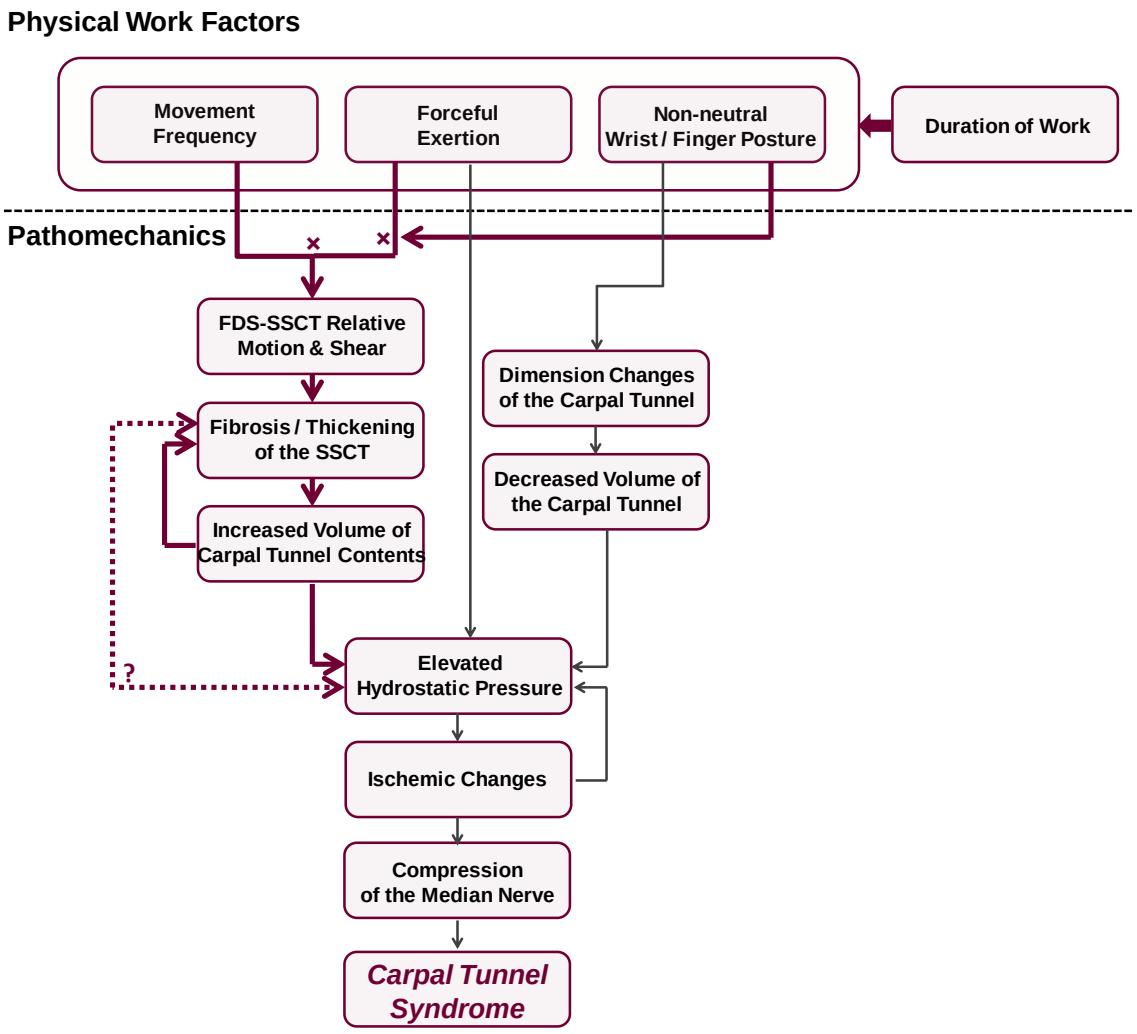

Figure 6.5. Theoretical model depicting the pathogenesis of work-related CTS. The red arrows indicate processes related to tendon motion and shear, which ultimately influence hydrostatic pressure in the carpal tunnel, leading to compression of the median nerve.

Regardless of the precise origins of shear, we developed two models to predict FDS-SSCT relative displacement and FDS tendon gliding resistance and frictional work based on common biomechanical risk factors, including non-neutral postures, speed of work, and forceful exertions. Future research will validate the models using a cross-sectional paradigm to quantify tendon motion and shear in work tasks with high incidence of flexor tendinitis, tenosynovitis, and CTS. Longitudinal studies with repeated measures over time may lend further support to confirming the role of tendon shear in injury development, and determining a dose-response relationship. Admittedly, longitudinal studies are extremely rare in ergonomics and biomechanics, and pose several challenges, including (but not limited to) worker turnover, evolving job characteristics, graduate student considerations, and typical funding structure of research grants. Regardless, this thesis demonstrated the relationship between well-established biomechanical risk factors and flexor tendon motion and shear, and supports histological evidence of repetitive shear in the development of CTS (Barr et al., 2004). Future research will aim to set protective thresholds based on tendon motion and shear for hand-intensive work.

6.6. Conclusions

I showed that concurrent exposure to several biomechanical risk factors multiplicatively increased tendon gliding resistance and frictional work in the cadaveric carpal tunnel. I also observed an exponential relationship between tendon displacement and friction, suggesting that strain-dependent tenosynovial gliding resistance is a large component of friction. Subsequently, I performed a series of studies to quantify relative displacement between tendon and adjacent SSCT using colour ultrasound (*in vivo*).

Repetitive long finger movements increased relative displacement with greater physical exposures, indicating greater tenosynovial shear, and increased risk of injury to the SSCT. I further developed two models to predict relative displacement between FDS and SSCT as well as FDS tendon gliding resistance and frictional work during repetitive wrist/finger movements. Ultimately, the two models will improve upon ergonomic risk assessments that consider cumulative tendon travel as a proxy for tendon friction. Future research will aim to set guidelines based on tendon motion and shear for hand-intensive work. Meanwhile, in the absence of protective thresholds, the relative displacement and friction models provide great utility for evaluating workplace interventions.

REFERENCES

Note: The references listed in this section are for the Introduction (Chapter 1) and Summary (Chapter 6). The references for each study in this thesis are listed in their respective chapters (Chapters 2 – 5).

ACGIH, 2002. *Threshold limit value for chemical substances and physical agents and biological exposure indices*. Cincnnati, OH: ACGIH.

Amadio, P.C., 2005. Friction of the gliding surface: implications for tendon surgery and rehabilitation. Journal of Hand Therapy 18 (2), 112–119.

An, K.N., 2007. Tendon excursion and gliding: clinical impacts from humble concepts. Journal of Biomechanics 40 (4), 713−718.

An, K.N., Berglund, L., Uchiyama, S., Coert, J.H., 1993. Measurement of friction between pulley and flexor tendon. Biomedical Sciences Instrumentation, 29, 1−7.

An, K.N., Ueba, Y., Chao, E.Y., Cooney, W.P., Linscheid, R.L., 1983. Tendon excursion and moment arm of index finger muscles. Journal of Biomechanics 16 (6), 419−425.

Armstrong, T.J., Chaffin, D.B., 1978. An investigation of the relationship between displacements of the finger and wrist joints and the extrinsic finger flexor tendons. Journal of Biomechanics 11 (3), 119−128.

Armstrong, T.J., Chaffin, D.B., 1979. Some biomechanical aspects of the carpal tunnel. Journal of Biomechanics 12 (7), 567−570.

Barr, A.E., Barbe, M.F., Clark, B.D., 2004. Work-related musculoskeletal disorders of the hand and wrist: epidemiology, pathophysiology, and sensorimotor changes. Journal of Orthopaedic & Sports Physical Therapy 34 (10), 610–627.

Bernard, B.P., 1997. *Musculoskeletal disorders and workplace factors: a critical review of epidemiologic evidence for work-related musculoskeletal disorders of the neck, upper extremity, and low back (Publication # 97-141).* Cincinnati, OH: National Institute for Occupational Safety and Health (Department of Health and Human Services).

Bonfiglioli, R., Mattioli, S., Fiorentini, C., Graziosi, F., Curti, S., Violante, F.S., 2007. Relationship between repetitive work and the prevalence of carpal tunnel syndrome in part-time and full-time female supermarket cashiers: a quasi-experimental study. International Archives of Occupational and Environmental Health 80 (3), 248−253.

Bongers, F.J., Schellevis, F.G., van den Bosch, W.J. van der Zee, J., 2007. Carpal tunnel syndrome in general practice (1987 and 2001): incidence and the role of occupational and non-occupational factors. British Journal of General Practice 57 (534), 36–39.

Bower, J.A., Stanisz, G.J., Keir, P.J., 2006. An MRI evaluation of carpal tunnel dimensions in healthy wrists: implications for carpal tunnel syndrome. Clinical Biomechanics 21 (8), 816−825.

Brand, P.W., Cranor, K.C., Ellis, J.C., 1975. Tendon and pulleys at the metacarpophalangeal joint of a finger. Journal of Bone and Joint Surgery 57 (6), 779−784.

Cigali, B.S., Buyruk, H.M., Snijders, C.J., Laméris, J.S., Holland, W.P.J., Mesut, R., Stam, H.J., 1996. Measurement of tendon excursion velocity with colour Doppler imaging: a preliminary study on flexor pollicus longus muscle. European Journal of Radiology 23 (3), 217−221.

Cobb, T.K., An, K.N., Cooney, W.P., 1995. Effect of lumbrical muscle incursion within the carpal tunnel on carpal tunnel pressure: a cadaveric study. Journal of Hand Surgery 20A, 186−192.

Davis, L., Wellman, H., Punnett, L., 2001. Surveillance of work-related carpal tunnel syndrome in Massachusetts, 1992-1997: a report from the Massachusetts sentinel event notification system for occupational risks (SENSOR). American Journal of Industrial Medicine 39 (1), 58−71.

Dennerlein, J.T., Diao, E., Mote, C.D., Rempel, D.M., 1999. In vivo finger flexor tendon force while tapping on a keyswitch. Journal of Orthopaedic Research 17 (2), 178−184.

Eladoumikdachi, F., Valkov, P.L., Thomas, J., Netscher, D.T., 2002a. Anatomy of the intrinsic hand muscles revisited: part I. Interossei. Journal of Plastic and Reconstructive Surgery 110 (5), 1211−1224.

Eladoumikdachi, F., Valkov, P.L., Thomas, J., Netscher, D.T., 2002b. Anatomy of the intrinsic hand muscles revisited: part II. Lumbricals. Journal of Plastic and Reconstructive Surgery 110 (5), 1225-1231.

Ettema, A.M., Amadio, P.C., Zhao, C., Wold, L.E., O'Byrne, M.M., Moran, S.L., An, K.N., 2006a. Changes in the functional structure of the tenosynovium in idiopathic carpal tunnel syndrome: a scanning electron microscope study. Journal of Plastic and Reconstructive Surgery 118 (6), 1413−1422.

Ettema, A.M., An, K.N., Zhao, C., O'Byrne, M.M., Amadio, P.C., 2008. Flexor tendon and synovial gliding during simultaneous and single digit flexion in idiopathic carpal tunnel syndrome. Journal of Biomechanics 41 (2), 292-298.

Ettema, A.M., Belohlavek, M., Zhao, C., Oh, S.H., Amadio, P.C., An, K.N., 2006b. High-resolution ultrasound analysis of subsynovial connective tissue in human cadaver carpal tunnel. Journal of Orthopaedic Research 24 (10), 2011−2020.

Ettema, A.M., Zhao, C., Amadio, P.C., O'Byrne, M.M., An, K.N., 2007. Gliding characteristics of flexor tendon and tenosynovium in carpal tunnel syndrome: a pilot study. Clinical Anatomy 20 (3), 292−299.

Filius, A., Thoreson, A.R., Wang, Y., Passe, S.M., Zhao, C., An, K.N., Amadio, P.C., 2015. The effect of tendon excursion velocity on longitudinal median nerve displacement: differences between carpal tunnel syndrome patients and controls. Journal of Orthopaedic Research, Accepted, December 4, 2014.

Filius, A., Thoreson, A.R., Yang, T.H., Vanhees, M., An, K.N., Zhao, C., Amadio, P.C., 2014. The effect of low- and high-velocity tendon excursion on the mechanical properties of human cadaver subsynovial connective tissue. Journal of Orthopaedic Research 32 (1), 123–128.

Franko, O.I., Winters, T.M., Tirrell, T.F., Hentzen, E.R., Lieber, R.L., 2011. Moment arms of the human digital flexors. Journal of Biomechanics 44 (10), 1987−1990.

Franzblau, A., Armstrong, T.J., Werner, R.A., Ulin, S.S, 2005. A cross-sectional assessment of the ACGIH TLV for Hand Activity Level. Journal of Occupational Rehabilitation 15 (1), 57−67.

Frost, P., Andersen, J.H., Nielsen, V.K., 1998. Occurrence of carpal tunnel syndrome among slaughterhouse workers. Scandinavian Journal of Work Environment and Health 24 (4), 285−292.

Garg, A., Kapellusch, J., Hegmann, K., Wertsch, J., Merryweather, A., Deckow-Schaefer, G., Malloy, E.J., & the WISTAH Hand Study Research Team, 2012. The Strain Index (SI) and Threshold Limit Value (TLV) for Hand Activity Level (HAL): risk of carpal tunnel syndrome (CTS) in a prospective cohort. Ergonomics 55 (4), 396−414.

Gelberman, R.H., Seiler, J.G., Rosenberg, A.E., Heyman, P., Amiel, D., 1992. Intercalary flexor tendon grafts: a morphological study of intrasynovial and extrasynovial donor tendons. Scandinavian Journal of Plastic and Reconstructive Surgery and Hand Surgery 26 (3), 257−264.

Gelfman, R., Melton, L.J., Yawn, B.P., Wollan, P.C., Amadio, P.C., Stevens, J.C., 2009. Long-term trends in carpal tunnel syndrome. Neurology 72 (1), 33–41.

Gerr, F., Marcus, M., Ensor, C., Kleinbaum, D., Cohen, S., Edwards, A., Gentry, E., Ortiz, D.J., Monteilh, C., 2002. A prospective study of computer users: study design and incidence of musculoskeletal symptoms and disorders. American Journal of Industrial Medicine 41 (4), 221−35.

Goetz, J.E., Baer, T.E., 2011. Mechanical behavior of carpal tunnel subsynovial connective tissue under compression. Iowa Orthopaedic Journal 31 (1), 127–132.

Goodman, H.J., Choueka, J., 2005. Biomechanics of the flexor tendons. Hand Clinics 21 (2), 129−149.

Guimberteau, J.C., Delage, J.P., McGrouther, D.A., Wong, J.K.F., 2010. The microvacuolar system: how connective tissue sliding works. Journal of Hand Surgery 35E (8), 614–622.

Hamanaka, I., Okutsu, I., Shimizu, K., Takatori, Y., Ninomiya, S., 1995. Evaluation of carpal canal pressure in carpal tunnel syndrome. Journal of Hand Surgery 20A, 848–854.

Harris-Adamson, C., Eisen, E.A., Kapellusch, J., Garg, A., Hegmann, K.T., Thiese, M.S., Dale, A.M., Evanoff, B., Burt, S., Bao, S., Silverstein, B., Merlino, L., Gerr, F., Rempel, D., 2014. Biomechanical risk factors for carpal tunnel syndrome: a pooled study of 2474 workers. Occupational and Environmental Medicine (OEM-2014).

Horii, E., Lin, G.T., Cooney, W.P., Linscheid, R.L., An, K.N., 1992. Comparative flexor tendon excursion after passive mobilization: an in vitro study. Journal of Hand Surgery 17A (3), 559−566.

Jinrok, O., Zhao, C., Amadio, P.C., An, K.N., Zobitz, M.E., Wold, L.E., 2004. Vascular pathologic changes in the flexor tenosynovium (subsynovial connective tissue) in idiopathic carpal tunnel syndrome. Journal of Orthopaedic Research 22 (6), 1310−1315.

Jinrok, O., Zhao, C., Zobitz, M.E., Wold, L.E., An, K.N., Amadio, P.C., 2006. Morphological changes of collagen fibrils in the subsynovial connective tissue in carpal tunnel syndrome. Journal of Bone & Joint Surgery 88 (4), 824−831.

Keir, P.J., Bach, J.M., Rempel, D.M., 1998. Effects of finger posture on carpal tunnel pressure during wrist motion. Journal of Hand Surgery 23A (6), 1004−1009.

Keir, P.J., Rempel, D.M., 2005. Pathomechanics of peripheral nerve loading: evidence in carpal tunnel syndrome. Journal of Hand Therapy 18 (2), 259−269.

Keir, P.J., Wells, R.P., 1999. Changes in geometry of the finger flexor tendons in the carpal tunnel with wrist posture and tendon load: MRI study on normal wrists. Clinical Biomechanics 14 (9), 335−345.

Kociolek, A.M., & Keir, P.J., 2011. Modelling tendon excursions and moment arms of the finger flexors: Anatomic fidelity versus function. *Journal of Biomechanics*, 44 (10), 1967-73.

Korstanje, J.W.H., Schreuders, T.R., van der Sijde, J., Hovius, S.E., Bosch, J.G., Selles, R.W., 2010b. Ultrasonographic assessment of long finger tendon excursion in zone v during passive and active tendon gliding exercises. Journal of Hand Surgery 35A (4), 559−565.

Korstanje, J.W.H., Selles, R.W., Stam, H.J., Hovius, S.E.R., Bosch, J.G., 2010a. Development and validation of ultrasound speckle tracking to quantify tendon displacement. Journal of Biomechanics 43 (7), 1373−1379.

Korstanje, J.W.H., Soeters, J.N., Schreuders, T.A., Amadio, P.C., Hovius, S.E., Stam, H.J., Selles, R.W., 2012. Ultrasonographic assessment of flexor tendon mobilization: effect of different protocols on tendon excursion. Journal of Bone & Joint Surgery 94 (5), 394−402.

Kukulski, T., Voigt, J.U., Wilkenshoff, U.M., Strotmann, J.M., Wranne, B., Hatle, L., Sutherland, G.R., 2000. A comparison of regional myocardial velocity information derived by pulsed and color Doppler techniques: an in vitro and in vivo study. Echocardiography 17 (7), 639−651.

Kursa, K., Diao, E., Lattanza, L., Rempel, D., 2005. In vivo forces generated by finger flexor muscles do not depend on the rate of fingertip loading during an isometric task. Journal of Biomechanics 38 (11), 2288–2293.

Landsmeer, J.M., 1961. Studies in the anatomy of articulation. I. The equilibrium of the ‘‘intercalated’’ bone. Acta Morphologica Neerlando-Scandinavica 3, 287−303.

Lopes, M.M., Lawson, W., Scott, T., Keir, P.J., 2011. Tendon and nerve excursion in the carpal tunnel in healthy and CTD wrists. Clinical Biomechanics 26 (9), 930−936.

Lundborg, G., Gelberman, R.H., Minteer-Convery, M., Lee, Y.F., Hargens, A.R., 1982. Median nerve compression in the carpal tunnel - functional response to experimentally induced controlled pressure. Journal of Hand Surgery 7A (3), 252−259.

Lundborg, G., Myers, R., Powell, H., 1983. Nerve compression injury and increased endoneurial fluid pressure: a "miniature compartment syndrome". Journal of Neurology, Neurosurgery & Psychiatry 46 (12), 1119−1124.

MacIntosh, A.R., Keir, P.J., 2014. Improving musculoskeletal hand modelling by incorporating intrinsic structures. 7th World Congress of Biomechanics, Boston, MA.

Manktelow, R.T., Binhammer, P., Tomat, L.R., Bril, V., Szalai, J.P., 2004. Carpal tunnel syndrome: cross-sectional and outcome study in Ontario workers. Journal of Hand Surgery 29A (2), 307−317.

Marieb, E.N., 2003. *Human anatomy and physiology (6th edition)*. San Francisco, CA: Pearson.

McAtamney, L., Corlett, E.N., 1993. RULA: a survey method for the investigation of work-related upper limb disorders. Applied Ergonomics 24 (2), 91−99.

Moore, A., Wells, R., Ranney, D., 1991. Quantifying exposure in occupational manual tasks with cumulative trauma disorder potential. Ergonomics 34 (12), 1433−1453.

Moore, J.S., Garg, A., 1995. The strain index: a proposed method to analyze jobs for risk of distal upper extremity disorders. American Industrial Hygiene Association 56 (5), 443−458.

National Research Council & Institute of Medicine, 2001. *Musculoskeletal disorders and the workplace*. Washington, DC: National Academy Press.

Nelson, J.E., Treaster, D.E., Marras, W.S., 2000. Finger motion, wrist motion and tendon travel as a function of keyboard angles. Clinical Biomechanics 15 (7), 489−498.

Occhipinti, E., 1998. OCRA: a concise index for the assessment of exposure to repetitive movements of the upper limbs. Ergonomics 41 (9), 1290−1311.

Oh, S., Belohlavek, M., Zhao, C., Osamura, N., Zobitz, M.E., An, K.N., 2007. Detection of differential gliding characteristics of the flexor digitorum superficialis tendon and subsynovial connective tissue using color Doppler sonographic imaging. Journal of Ultrasound Medicine 26 (2), 149−155.

Osamura, N., Zhao, C., Zobitz, M.E., An, K.N., Amadio, P.C., 2007a. Evaluation of the material properties of the subsynovial connective tissue in carpal tunnel syndrome. Clinical Biomechanics 22 (9), 999−1003.

Osamura, N., Zhao, C., Zobitz, M.E., An, K.N., Amadio, P.C., 2007b. Permeability of the subsynovial connective tissue in the human carpal tunnel: A cadaver study. Clinical Biomechanics 22 (5), 524−528.

Peolsson, M., Löfstedt, T., Vogt, S., Stenlund, H., Arndt, A., Trygg, J., 2010. Modelling human musculoskeletal functional movements using ultrasound imaging. BioMed Central (BMC) Medical Imaging 10 (1), 1−11.

Rempel, D.M., Bach, J.M., Gordon, L., So, Y., 1998. Effects of forearm pronation/supination on carpal tunnel pressure. Journal of Hand Surgery 23A, 38–42.

Rempel, D., Keir, P.J., Smutz, W.P., Hargens, A., 1997. Effects of static fingertip loading on carpal tunnel pressure. Journal of Orthopaedic Research 15 (3), 422−426.

Russo, A., Murphy, C., Lessoway, V., Berkowitz, J., 2002. The prevalence of musculoskeletal symptoms among British Columbia sonographers. Applied Ergonomics 33 (5), 385−393.

Rydevik, B., Lundborg, G., Bagge, U., 1981. Effects of graded compression on intraneural blood blow. An in vivo study on rabbit tibial nerve. Journal of Hand Surgery 6A (1), 3−12.

Scheuerle, J., Guilford, A.M., Habal, M.B., 2000. Work-related cumulative trauma disorders and interpreters for the deaf. Applied Occupational and Environmental Hygiene 15 (5), 429−434.

Schuind, F., Ventura, M., Pasteels, J.L., 1990. Idiopathic carpal tunnel syndrome: histologic study of the flexor synovium. Journal of Hand Surgery 15A (3), 497−503.

Seradge, H., Jia, Y.C., Owens, W., 1995. In vivo measurement of carpal tunnel pressure in the functioning hand. Journal of Hand Surgery 20A, 855–859.

Silverstein, B.A., Fine, L.J., Armstrong, T.J., 1986. Hand wrist cumulative trauma disorders in industry. British Journal of Industrial Medicine 43 (11), 779−784.

Silverstein, B.A., Fine, L.J., Armstrong, T.J., 1987. Occupational factors and the carpal tunnel syndrome. American Journal of Industrial Medicine 11 (3), 343−358.

Silverstein, B.A., Welp, E., Nelson, N., Kalat, J., 1998. Claims incidence of work-related disorders of the upper extremities: Washington State, 1987 through 1995. American Journal of Public Health 88 (12), 1827−33.

Smutz, W.P., Miller, S.C., Eaton, C.J., Bloswick, D.S., France, E.P., 1994. Investigation of low-force high-frequency activities on the development of carpal-tunnel syndrome. Clinical Biomechanics 9 (1), 15−20.

Sommerich, C.M., Marras, W.S., Parnianpour, M., 1998. A method for developing biomechanical profiles of hand-intensive tasks. Clinical Biomechanics 13 (4), 261−271.

Staal, J.B., de Bie, R.A., Hendriks, E.J.M., 2007. Aetiology and management of work-related upper extremity disorders. Best Practice & Research Clinical Rheumatology 21 (1), 123−133.

Tanaka, S., McGlothlin, J.D., 1993. A conceptual quantitative model for prevention of work-related carpal tunnel syndrome (CTS). International Journal of Industrial Ergonomics 11 (3), 181–193.

Tat, J., 2014. *Ultrasound assessment of finger flexor tendon shear: implications for carpal tunnel syndrome*. Master's Thesis, McMaster University, Hamilton, Ontario.

Tat, J., Kociolek, A.M., Keir, P.J., 2013. Repetitive differential finger motion increases shear strain between the flexor tendon and subsynovial connective tissue. Journal of Orthopaedic Research 31 (10), 1533−1539.

Tat, J., Kociolek, A.M., Keir, P.J., 2015. Validation of colour Doppler ultrasonography for evaluating relative displacement between flexor tendon and subsynovial connective tissue. Journal of Ultrasound in Medicine 34 (4), 679−687.

Taylor, D.C., Dalton, J.D., Seaber, A.V., Garrett, W.E., 1990. Viscoelastic properties of muscle-tendon units the biomechanical effects of stretching. American Journal of Sports Medicine 18 (3), 300–309.

Thomsen, J.F., Hansson, G.Å., Mikkelsen, S., Lauritzen, M., 2002. Carpal tunnel syndrome in repetitive work: A follow-up study. American Journal of Industrial Medicine 42 (4), 344−353.

Treaster, D.E., Marras, W.S., 2000. An assessment of alternate keyboards using finger motion, wrist motion and tendon travel. Clinical Biomechanics 15 (7), 499−503.

Uchiyama, S., Coert, J.H., Berglund, L., Amadio, P.C., An, K.N., 1995. Method for the measurement of friction between tendon and pulley. Journal of Orthopaedic Research 13 (1), 83−89.

Ugbolue, U.C., Nicol, A.C., 2010. A comparison of two interventions designed to promote neutral wrist postures during simple computer operations. Work: A Journal of Prevention, Assessment and Rehabilitation 37 (4), 413–424.

Ugbolue, U.C., Nicol, A.C., 2012. A wrist tendon travel assessment of hand movements associated with industrial repetitive activities. Work 42 (3), 311−320.

Ugbolue, U.C., Nicol, A.C., 2014. An assessment of hand volumetric and temperature changes during office related repetitive activities. Work 48 (1), 53−64.

Valero-Cuevas, F.J., Johanson, M.E., Towles, J.D., 2003. Towards a realistic biomechanical model of the thumb: the choice of kinematic description may be more critical than the solution method or the variability/uncertainty of musculoskeletal parameters. Journal of Biomechanics 36 (7), 1019–1030.

van Doesburg, M.H.M., Yoshii, Y., Henderson, J., Villarraga, H.R., Moran, S.L., Amadio, P.C., 2012. Speckle-tracking sonographic assessment of longitudinal motion of the flexor tendon and subsynovial tissue in carpal tunnel syndrome. Journal of Ultrasound in Medicine 31 (7), 1091−1098.

Violante, F.S., Armstrong, T.J., Fiorentini, C., Graziosi, F., Risi, A., Venturi, S., Curti, S., Zanardi, F., Cooke, R.M.T., Bonfiglioli, R., Mattioli, S., 2007. Carpal tunnel syndrome and manual work: a longitudinal study. Journal of Occupational and Environmental Medicine 49 (11), 1189–1196.

Weiss, N.D., Gordon, L., Blooms, T., So, Y., Rempel, D.M., 1995. Position of the wrist associated with the lowest carpal-tunnel pressure: implications for splint design. Journal of Bone and Joint Surgery 77A (11), 1695−1699.

Werner, R., Armstrong, T.J., Bir, C., Aylard, M.K., 1997. Intracarpal canal pressures: the role of finger, hand, wrist and forearm position. Clinical Biomechanics 12 (1), 44–51.

Workplace Safety and Insurance Board of Ontario, 2013. *Statistical supplement of the 2013 annual report*. Toronto, ON: Workplace Safety and Insurance Board of Ontario (Communications Division).

Yamaguchi, T., Osamura, N., Zhao, C., An, K.N., Amadio, P.C., 2008. Relative longitudinal motion of the finger flexors, subsynovial connective tissue, and median nerve before and after carpal tunnel release in a human cadaver model. Journal of Hand Surgery 33A (6), 888−892.

Yoshii, Y., Villarraga, H.R., Henderson, J., Zhao, C., An, K.N., Amadio, P.C., 2009a. Speckle tracking ultrasound for assessment of the relative motion of flexor tendon and

subsynovial connective tissue in the human carpal tunnel. Ultrasound in Medicine and Biology 35 (12), 1973−1981.

Yoshii, Y., Zhao, C., Henderson, J., Zhao, K.D., An, K.N., Amadio, P.C., 2009b. Shear strain and motion of the subsynovial connective tissue and median nerve during single-digit motion. Journal of Hand Surgery 34A (1), 65−73.

Yoshii, Y., Zhao, C., Henderson, J., Zhao, K.D., An, K.N., Amadio, P.C., 2011. Velocity-dependent changes in the relative motion of the subsynovial connective tissue in the human carpal tunnel. Journal of Orthopaedic Research 29 (1), 62−66.

Yoshii, Y., Zhao, C., Zhao, K.D., Zobitz, M.E., An, K.N., Amadio, P.C., 2008. The effect of wrist position on the relative motion of tendon, nerve, and subsynovial connective tissue within the carpal tunnel in a human cadaver model. Journal of Orthopaedic Research 26 (8), 1153−1158.

Zakaria, D. (2004). Rates of carpal tunnel syndrome, epicondylitis, and rotator cuff claims in Ontario workers during 1997. Chronic Diseases in Canada 25 (2), 32−39.

Zakaria, D., Robertson, J., Koval, J., MacDermid, J., Hartford, K., 2004. Rates of claims for cumulative trauma disorder of the upper extremity in Ontario workers during 1997. Chronic Diseases in Canada 25 (1), 22−31.

Zhao, C., Ettema, A.M., Osamura, N., Berglund, L.J., An, K.N., Amadio, P.C., 2007. Gliding characteristics between flexor tendons and surrounding tissues in the carpal tunnel: a biomechanical cadaver study. Journal of Orthopaedic Research 25 (2), 185−190.

APPENDIX A ETHICS APPROVAL FOR CHAPTER 2

Hamilton Health Sciences

RESEARCH ETHICS BOARD

McMaster University

REB Office, 293 Wellington St. N., Suite 102, Hamilton, ON L8L 8E7
Telephone: 905-521-2100, Ext. 42013
Fax: 905-577-8378

September 28, 2012

PROJECT NUMBER: **12-571-T**

PROJECT TITLE: Measuring Flexor Tendon Motion and Gliding Resistance in a Cadaveric Model

PRINCIPAL INVESTIGATOR: **Dr. Peter Keir**

This will acknowledge receipt of your tissue application for the study entitled "*Measuring Flexor Tendon Motion and Gliding Resistance in a Cadaveric Model*". This study has been reviewed by the members of the Human Tissue Committee and we wish to confirm the study has been given ***final*** approval. The submission was found to be acceptable on both ethical and scientific grounds.

We are pleased to issue final approval for the above-named study for a period of 12 months from the date of this approval letter. Continuation beyond that date will require further review and renewal of REB approval. Any changes or amendments to the protocol or information sheet must be approved by the Research Ethics Board.

We wish to advise the Human Tissue Committee (HTC) is a sub-committee of the Hamilton Health Sciences/Faculty of Health Sciences Research Ethics Board operates in compliance with ICH Good Clinical Practice Guidelines and the Tri-Council Policy Statement.

PLEASE QUOTE THE ABOVE-REFERENCE PROJECT NUMBER ON ALL FUTURE CORRESPONDENCE

Sincerely,

S. Salama

Suzette Salama PhD.
Chair, Research Ethics Board

APPENDIX B ETHICS APPROVAL FOR CHAPTERS 3 & 4

Hamilton Health Sciences

RESEARCH ETHICS BOARD

McMaster University

REB Office, 293 Wellington St. N., Suite 102, Hamilton, ON L8L 8E7
Telephone: 905-521-2100, Ext. 42013
Fax: 905-577-8378

January 3, 2012

PROJECT NUMBER: **11-551**

PROJECT TITLE: Ultrasound Assessment of Flexor Tendon Excursion in the Carpal Tunnel

PRINCIPAL INVESTIGATOR: **Aaron Kociolek**
LOCAL PI: **Dr. Peter Keir**

This will acknowledge receipt of your letter dated December 13, 2011 which enclosed revised copies of the Information/Consent Form and the Poster for the above-named study. These issues were raised by the Research Ethics Board at their meeting held on November 15, 2011. Based on this additional information, we wish to advise your study has been given ***final*** approval from the full REB. The submission, Study Protocol version 1 dated October 25, 2011 including the Information/Consent Form version 2 dated December 13, 2011 together with Study Poster version 2 dated December 13, 2011; Participant Questionnaire version 3 dated January 1, 2012 and Participant Screening Telephone Script version 1 dated October 25, 2011 were found to be acceptable on both ethical and scientific grounds. ***Please note*** attached you will find the Information/Consent Form and the Study Poster with the REB approval affixed; all consent forms/posters used in this study must be copies of the attached materials.

We are pleased to issue final approval for the above-named study for a period of 12 months from the date of the REB meeting on November 15, 2011. Continuation beyond that date will require further review and renewal of REB approval. Any changes or revisions to the original submission must be submitted on an REB amendment form for review and approval by the Research Ethics Board.

The Hamilton Health Sciences/McMaster Health Sciences Research Ethics Board operates in compliance with and is constituted in accordance with the requirements of: The Tri-Council Policy Statement on Ethical Conduct of Research Involving Humans; The International Conference on Harmonization of Good Clinical Practices; Part C Division 5 of the Food and Drug Regulations of Health Canada; and the provisions of the Ontario Personal Health Information Protection Act 2004 and its applicable Regulations.

PLEASE QUOTE THE ABOVE-REFERENCE PROJECT NUMBER ON ALL FUTURE CORRESPONDENCE

Sincerely,

S. Salama

Suzette Salama PhD.,
Chair, Research Ethics Board

APPENDIX C ETHICS APPROVAL FOR CHAPTER 5

Hamilton Health Sciences | McMaster University | St. Joseph's Healthcare Hamilton

Hamilton Integrated Research Ethics Board
AMENDMENT REQUEST

REB Project #: 11-551

Principal Investigator: Dr. Peter Keir

Project Title: Ultrasound assessment of flexor tendon excursion in the carpal tunnel

Document(s) Amended with version # and date:

- Protocol Amendment - Protocol Ver: 3 Dated: 25 November, 2013
- Consent Form Amendment - Letter of Information and Consent Ver: 3 Dated: 25 November, 2013
- Recruitment Poster - Advertisement Poster Ver: 3 Dated: 25 November, 2013
- Participant Letter - Thank You Letter with Screening Questions Ver: 3 Dated: 25 November, 2013
- Questionnaire - Participant Questionnaire Ver: 4 Dated: 25 November, 2013
- Other - PI's Letter dated November 25, 2013 re rationale and summary of changes

Research Ethics Board Review
(this box to be completed by HIREB Chair only)

[X] **Amendment approved as submitted**

[ ] **Amendment approved conditional on changes noted in "Conditions" section below**

[ ] **New enrolment suspended**

[ ] **Study suspended pending further review**

Level of Review:

[ ] Full Research Ethics Board
[X] Research Ethics Board Executive

The Hamilton Integrated Research Ethics Board operates in compliance with and is constituted in accordance with the requirements of: The Tri-Council Policy Statement on Ethical Conduct of Research Involving Humans; The International Conference on Harmonization of Good Clinical Practices; Part C Division 5 of the Food and Drug Regulations of Health Canada, and the provisions of the Ontario Personal Health Information Protection Act 2004 and its applicable Regulations; For studies conducted at St. Joseph's Hospital, HIREB complies with the health ethics guide of the Catholic Alliance of Canada

Raelene Rathbone

Suzette Salama PhD., Chair
Raelene Rathbone, MB, BS, MD, PhD, Chair

12/3/2013
Date

All Correspondence should be addressed to the HIREB Chair(s) and forwarded to:
HIREB Coordinator
293 Wellington St. N, Suite 102, Hamilton ON L8L 8E7
Tel. 905-521-2100 Ext. 42013 Fax: 905-577-8378

APPENDIX D **CONSENT FORM FOR CHAPTERS 3 & 4**

McMaster University
Inspiring Innovation and Discovery

Letter of Information and Consent

Ultrasound Assessment of Tendon Excursion in the Carpal Tunnel

Local Principal Investigator: Peter Keir, PhD
Department of Kinesiology
McMaster University
Hamilton, Ontario, Canada
Phone: (905) 525-9140 (× 23543)
Email: pjkeir@mcmaster.ca

Principal Investigator: Aaron Kociolek, MSc
Department of Kinesiology
McMaster University
Hamilton, Ontario
Phone: (905) 525-9140 (× 20175)
Email: kociolam@mcmaster.ca

Co-investigator: Jimmy Tat, BSc
Department of Kinesiology
McMaster University
Hamilton, Ontario
Phone: (905) 525-9140 (× 20175)
Email: tatj2@mcmaster.ca

Sponsor: This study is funded by the Natural Sciences and Engineering Research Council of Canada

Introduction

You are being invited to participate in a study about musculoskeletal disorders of the wrist and hand. Common musculoskeletal disorders include tendonitis and carpal tunnel syndrome. Understanding how the tendons and nerves move inside the carpal tunnel (or wrist) is important in determining the development of wrist and hand musculoskeletal disorders. Tendons and nerves can be seen non-invasively using ultrasound.

Purpose of the Study

The purpose of this study is to observe and measure movement of the tendons that travel through the carpal tunnel using ultrasound.

Procedures Involved in the Research

You will be asked to complete a survey with questions about your handedness (i.e. left-handed or right-handed), general health, as well as musculoskeletal disorders of the wrist and hand. Following the questionnaire, you will complete a testing protocol no longer than 2 hours. You will be seated comfortably while the ultrasound technician applies ultrasound gel on the wrist of your dominant hand. Small spherical markers will also be taped to your arm so that a camera system can measure joint angles of the wrist and fingers. Next, you will be asked to complete a series of wrist and finger movements while an ultrasound probe records images of the tendons in the carpal tunnel. Each type of movement will last no longer than 30 seconds (with rest in between the different movements). You may also be asked to perform a different series of wrist and finger movements on another day. This second testing session will be similar to the first but between the ultrasound measurements you will be asked to perform simple hand and finger motions for up to 30 minutes. This portion of the study is to see if activity alters the ultrasound measurements.

Potential Harm, Risk or Discomfort

Ultrasound is a safe imaging tool used to visualize tissues within your body. The cameras that measure your wrist and finger angles only record the markers attached to your skin and do not acquire your image itself. The wrist and finger movements in this study might cause you minimal discomfort due to fatigue in some rare cases. However, we do not foresee any risks from your participation in this research. If you do feel any muscular discomfort or pain, please tell the ultrasound technician. In the event that you do feel pain while performing any of the tasks, the study will be stopped immediately to ensure your safety.

Potential Benefits

This research will not benefit you directly, except for knowing that you are helping further our understanding about the movement of tendons in the wrist. Ultimately, we hope to prevent musculoskeletal disorders in the workplace.

Payment and Reimbursement

You will receive $30.00 for your time for participating in this study. If you withdraw from this study at any time, you will still receive prorated compensation.

Confidentiality

Your identity will be kept confidential. We will not use your name or any information that would allow you to be identified. The data obtained in this study will be used for research and

teaching purposes only. Information directly pertaining to you will be stored in a locked cabinet or on a password protected computer. Your individual data will be kept confidential to the fullest extent of the law. We will treat all information provided to us as subject to researcher-participant privilege.

Participation

Your participation in this study is voluntary. If you decide to participate, you can choose to stop at any time, even after signing the consent form, or partway through the study. If you decide to stop participating in this study, there will be no consequences to you. Also, all of your data will be permanently deleted.

This study has been reviewed by the Hamilton Health Sciences/McMaster Faculty of Health Sciences Research Ethics Board (HHS/FHS REB). If you have any concerns or questions about your rights as a participant or about the way this study is conducted, contact the Office of the Chair of the HHS/FHS REB at (905) 521-2100 (× 42013).

Information about the Study Results

You may obtain information about the study results by contacting Aaron Kociolek at (905) 525-9140 (× 20175) or Peter Keir at (905) 525-9140 (× 23543).

Information about Participating in this Study

If you have questions or require more information about the study itself, please contact Aaron Kociolek or Peter Keir.

INFORMED CONSENT

I have read the information in this information and consent form about a study being conducted by Aaron Kociolek and Peter Keir at McMaster University. I have had the opportunity to ask questions about my involvement in this study, and to receive any additional details I wanted to know about the study. I understand that I may withdraw from the study at any time, if I choose to do so. I have been given a signed copy of this form. I agree to participate in this study.

_____	_____	_____
Name of Participant (Print)	Signature	Date

In my opinion, the person who has signed above is agreeing to participate in this study voluntarily, and understands the nature of the study and the consequences of participation in it.

_____	_____	_____
Name of Research Investigator Obtaining Consent (Print)	Signature	Date

APPENDIX E **CONSENT FORM FOR CHAPTER 5**

McMaster University
Inspiring Innovation and Discovery

Letter of Information and Consent

Ultrasound Assessment of Tendon Excursion in the Carpal Tunnel

Local Principal Investigator:
Peter Keir, PhD
Department of Kinesiology
McMaster University
Hamilton, Ontario, Canada
Phone: (905) 525-9140 (× 23543)
Email: pjkeir@mcmaster.ca

Principal Investigator:
Aaron Kociolek, MSc
Department of Kinesiology
McMaster University
Hamilton, Ontario
Phone: (905) 525-9140 (× 20175)
Email: kociolam@mcmaster.ca

Co-investigators:
Joanne Hodder, PhD
Department of Kinesiology
McMaster University
Hamilton, Ontario
Phone: (905) 525-9140 (× 20175)
Email: hodderjn@mcmaster.ca

Jimmy Tat, BSc
Department of Kinesiology
McMaster University
Hamilton, Ontario
Phone: (905) 525-9140 (× 20175)
Email: tatj2@mcmaster.ca

Sponsor:
This study is funded by the Natural Sciences and Engineering Research Council of Canada

Introduction

You are being invited to participate in a study about musculoskeletal disorders of the wrist and hand. Common musculoskeletal disorders include tendonitis and carpal tunnel syndrome. Understanding how the tendons and nerves slide past each other inside the carpal tunnel (or wrist) is important in determining the development of wrist and hand musculoskeletal disorders. Tendons and nerves can be seen non-invasively using ultrasound.

Purpose of the Study

The purpose of this study is to observe and measure movement of the tendons that travel through the carpal tunnel using ultrasound.

Procedures Involved in the Research

You will be asked to complete a survey with questions about your handedness (i.e. left-handed or right-handed), general health, and musculoskeletal disorders of the wrist and hand. Following the questionnaire, you will complete a testing protocol no longer than 2 hours. You will be seated comfortably while an ultrasound technician applies ultrasound gel on the wrist of your dominant hand. We will also measure the activity of two forearm muscles while you are performing the wrist and finger motions. Small electrodes will be inserted into the muscle belly with a small needle. Measuring muscle activity while imaging tendon motion in the wrist will help us to determine how the tendons slide past each other with different wrist and finger movements. We will also assess wrist and finger posture using electrogoniometers (small electrical devices that measure angles) taped onto your hand.

Next, you will be asked to complete a series of wrist and finger movements while an ultrasound probe records images of the tendons in the carpal tunnel. Each movement will last no longer than 30 seconds (with rest in between the different movements). You may also be asked to perform a different series of wrist and finger movements on another day. This second testing session will be similar to the first but between the ultrasound measurements you will be asked to perform simple hand and finger motions for up to 30 minutes. This part of the study is to see if repeated finger movements change tendon motion over longer periods of time.

Potential Harm, Risk or Discomfort

Ultrasound is a safe imaging tool used to visualize tissues within your body. Electrogoniometers are also a safe method to measure angles of the wrist and finger joints. Placing electrodes in muscles may cause mild discomfort and minor bruising. However, the electrodes are inserted with very fine, sterile, single-use needles to minimize any discomfort and prevent infection. Also, if you do experience any pain while placing the electrodes we will move to another area on your forearm. Once the fine-wire electrode is in place the needle is removed and disposed. The wires are taped to your forearm (using medical tape) so they do not move during the study. The electrodes will remain in the muscles until the end of study, and are easily removed by gently pulling on the wire.

Once the electrodes are placed, you will be asked to maximally flex (bend forwards) and extend (bend backwards) your fingers against a rigid structure. This structure will prevent your fingers from moving as you try to bend them. These maximal efforts may cause delayed onset muscle soreness after the study. However, this muscle discomfort should go away within 72 hours. Next, you will complete different wrist and finger movements, which might cause minimal discomfort due to fatigue in some rare cases. If you do feel any muscular discomfort or pain, please tell the ultrasound technician. In the event that you do feel pain while performing any of the tasks, the study will be stopped immediately to ensure your safety.

Potential Benefits

This research will not benefit you directly, except for knowing that you are helping further our understanding about the movement of tendons in the wrist. Ultimately, we hope to prevent musculoskeletal disorders in the workplace.

Payment and Reimbursement

You will receive $30.00 for your time for participating in this study. If you withdraw from this study at any time, you will still receive compensation.

Confidentiality

Your identity will be kept confidential. We will not use your name or any information that would allow you to be identified. The data obtained in this study will be used for research and teaching purposes only. Information directly pertaining to you will be stored in a locked cabinet or on a password protected computer. Your individual data will be kept confidential to the fullest extent of the law. We will treat all information provided to us as subject to researcher-participant privilege.

Participation

Your participation in this study is voluntary. If you decide to participate, you can choose to stop at any time, even after signing the consent form, or partway through the study. If you decide to stop participating in this study, there will be no consequences to you. Also, all of your data will be permanently deleted.

This study has been reviewed by the Hamilton Integrated Research Ethics Board (HIREB). If you have any concerns or questions about your rights as a participant or about the way this study is conducted, contact the Office of the Chair of HIREB at (905) 521-2100 (× 42013).

Information about the Study Results

You may obtain information about the study results by contacting Aaron Kociolek at (905) 525-9140 (× 20175) or Peter Keir at (905) 525-9140 (× 23543).

Information about Participating in this Study

If you have questions or require more information about the study itself, please contact Aaron Kociolek or Peter Keir.

INFORMED CONSENT

I have read the information in this information and consent form about a study being conducted by Aaron Kociolek and Peter Keir at McMaster University. I have had the opportunity to ask questions about my involvement in this study, and to receive any additional details I wanted to know about the study. I understand that I may withdraw from the study at any time, if I choose to do so. I have been given a signed copy of this form. I agree to participate in this study.

_____	_____	_____
Name of Participant (Print)	Signature	Date

In my opinion, the person who has signed above is agreeing to participate in this study voluntarily, and understands the nature of the study and the consequences of participation in it.

_____	_____	_____
Name of Research Investigator Obtaining Consent (Print)	Signature	Date

APPENDIX F QUESTIONNAIRE FOR CHAPTERS 3 − 5

Participant Questionnaire:

Ultrasound Assessment of Tendon Motion in the Carpal Tunnel

PARTICIPANT IDENTIFIACTION

Date: _____

Name: _____

Subject Code: _____

HANDEDNESS

1) Are you are you right-handed or left-handed or ambidextrous?

right-handed ☐ ***left-handed*** ☐ ***ambidextrous*** ☐

HEALTH HISTORY

1) Have you ever had any of the following health conditions and/or treatment protocols performed on you currently and/or in the past? [*please check all that apply*]

☐ Diabetes mellitus
☐ Thyroid condition (e.g. hypothyroidism)
☐ Gout
☐ Amyloidosis
☐ Sarcoidosis
☐ Renal failure (or hemodialysis)
☐ Degenerative joint disease
☐ Arthritis of the wrist/hand
☐ Corticosteroid injection
☐ Cervical radiculopathy
☐ Peripheral neuropathy
☐ Radial malunion
☐ Colles fracture
☐ Wrist/hand musculoskeletal disorder
☐ Flexor tendonopathy
☐ Carpal tunnel syndrome
☐ Ultrasound/laser/soft tissue treatment
☐ Wrist/hand surgery
☐ Pain/tingling/numbness of the hand

2) Are you currently on any medications? *Yes* ☐ *No* ☐

** If *yes*, please list:

_____
_____
_____

WORK HISTORY

1) Occupation: _____

2) Location of work: _____

3) Hours at work per week: _____

4) Years at current job: _____

5) Typical tasks performed at work: _____
_____
_____
_____
_____
_____

6) Have you ever-experienced a work-related wrist or hand injury? *Yes* ☐ *No* ☐

** If *yes*, please elaborate (type of injury, onset of injury, what do you attribute it to, how long have you have had the injury, symptoms, treatment of injury, time off work): _____
_____
_____
_____
_____
_____

I verify that I have answered the above questions to the best of my knowledge. I understand that no confidential health information will be released without my written consent.

_____	_____	_____
Name of Participant (Print)	Signature	Date
_____	_____	_____
Name of Research Investigator Obtaining Consent (Print)	Signature	Date